Clinical Relevance of the Immune Contexture and AXL Kinase in Triple-Negative Breast Cancer

Giulia Bottai, MSc

Humanitas Clinical and Research Institute

Milan, Italy

Affiliated Research Centre to the "Open University" Milton Keynes, UK

(*International PhD Programme in Immunology and Immunopathology*)

Director of Studies: Dr. Libero Santarpia

Humanitas Clinical and Research Institute, Milan, Italy

External Supervisor: Prof. Christos Sotiriou

Institut Jules Bordet, Université Libre de Bruxelles, Brussels, Belgium

Thesis submitted in accordance with the requirements of

The Open University

for the degree of Doctor of Philosophy

4th October 2017

Abstract

Triple-negative breast cancers (TNBC) are usually associated with an aggressive phenotype, an increased risk of early relapse, and poor outcome. Burgeoning evidence demonstrates that TNBC encompasses distinct molecular entities that are differentially characterized by specific hallmarks of cancer, including chromosomal instability (CIN), epithelial-to-mesenchymal transition (EMT), and cancer-related immune responses. In particular, the tumour immune microenvironment and the interaction between immune and cancer cells are emerging as crucial factors in tumour progression, prognosis, and response to therapy in TNBC. In this study, we aimed to evaluate the relationship between these three major hallmarks of TNBC. In particular, we assessed the composition and functionality of immune infiltrates in TNBC samples with different levels of CIN and investigated their clinical relevance in patients treated with adjuvant chemotherapy. Additionally, we explored the interactions between tumour-associated macrophages (TAM) and TNBC cells, particularly those with mesenchymal traits.

For this purpose, we integrated *in vivo* analysis of human TNBC tissues, *in vitro* experiments, and bioinformatics data. To assess the tumour immune microenvironment heterogeneity, we first identified different gene signatures from mRNA expression data, representing distinct immune components, and then evaluated their expression in different molecular subtypes of TNBC and in tumour samples characterized by low and high levels of CIN. To further explore the composition and functionality of immune infiltration in TNBC *in vivo*, formalin-fixed, paraffin-embedded tissues were retrospectively collected from large cohorts of early-stage TNBC patients treated with anthracycline-based chemotherapy. Stromal tumour-infiltrating lymphocytes (TIL) were evaluated on haematoxylin and eosin-stained sections. The density of CD4+, CD8+, CD103+, and FOXP3+ lymphocytes, CD68+ and CD163+ macrophages, and the expression of the immune checkpoints PD-1 and LAG-3 were assessed by immunohistochemistry.

Furthermore, to understand the biological and clinical relevance of the interaction between TNBC cells and innate immune cells, we investigated several kinases functioning in the EMT process and their association with TAM in patients treated with adjuvant chemotherapy and in several TNBC cell lines.

We demonstrated that immune expression signatures were differentially expressed in TNBC characterized by varying levels of CIN and that TNBC molecular subgroups with a mesenchymal phenotype were enriched for immune signatures related to pro-tumour M2 macrophages. Conjunctly, by analysing human TNBC tissues, we showed that the presence of elevated TIL positively correlated with the density of all T cell subtypes, especially cytotoxic CD8+ lymphocytes. Among immune subpopulations, CD8+ lymphocytes were the main effectors of anti-tumour immune responses. We also found that PD-1 and LAG-3 were concurrently expressed in nearly 15% of TNBC. The expression of both checkpoint receptors positively correlated with the presence of TIL, but was not significantly associated with patient outcome. Furthermore, we showed that intraepithelial CD8+ cells frequently expressed the integrin CD103, which mediates the localization of cytotoxic lymphocytes within epithelial tissues. Importantly, the massive intraepithelial infiltration of cytotoxic CD103+ TIL co-expressing PD-1, correlated with prolonged survival in TNBC. In addition to TIL, we have demonstrated that the activation of the innate immune cells within the TNBC tumour stroma had a crucial role in tumour progression and chemoresistance, especially through the modulation of EMT. Accordingly, the EMT-related kinase AXL was highly associated with the presence of CD163+ TAM. Tumours from relapsing patients presented a high expression of AXL and CD163, although only AXL retained independent prognostic significance in multivariate analysis. *In vitro* analysis demonstrated that *AXL*-expressing TNBC cells were able to polarize human macrophages toward an M2-like phenotype. A selective inhibition of AXL impaired the activity of M2-like macrophages, reducing cancer cell invasiveness and restoring the sensitivity of breast cancer cells to chemotherapeutic drugs, especially anthracyclines.

Overall, our data indicate that TNBC subgroups with different biological and genomic features are characterized by distinct compositions of the immune microenvironment. Our results confirm that the evaluation of stromal TIL is the most reliable immune prognostic marker in TNBC patients. Our data also support the pharmacological and clinical evaluation of anti-PD-1/PD-L1 and anti-LAG-3 in a specific subset of TNBC patients and the inhibition of AXL as a novel strategy to simultaneously target TNBC cells and tumour promoting TAM.

Table of contents

1. Introduction

1.1 Breast cancer

Breast cancer is the most frequently diagnosed cancer and a major cause of cancer death in women worldwide (Ferlay et al., 2015). Hereditary breast cancer found in women with a strong inherited germline component accounts only for 5-10% of all breast cancers, whereas the majority of breast tumours are sporadic (Nielsen et al., 2016). Overall, breast cancer represents a complex and heterogeneous disease, encompassing several distinct entities with different molecular features and clinical behaviour. The intrinsic diversity between and within tumours is widely affected by genetic and molecular heterogeneity, which impact breast cancer development and progression as well as individual patients' outcome and response to treatment. Furthermore, the tumour immune microenvironment and the interactions between cancer cells and immune cells have a crucial role in sustaining breast carcinogenesis and metastatic spread, and are emerging as important predictors of outcome and response to therapies in distinct breast cancer subtypes. Overall, understanding the complex relationships and signalling networks between different cells within a tumour may allow a better stratification of breast cancer patients into different risk groups and help to develop new targeted therapies inhibiting key oncogenic pathways.

1.1.1 Molecular and clinical portraits of breast cancer

The heterogeneity of breast cancer is not fully reflected by the main clinical parameters and histopathological markers, including age, tumour size, histological grade, lymph node status, estrogen receptor (ER), progesterone receptor (PR), and human epidermal growth factor receptor 2 (HER2) (Figure 1, Table 1) (Prat and Perou, 2011). Gene-expression profiling and recent advances in sequencing-based technologies have enabled the recognition of this complexity in previously unprecedented depth and have begun to reshape research directions. The "intrinsic" classification identifies four classes of breast

cancer – luminal A, luminal B, HER2-enriched, and basal-like – showing extensive differences in biological features, incidence, prognosis, and response to treatment (Figure 1, Table 1) (Perou et al., 2000; Sotiriou and Pusztai, 2009). However, although not completely interchangeable, these subtypes are commonly overlapped with the subgroups defined on the basis of hormone receptors and HER2 status, and proliferation markers, which are routinely used in the clinic to stratify patients for prognostic predictions and treatment selection (Figure 1) (Sotiriou and Pusztai, 2009).

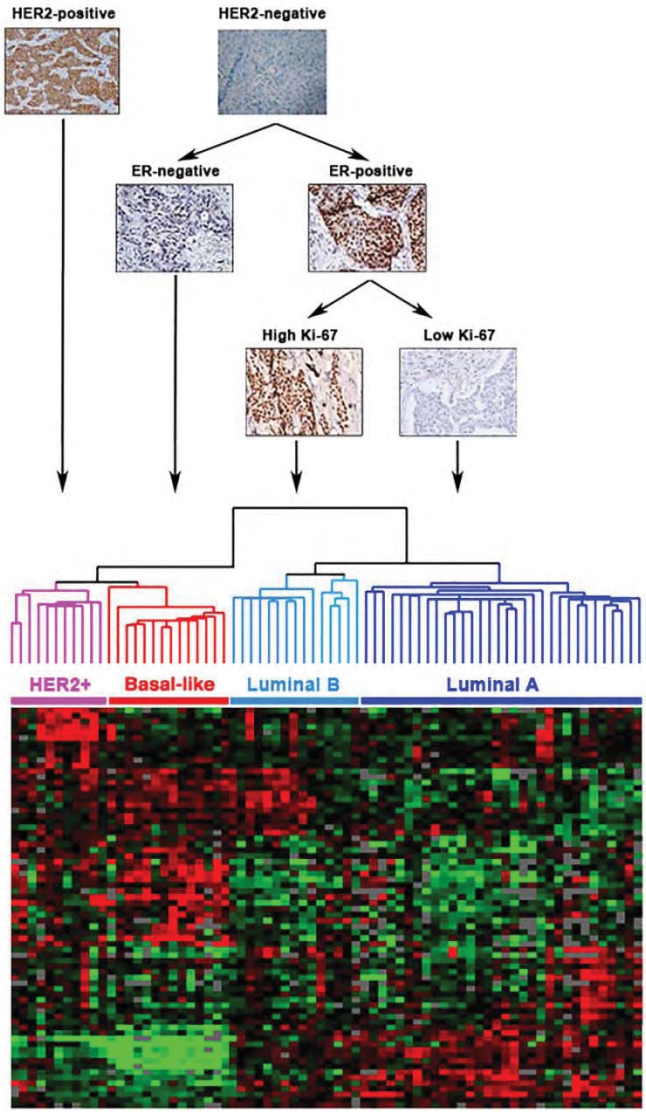

Figure 1. Correspondence between breast cancer subtypes defined by standard pathological characteristics and gene expression profiles. Classical pathological markers, including ER, PR and HER2 status, and proliferation markers (Ki-67) are routinely used as a surrogate of breast cancer intrinsic subtype classification.

Table 1. Clinicopathological characteristics of the four major breast cancer subtypes

Subtype	Pathological Characteristics[a]	Frequency[b]	Clinical Features	Treatment[a]
Luminal A	ER-positive PR-positive (≥ 20%) HER2-negative Low Ki-67 (< 20%)	30-70%	Low grade, good prognosis	Endocrine therapy; Chemotherapy in case of ≥ 4 positive LN, tumour size ≥ 5 cm, or grade 3
Luminal B	ER-positive HER2-negative High Ki-67 (≥ 20%) or PR (< 20%)	10-20%	High grade, large tumour size, LN involvement, LVI, poorer prognosis than luminal A tumours	Endocrine therapy; Chemotherapy
	ER-positive HER2-positive Any Ki-67 and PR			Endocrine therapy; Chemotherapy; Anti-HER2 therapy
HER2-positive	ER-negative PR-negative HER2-positive	5-15%	High grade, LN involvement, intermediate prognosis between luminal and TNBC	Chemotherapy; Anti-HER2 therapy
TNBC/ Basal-like	ER-negative PR-negative HER2-negative CK5/6-positive EGFR-positive	15-20%	Aggressive, high grade, high rate of early relapse, worst prognosis among all subtypes	Chemotherapy

[a]According to the 2013 St Gallen Consensus Conference and ESMO Clinical Practice Guidelines 2015 (Goldhirsch et al., 2013; Senkus et al., 2015)

[b]According to the Susan G. Komen organization (Susan G. Komen, 2015)

Abbreviations: CK, cytokeratins; EGFR, epidermal growth factor receptor; ER, estrogen receptor; HER2, human epidermal growth factor receptor 2; LN, lymph node; LVI, lymphovascular invasion; PR, progesterone receptor; TNBC, triple-negative breast cancer.

ER-positive/luminal breast cancers are the most numerous and heterogeneous in terms of genetic characteristics, molecular features, and patient outcomes (Cancer Genome Atlas Network, 2012; Ignatiadis and Sotiriou, 2013). Luminal A tumours are characterized by the high expression of estrogen-related genes and low expression of proliferation-related genes (Table 1) (Goldhirsch et al., 2013; Ignatiadis and Sotiriou, 2013).

Conversely, luminal B tumours usually present low expression of estrogen-related genes, high expression of proliferation-related genes, low or no PR expression, possible overexpression and/or amplification of *HER2*, and high tumour grade (Goldhirsch et al., 2013; Ignatiadis and Sotiriou, 2013). In luminal A cancers, the most frequent mutated gene is *PIK3CA* (45%), followed by *GATA3* (14%), *MAP3K1* (13%), *TP53* (12%), *CDH1* (9%), *MLL3* (8%), *MAP2K4* (7%), *NCOR1* (5%) and *RUNX1* (5%), while luminal B tumours have a lower frequency of *PIK3CA* mutations (29%) and a higher frequency of *GATA3* (15%) and *TP53* (29%) mutations (Table 2) (Cancer Genome Atlas Network, 2012; Santarpia et al., 2016). Another striking feature of ER-positive/luminal subtype is the association with few common copy number alterations (CNA), even though luminal A and luminal B are unique entities also regarding the CNA profile (Table 2) (Santarpia et al., 2016). Clinically, luminal A breast cancer is generally associated with a favourable outcome, while luminal B tumours are characterized by an aggressive clinical behaviour and poor prognosis (Goldhirsch et al., 2013). Adjuvant endocrine therapy with ER antagonists such as tamoxifen or aromatase inhibitors, including anastrozole, exemestane and letrozole, is the mainstay of treatment for ER-positive/luminal breast cancer. However, the risk of relapse extends for at least 20 years in women with ER-positive tumours despite adjuvant endocrine treatment (Ignatiadis and Sotiriou, 2013). Thus, in specific settings, including high histological grade, high Ki-67, low hormone receptor status, HER2 positivity, and the involvement of more than three lymph nodes, the addition of cytotoxic chemotherapy to standard endocrine treatment is recommended (Goldhirsch et al., 2013; Senkus et al., 2015).

Table 2. Most common gene mutations and copy number alterations in different molecular subtypes of primary breast cancer

	Luminal A	Luminal B	HER2-positive	Triple-negative
Gene mutations	*PIK3CA*, *GATA3*, *MAP3K1*, *TP53*, *CDH1*, *MLL3*, *MAP2K4*, *AKT1*, *FOXA1*, *CDH1* and *RUNX1*	*PIK3CA*, *GATA3*, and *TP53*	*PIK3CA*, and *TP53*	*TP53*, and *PIK3CA*
Gene gains, losses and amplifications	-	loss of ATM; amplification of *CCND1*, *CDK4*, *CDK6*, and *MDM2*	amplification of multiple genes based on the *HER2* amplicon size	loss of *INPP4B*, *PTEN*, and *RB1*; amplification of *BRAF*, *CCNE1*, *EGFR*, and *KRAS*
Copy number alterations				
Gains	1q and 16p	1q, 8q, 17q, and 20q	1p36.33-p36.32, 4q13.3, 5p15-p12, 8q23.3-q24.21, 11q13.5-q14.1, 14q11.1-q11.2, 17q23-q24, and 19q12	1q12-q41, 3q, 6p12-p25, 7p12, 7q22-q36, 8q23.2-24.3, 10p12-p15, 12p, 17q25, and 21q22
Losses	16q	1p, 3q, 8p, 13q, 16q, 17p, and 22q	1p39, 1p36, 1p35, 1p32, 4p16.3, 7q21-q22, 7p22.3, 7q34, 7q36.1-q36.3, 8p23.3-p23.2, 8p11.23-p11.22, 9p21.3, 9q34.3, 10q26.3, 11q13.5, 11p15.5, 14q32.33, 15q11.2, 16p13.3, and 19p13.3	3p, 3q12, 4p15-p32, 4q31-q35, 5q11-q31, 8p, 12q14-23, 13q, 14q22-q23, and 15q
Amplifications	8p11-12, 8q , 11q13-14, 12q13-14, 17q11-12, 17q21-24, and 20q13	7p22, 8p11-12, 8q11-24, 11q13-14, 17q23, 19q13, and 20q13	4q13.3, 8q23.3-q24.21, 11q13.5-q14.1, 14q11.1-q11.2, 17q12-q21, and 19q12	-

HER2-positive breast cancers are characterized by the overexpression and/or amplification of *HER2*, which is an oncogene coding for a tyrosine kinase receptor that activates critical signalling pathways resulting in an aggressive tumour phenotype and poor outcome (Prat et al., 2014). Even though the HER2 positivity determined by immunohistochemistry (IHC) and/or fluorescence in situ hybridization (FISH) largely overlaps with the HER2-enriched intrinsic subtype, HER2 amplification occurs in all four subtypes with varying frequencies, indicating the presence of biological and molecular heterogeneity within this breast cancer subgroup (Prat et al., 2014). The complex scenario of HER2-positive disease was confirmed by its somatic mutation landscape (Table 2). A source of genomic heterogeneity within HER2-positive tumours is dependent on the size of the HER2 amplicon. Beyond the core of the amplicon, which includes at least *HER2-C17orf37-GRB7* genes, co-amplifications of *GSDML*, *NEUROD2*, *PERLD1*, *PNMT*, *PPP1R1B*, *PSMD3*, *STARD3*, *TCAP*, *THRAP4* and *TOP2A* genes have been described (Santarpia et al., 2016). In addition to the common amplification at 17q12 (containing the *HER2* oncogene), other recurrent CNA and gene mutations, particularly *TP53* (72%) and *PIK3CA* (39%), have been reported in HER2-positive cancers (Table 2) (Cancer Genome Atlas Network, 2012; Santarpia et al., 2016). Fortunately, the HER2 positivity is associated with a high benefit from anti-HER2 therapies (*e.g.,* trastuzumab and lapatinib) in combination with chemotherapy (Goldhirsch et al., 2013; Senkus et al., 2015).

1.1.2 Triple-negative breast cancer

Triple-negative breast cancer (TNBC) is generally more aggressive, with a higher rate of early relapse and poorer overall survival compared with the other breast cancer subtypes (Dawson et al., 2009). Molecularly, this cohort of cancers exhibits high levels of genomic instability and shows the highest frequency of *TP53* mutations (80%). Among all other alterations, *PIK3CA* (9%), *MLL3* (5%), and *GATA3* (2%) mutations, *RB1* mutations and/or deletions (20%), and *CCNE1* amplifications (9%) occur at a relatively low frequency

(Table 2) (Cancer Genome Atlas Network, 2012; Santarpia et al., 2016). Despite the low proportion of *PIK3CA* mutations, the associated pathway shows a quite high activity, likely due to the loss of *PTEN* (35%) and *INPP4B* (30%) (Cancer Genome Atlas Network, 2012; Santarpia et al., 2016). The pattern of CNA in TNBC includes a relatively large number of losses and gains (Table 2). In particular, 5q deletions have been associated with the high expression of several genes involved in cell cycle checkpoints, DNA damage repair and apoptosis signalling (Santarpia et al., 2016).

Clinically, the vast majority of TNBC are high-grade invasive ductal carcinomas that are characterized by atypical and pleomorphic neoplastic cells, high mitotic rates, areas of central necrosis, stromal lymphocytic infiltrate, and pushing borders (Metzger-Filho et al., 2012). In contrast to hormone receptor-positive breast cancer, TNBC patients have an early peak of relapse within the first three years after diagnosis, and an increased likelihood of visceral metastases and death within five years of follow-up (Metzger-Filho et al., 2012). These characteristics and the lack of therapeutic targets represent an important clinical challenge. In fact, conventional chemotherapy containing anthracyclines and taxanes remains the only treatment option with effect, even though the long-term results are not satisfactory (Metzger-Filho et al., 2012). Although numerous efforts have been made to identify novel targets in TNBC, the molecular and clinical heterogeneity of this disease has led to limited success.

Following the identification of intrinsic subtypes, triple-negative tumours have been often classified as basal-like cancers due to their extensive overlap (approximately 70-80%) (Lehmann and Pietenpol, 2014). However, a number of studies have subsequently attempted to further decipher the heterogeneity within TNBC. An additional intrinsic subtype, known as claudin-low, representing approximately 30% of TNBC, has been defined as a poor prognosis group of tumours, which is enriched for features linked to cancer stem cells (CSC) and epithelial to mesenchymal transition (EMT) (Prat and Perou, 2011). Then, six molecular subtypes of TNBC have been described, including basal-like 1

(BL1), basal-like 2 (BL2), immunomodulatory (IM), luminal androgen receptor (AR)-like (LAR), mesenchymal (M), and mesenchymal stem cell-like (MSL) (Figure 2A) (Lehmann et al., 2011). BL1, BL2, IM, and M subgroups are mainly composed of the basal-like intrinsic subtype, while MSL and LAR comprises a consistent proportion of luminal B, and luminal B and HER2-positive tumours , respectively (Figure 2A) (Lehmann et al., 2011). The BL1 cancers are enriched for cell division-related genes and for the expression of genes involved in the DNA damage response (ATR/BRCA) pathways (Figure 2B). Conversely, the BL2 subtype is characterized by the expression of myoepithelial markers and of genes associated with growth factor signalling (*e.g.,* epidermal growth factor [EGF] pathway, nerve growth factor [NGF] pathway, WNT/β-catenin, and insulin-like growth factor 1 receptor [IGF1R] pathway), glycolysis and gluconeogenesis (Figure 2B). The IM subtype is enriched for genes regulating immune cell processes, including immune cell signalling (*e.g.,* B lymphocytes, T lymphocytes, and natural killer [NK] cells), cytokine signalling, and antigen processing and presentation (Figure 2B) (Le Du et al., 2015; Lehmann and Pietenpol, 2014). It is still unclear whether this signature truly reflects the features of tumour cells or is a consequence of lymphocytic infiltration. Thus, it is plausible that the IM subtype includes cancers that biologically are basal-like and mesenchymal-like tumours heavily infiltrated by lymphocytes (Turner and Reis-Filho, 2013). The LAR subtype displays luminal patterns and is consistently enriched for genes involved in steroid synthesis and androgen/estrogen metabolism (Figure 2B). Both the M and MSL subtypes, which represent the vast majority of claudin-low tumours, are characterized by gene expression patterns associated with extracellular matrix, cell differentiation and motility pathways, and EMT (Figure 2B). Interestingly, the MSL subtype diverges from M tumours as it expresses low levels of proliferation genes and is enriched for the expression of genes associated with a CSC phenotype (Figure 2B) (Lehmann and Pietenpol, 2014).

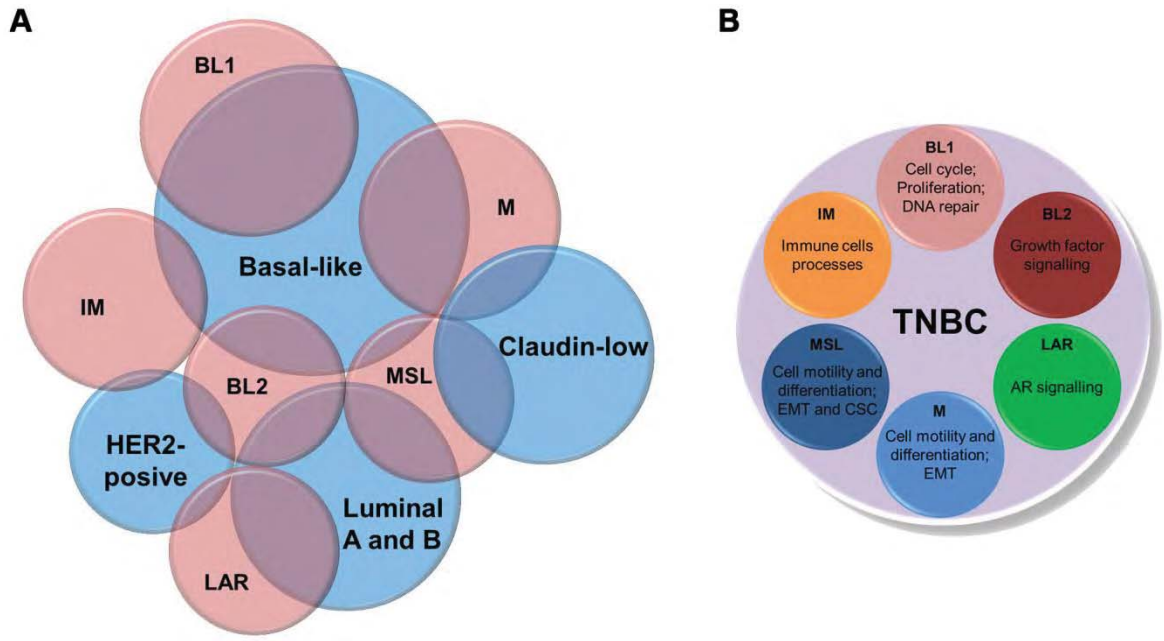

Figure 2. Classification of triple-negative breast cancer. A) Intrinsic subtypes (light blue) (Prat and Perou, 2011) and Lehmann's classification (pink) (Lehmann et al., 2011), and their potential overlaps. B) Lehmann's TNBC subtypes are molecularly different and are characterized by distinct sets of genes and pathways.

1.1.3 Therapies for triple-negative breast cancer

Due to the lack of specific molecular targets, cytotoxic chemotherapy remains the mainstay of systemic therapy for TNBC, and therefore adjuvant anthracycline-taxane-based chemotherapy is recommended for patients with stage I-III disease (Le Du et al., 2015). Even though patients with TNBC are initially more responsive to chemotherapy than patients with other breast cancer subtypes, a substantial proportion of patients with early-stage TNBC (30-40%) develop distant metastasis and die of cancer (Le Du et al., 2015; Metzger-Filho et al., 2012).

The recognition of the heterogeneity of TNBC by molecular classification has begun to reshape research directions. Firstly, different TNBC subtypes have been demonstrated to have distinct response to neoadjuvant anthracycline-taxane-based chemotherapy (Carey et al., 2007; Masuda et al., 2013; Rouzier et al., 2005). These findings, following extensive retrospective and prospective validations in large cohorts of patients, may have the potential to guide differential use of chemotherapy-containing

regimens based on molecular classification. Furthermore, the increased understanding of TNBC biology will reveal new therapeutic targets and may help to refine the selection of patients in novel biology-oriented clinical trials. For instance, targeting DNA-repair deficiency appears to be a promising strategy for triple-negative/basal-like cancers, which have the highest pathologic complete response (pCR) rates following neoadjuvant chemotherapy (Carey et al., 2007; Rouzier et al., 2005). In particular, patients with BL1 tumours displaying *BRCAness* characteristics – traits that cancers share with *BRCA1*-mutated tumours – could be entered into clinical trials investigating platinum agents or poly(ADP-ribose) polymerase (PARP) inhibitors (Le Du et al., 2015; Masuda et al., 2013). Conversely, patients with BL2 cancers, which have the lowest pCR rate among TNBC subtypes, may benefit from the inhibition of growth factor/receptor tyrosine kinase (RTK) pathways like mesenchymal-like cancers (Le Du et al., 2015; Masuda et al., 2013). Mesenchymal-like cancers (M and MSL), which harbour features associated with metastatic potential and are associated with the worst prognosis among the other TNBC subtypes, likely due to the development of resistance to chemotherapy, could be eligible for treatment with EMT- and CSC-targeted therapies (*e.g.,* hedgehog and notch inhibitors) that are under investigation in early stage clinical trials (Le Du et al., 2015). Furthermore, these tumours have demonstrated an exquisite sensitivity to ABL/SRC and phosphatidylinositol 3-kinase (PI3K)/ mammalian target of rapamycin (mTOR) inhibitors (Lehmann and Pietenpol, 2014).

Immune-based therapies can be effective for patients with TNBC of the IM subgroup. Noteworthy, the claudin-low subset of TNBC tumours is characterized not only by the presence of EMT and CSC-like features, but also by the high expression of immune genes and by an intense immune cell infiltrate, making this subgroup a potential candidate for selective immunotherapy (Le Du et al., 2015; Lehmann and Pietenpol, 2014). Finally, as the AR can replace the ER as a major component of steroid-related signalling in the LAR subtype, AR inhibitors or histone deacetylase inhibitors that regulate AR target genes

may provide an attractive therapeutic opportunity for this TNBC subset of tumours (Le Du et al., 2015).

Even though the future success of clinical trials in patients with TNBC will likely benefit from the stratification of their tumours by molecular subgroups or genomic alterations, the multiplication of subtypes could yield to an excessive splitting that can be deleterious for the design of powerful studies with sufficient number of patients. So far, triple-negative/basal-like breast cancers are still considered as a unique entity in clinical trials.

1.2 Hallmarks of breast cancer

The development of clinical breast cancer is a multistep process, which involves the acquisition of multiple molecular alterations and the evolution of cellular populations with malignant phenotypes. Cancer progression may occur over long periods of time and can vary depending on the tumour genetic background and other intrinsic features. The classic model of breast cancer development is a linear, non-obligatory and multistage progression from atypical hyperplasia to ductal carcinoma *in situ* (DCIS), eventually followed by the evolution to invasive breast cancer (IBC) and metastatic disease (Rivenbark et al., 2013). DCIS is the first step in the neoplastic progression of breast cancer and harbours many of the same molecular abnormalities that invasive cancers have. Despite being by definition non-invasive, DCIS has the potential for further progress to invasive cancer (Rivenbark et al., 2013).

For the progression through each step, cells are expected to acquire new oncogenic abilities that provide a selective growth advantage, including sustaining proliferative signals, evading growth suppressors, resisting cell death, inducing angiogenesis, enabling replicative immortality, triggering metastatic dissemination, deregulating cellular energetics, and avoiding immune responses (Figure 3) (Hanahan and Weinberg, 2011). The acquisition of these eight hallmarks of cancer is enabled by genomic instability and cancer-

related immune responses, and broadly depends on the interactions between cancer cells and the tumour immune microenvironment (Figure 3) (Hanahan and Weinberg, 2011). Distinct breast cancer subtypes clearly differ in the hallmarks and pathways affecting their specific molecular and clinical features. In particular, three major tumour-associated properties – genomic instability, EMT and cancer-related immune responses – comprehensively characterize TNBC and are distinctive of different TNBC subtypes (Figure 4).

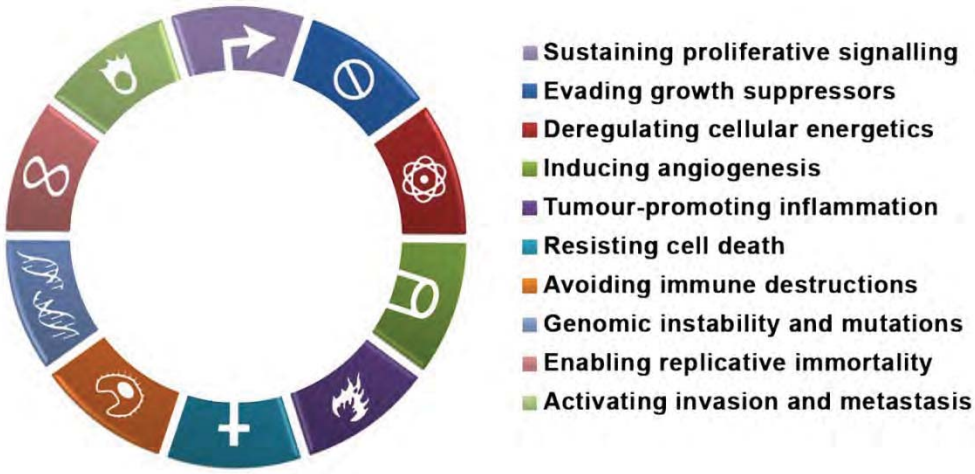

Figure 3. The hallmarks of cancer. The eight major hallmarks of cancer and the two enabling characteristics – genomic instability and tumour-promoting inflammation – reported by Hanahan and Weinberg describe the crucial oncogenic properties acquired during the multistep development of human cancers (Hanahan and Weinberg, 2011).

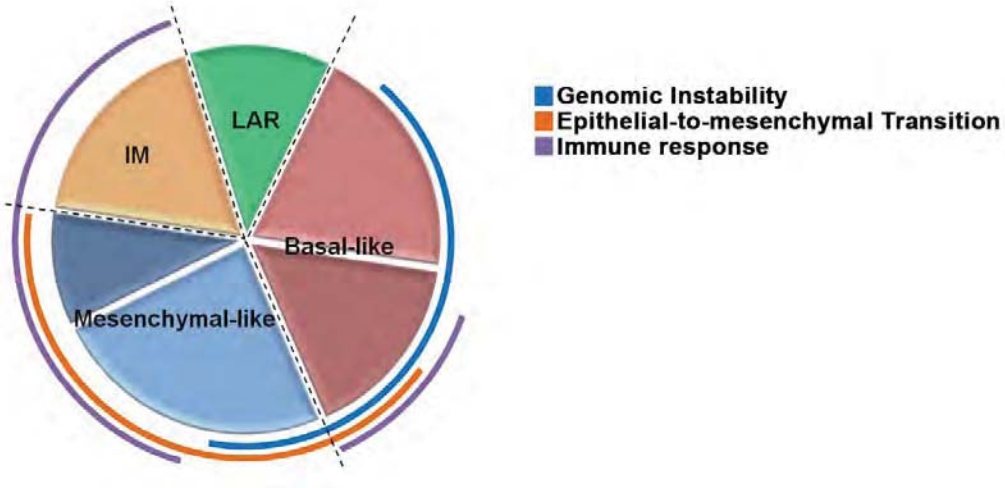

Figure 4. Hallmarks of triple-negative breast cancers. The three major hallmarks that best characterize TNBC.

1.2.1 Genomic instability

Genomic instability is a characteristic common to the majority of human cancers. The disruption of the mechanisms that maintain genome integrity increases the rate of genomic scars, causing genetic heterogeneity during cancer evolution and tumour aggressiveness, thus providing a biological fitness advantage to tumour cells (Burrell et al., 2013; Negrini et al., 2010). Among the different types of genomic instability, most cancers show chromosomal instability (CIN), which refers to an increased rate of change in chromosome number or structure, resulting in whole-chromosome and segmental aneuploidies as well as translocations, inversions, and deletions (Burrell et al., 2013). CIN can arise through a range of mechanisms, including mitotic defects, proliferation of mesenchymal-like cells, and defective DNA repair pathways (Burrell et al., 2013; Comaills et al., 2016). For instance, mutations in *BRCA1*, *BRCA2*, and *TP53* genes result in aberrant DNA damage response (Burrell et al., 2013; Turner et al., 2004). Importantly, a higher frequency of CNA and *TP53* mutations have been observed in triple-negative/basal-like tumours compared with other breast cancer subtypes, suggesting extensive genomic instability in this group (Cancer Genome Atlas Network, 2012; Turner and Reis-Filho, 2013). Furthermore, inherited *BRCA1*-mutated breast cancers share several characteristics with sporadic TNBC such as *BRCAness* traits (Santarpia et al., 2013; Turner et al., 2004). Accordingly, familial *BRCA1*-mutated tumours segregate strongly with sporadic basal-type cancers, are of a high mitotic count, commonly show lymphocytic infiltration, and are more likely to have pushing margins (Rakha et al., 2008; Turner et al., 2004). Moreover, triple-negative/basal-like cancers, especially tumours of the BL1 subtype, are heavily enriched for genes involved in the DNA damage response (Lehmann and Pietenpol, 2014; Santarpia et al., 2013). Even though TNBC globally displays the most instable genome, it is worth noting that CIN is not a feature common to all TNBC. Indeed, a combined analysis of CNA and gene expression revealed that the vast majority of TNBC (~ 59%), identified as integrative cluster (IC) 10 and representing the core basal subgroup, show an intermediate level of

CIN, a high rate of *TP53* mutations, and a gene expression profile associated with cell-cycle, DNA damage repair, and apoptosis (Curtis et al., 2012; Dawson et al., 2013). Conversely, the IC4, which includes 25% of TNBC, displays a reduced level of genomic instability and massive lymphocytic infiltration (Curtis et al., 2012; Dawson et al., 2013).

Beside its role in affecting tumour biology and driving tumour evolution, genomic instability has important implications for the clinical management of breast cancer patients. Several gene expression surrogates and DNA-based measures of genomic instability have been evaluated as predictors of clinical outcome and response to chemotherapy in TNBC (Carter et al., 2006; Habermann et al., 2009; Mulligan et al., 2014; Pitroda et al., 2017; Telli et al., 2016; Vollan et al., 2015). Overall, genomically unstable tumours have a poorer outcome compared with stable tumours. Accordingly, the CIN70 gene expression signature, which is highly associated with aneuploidy and genomic instability quantified by DNA image cytometry, is predictive of poor prognosis in breast cancer (Carter et al., 2006; Swanton et al., 2009). Interestingly, two distinct measurements of CIN – the CIN70 signature and the dual centromeric FISH assay – demonstrated a non-monotonic relationship between genomic instability and survival outcome in TNBC (Birkbak et al., 2011; Jamal-Hanjani et al., 2015; Roylance et al., 2011). TNBC with an extreme CIN were associated with improved long-term prognosis relative to tumours with intermediate CIN. This paradoxical relationship could be explained by the negative impact of intolerable CIN on cellular fitness. Conceivably, the favourable outcome of TNBC with extreme CIN could also be due to the increased sensitivity to chemotherapy regimens containing DNA damaging agents. Consistently, high levels of genomic instability have been shown to predict sensitivity to anthracycline- and platinum-based chemotherapy (Ignatiadis et al., 2012; Mulligan et al., 2014; Pitroda et al., 2017; Telli et al., 2016). Thus, the intrinsic genomic instability of a subset of TNBC, which positively affects tumour evolution and correlates with tumour aggressiveness at baseline and poor outcome, may also determine the success of specific chemotherapy regimens.

1.2.2 Epithelial-to-mesenchymal transition

EMT is a fundamental step in several physiologic processes such as morphogenesis and wound healing and has been demonstrated to be closely associated with cancer progression (De Craene and Berx, 2013). During EMT, cells lose their epithelial characteristics to gain mesenchymal features and acquire multiple traits that, in combination with genetic aberrations and appropriate signals at the tumour site, enable invasion and metastatic dissemination (De Craene and Berx, 2013). This complex, multistep, and reversible process is accompanied by the loss of cell cohesiveness, the reorganization of the cytoskeleton that induces a switch in cell polarity, and the increased expression of matrix-degrading enzymes, cell motility and resistance to senescence and apoptosis (Hanahan and Weinberg, 2011). In particular, cell surface proteins such as E-cadherin, integrins, or claudin are loss, while the expression of mesenchymal markers, including N-cadherin, fibronectin, or vimentin is enhanced (Mallini et al., 2014).

The entire EMT programme is tightly regulated by a network of signalling pathways and is also influenced by microenvironmental factors such as hypoxia and heterotypic interactions between cancer cells and adjacent stromal cells (Figure 5) (Hanahan and Weinberg, 2011). In particular, transforming growth factor-β (TGF-β), a cytokine produced by both tumour cells and a variety of cells in the tumour microenvironment, downregulates epithelial markers and increases the expression of mesenchymal markers through the SMAD-dependent activation of several EMT master regulators such as the components of SNAIL, TWIST, and ZEB families (Figure 5A) (Lamouille et al., 2014). Furthermore, TGF-β can activate and interact with multiple other oncogenic pathways, including Rho-like GTPases, PI3K/AKT/mTOR, mitogen-activated protein kinases (MAPK), and integrin signalling ultimately inducing cytoskeletal changes, the dissolution of cell junctions, and the acquisition of mesenchymal and invasive properties (Figure 5A) (Lamouille et al., 2014; Polyak and Weinberg, 2009).

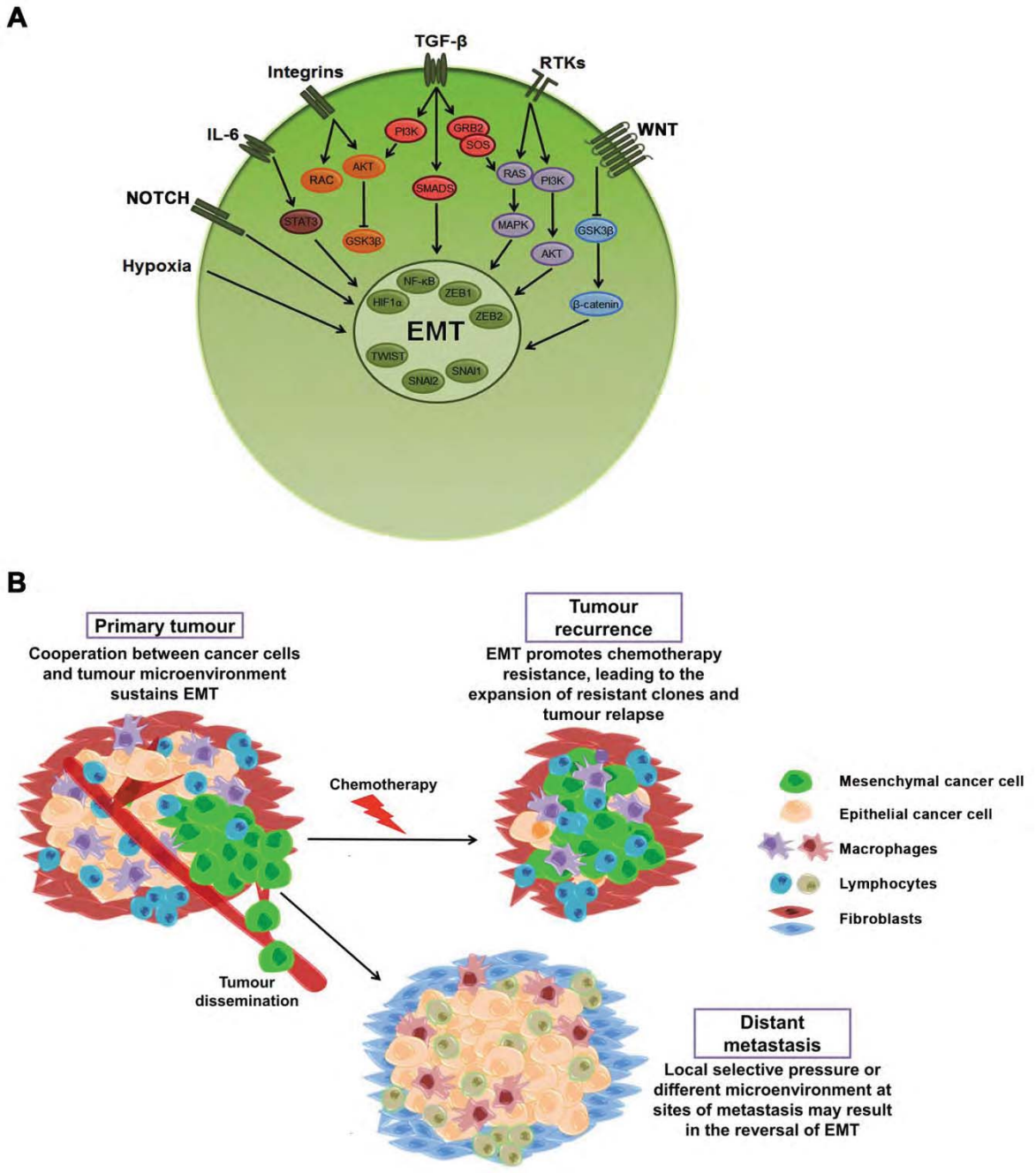

Figure 5. Epithelial-to-mesenchymal transition. A) A simplified overview of signalling networks that regulate EMT. B) In the primary tumour, the EMT process is broadly sustained by the interactions of cancer cells with cells of the tumour microenvironment, including cancer-associated fibroblasts, tumour-associated macrophages, and tumour infiltrating lymphocytes. Cancer cells with mesenchymal-like properties acquire the ability to disseminate to distant sites. Different local environments (represented by different colours of cells at the metastatic site compared with the primary tumour) may result in the reversal of EMT (MET process). EMT may also promote resistance to chemotherapy, leading to the expansion of resistant clones and tumour recurrence.

In addition, other signalling pathways, including interleukin [IL]-6, nuclear factor-κB (NF-κB), NOTCH, WNT/β-catenin, and several RTKs (*e.g.,* EGFR) are involved in the acquisition of a mesenchymal-like phenotype and cooperate to sustain the whole EMT process (Figure 5A) (Lamouille et al., 2014). Noteworthy, oncogenic mutations and genomic instability may also contribute to EMT. For instance, activating mutations in RTKs or oncogenes downstream of receptors can lead to an enhanced signalling along the RAS/MAPK or PI3K/AKT/mTOR axes, resulting in the upregulation of EMT master regulators (Zhang et al., 2013). Beside these cell-autonomous processes, the establishment of a permissive tumour microenvironment is crucial for supporting EMT. Indeed, a consistent enrichment of several immune targets such as immune checkpoints and cytokines has been recently found in multiple cancers that have undergone EMT, including breast cancer (Mak et al., 2016). Furthermore, inflammatory cells (*e.g.,* tumour-associated macrophages [TAM]) and several soluble mediators (*e.g.,* chemokine (C-C motif) ligand [CCL] 18, EGF, IL-1, IL-6, IL-8, TGF-β, and tumour necrosis factor [TNF]-α) have been identified as key inducers of EMT (Elinav et al., 2013).

As a result of EMT, epithelial cells can detach from the basal membrane, becoming more invasive and potentially entering the blood and lymphatic systems (Figure 5B). In addition to the mesenchymal switch, the EMT programme can endow cancer cells with stem-like properties, generating a tumour niche enriched for CSC, which are generally defined as CD44+CD24- cells with a high propensity to invade surrounding tissue and metastasize (Polyak and Weinberg, 2009). Interestingly, it is conceivable that local selective pressure for the outgrowth of more differentiated cancer cells or the absence of EMT-inducing signals at sites of metastasis may result in the reversal of EMT (mesenchymal-to-epithelial [MET] process) (Figure 5B) (Polyak and Weinberg, 2009).

EMT plays a central role in the control of invasion and progression of specific subtypes of breast cancer. The claudin-low subgroup, which includes a large proportion of M and MSL tumours, is characterized by the high expression of gene modules related to

EMT and CSC and a significant amount of different infiltrating leukocytes (Prat et al., 2010). Furthermore, CD44+CD24- stem-like cells are enriched in basal-like intrinsic subtype and the JAK2/STAT3 pathway, which is activated by EMT signals such as IL-6 and EGF, was found to be preferentially active in CD44+CD24- basal-like breast cancer cells (Marotta et al., 2011; Park et al., 2010). Even though these latter findings were generated without taking into account the distinction between basal-like and claudin-low subgroups, the possibility that EMT may be involved in the progression of a proportion of basal-like cancers cannot be ruled out.

Clinically, even though several single markers and gene signatures related to EMT and CSC have been associated with poor outcome of breast cancer patients, the prognostic value of EMT in breast cancer is still debated and need further validation (Bill and Christofori, 2015; Creighton et al., 2010; Foroutan et al., 2017; Liu et al., 2007; Mak et al., 2016; Polyak and Weinberg, 2009; Shipitsin et al., 2007; Tan et al., 2014; Taube et al., 2010). Conversely, EMT has been consistently associated with resistance to chemotherapy, resulting in the expansion of resistant clones and tumour recurrence (Figure 5B) (De Craene and Berx, 2013). Indeed, CD44+CD24- cells expressing EMT-associated genes have been found to be enriched in the residual tumours following anthracycline-taxane chemotherapy (Polyak and Weinberg, 2009). Furthermore, culture of epithelial tumour cells with stromal cells or in hypoxic conditions can lead to increased therapeutic resistance, potentially due to the ability of the tumour microenvironment to induce EMT (Jinushi et al., 2011; Polyak and Weinberg, 2009). Accordingly, several EMT-related gene expression signatures have been associated with a poor response to standard chemotherapy in breast cancer (Farmer et al., 2009; Tan et al., 2014; Taube et al., 2010).

1.2.3 Tumour-associated immune responses

The development and progression of a lesion toward a malignant phenotype partly rely on the interactions between cancer cells and the immune microenvironment. The tumour mass can be infiltrated by both innate and adaptive immune cells (Figure 6A) (Ruffell et al., 2012b). Historically, the presence of immune infiltrates at the tumour site has been related to the ability of the host defence to recognize and eliminate cancer cells (Hanahan and Weinberg, 2011). However, tumour-associated inflammation can also enhance tumourigenesis and cancer progression (Hanahan and Weinberg, 2011). Indeed, inflammation predisposes to various cancer types and tumours can develop at sites of chronic inflammation (Colotta et al., 2009). This tumour-promoting effect has been mainly ascribed to the innate immune system (Colotta et al., 2009; DeNardo et al., 2010; Qian and Pollard, 2010; Ruffell et al., 2012a). Under physiological conditions, innate immune cells, including macrophages, granulocytes, dendritic cells (DC), and NK cells protect the organism against foreign agents by secreting soluble mediators (*e.g.,* interferon [IFN]-γ and IL-1) that stimulate the recruitment of circulating leukocytes into damaged tissue (acute inflammation), and presenting foreign antigens to lymphocytes, which in turn mount specific "adaptive responses". Following the elimination of the foreign agents, inflammation resolves and tissue homeostasis is re-established (Figure 6B) (DeNardo and Coussens, 2007). In tumours, these balanced events fail to resolve, resulting in chronic inflammation of the neoplastic tissue. Chronically activated leukocytes can contribute to the acquisition of multiple hallmark abilities by supplying a variety of molecules to the tumour microenvironment such as growth and survival factors, proangiogenic molecules, extracellular matrix-modifying enzymes, and other signals that lead to the activation of EMT or to the induction of genetic instability (Figure 6B) (Colotta et al., 2009; Hanahan and Weinberg, 2011). Notable examples include CCL2, EGF, IL-4, IL-6, IL-10, IL-13, reactive oxygen species (ROS), TGF-β, and vascular endothelial growth factors (VEGF) (Colotta et al., 2009; Coussens et al., 2013).

Overall, the immune system specifically detects and targets foreign agents with adaptive immune cells. Lymphocytes are sustained by cells of the innate immunity, which are primarily involved in inflammation, wound healing and clearing dead cells and cellular debris. However, the general concept that innate immune cells have a tumour-promoting activity, while adaptive cells exert anti-tumour functions is oversimplified. Indeed, it is now well established that the tumour microenvironment is composed by different specialized classes of leukocytes with distinct functions.

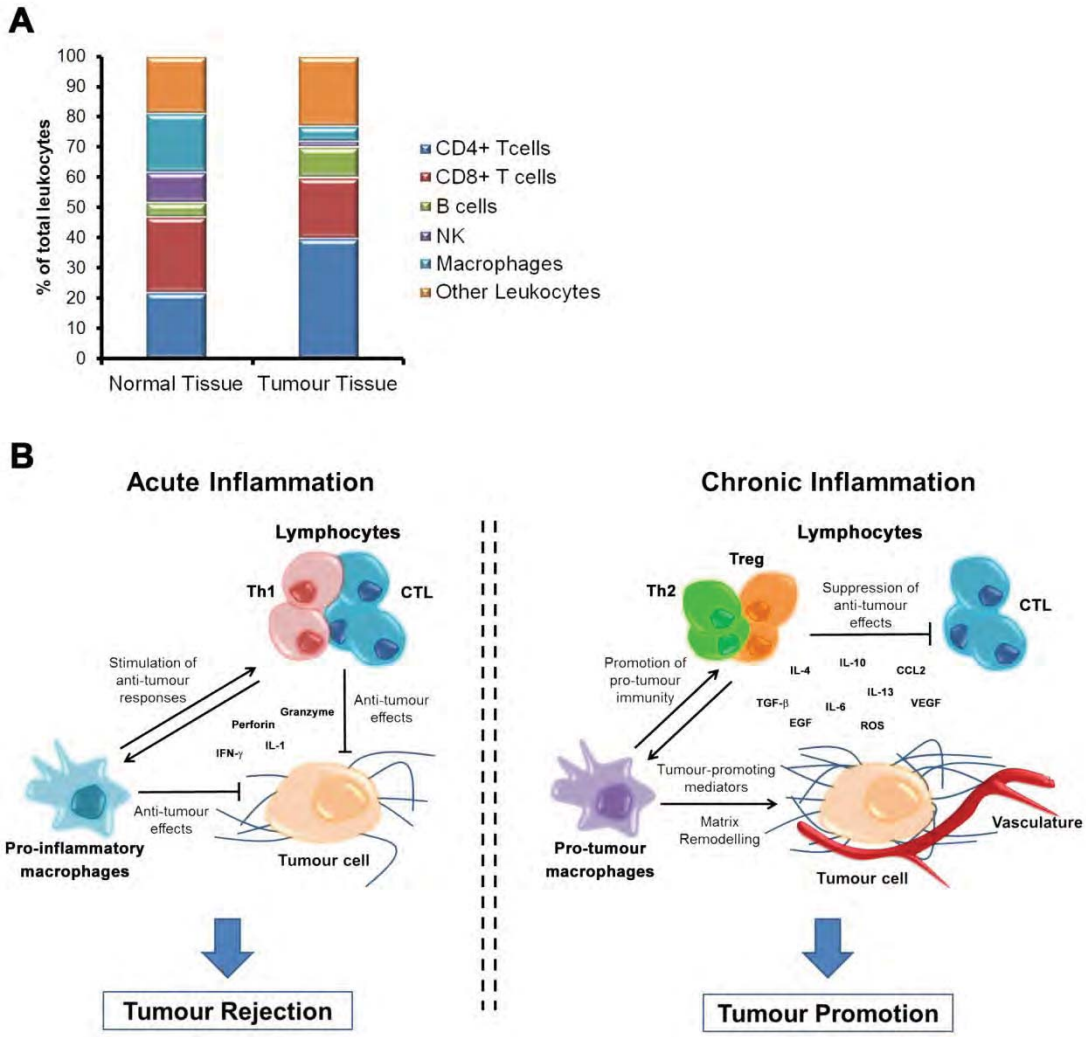

Figure 6. Immune infiltrates in breast tumours. A) Immune cell composition of adjacent normal and breast tumour tissues (Ruffell et al., 2012b). B) Contrasting roles of leukocytes during acute inflammation and cancer development. The presence of specialized classes of leukocytes with anti- and pro-tumour functions is represented by different colours of cells in the two scenarios. Abbreviations: CTL: cytotoxic lymphocytes; Th1: T helper 1 lymphocytes; Th2: T helper 2 lymphocytes; Treg: T regulatory lymphocytes.

1.3 The immune contexture of human breast cancer

1.3.1 Tumour-infiltrating lymphocytes

It is becoming increasingly evident that tumour-infiltrating lymphocytes (TIL) are able to control the clinical progression of epithelial cancers. T cells display broad diversity in terms of phenotype, function and tissue distribution. Breast tumours can be infiltrated by helper (Th; CD4+), cytotoxic (CD8+), and regulatory (Treg; FOXP3+) T lymphocytes. Cytotoxic CD8+ T lymphocytes (CTL) are recognized as the crucial component of the anti-tumour immune response. Effector CTL can interact with tumour antigen and promote the apoptotic death of the target cell by releasing cytokines such as interferon (IFN)-γ, TNF-α, granzyme, and perforin (Figure 7) (Andersen et al., 2006; DeNardo and Coussens, 2007; Martinez-Lostao et al., 2015). Also CD4+ cells can be activated by the encounter with the antigen. Depending on the intensity of stimulation and the presence of specific environmental signals, CD4+ cells can differentiate into two major subpopulations of T cells – Th1 and Th2 – with specific characteristics and functions (Figure 7) (Kim and Cantor, 2014). Th1 cells are induced in response to IL-12, and are characterized by the production of IL-2, IFN-γ, and TNF-α, which create a positive feedback loop reinforcing the Th1 polarization, collaborate with the functions of antigen-presenting cells (APC) and CTL, and influence the functions of the innate immune systems (Burkholder et al., 2014; Kim and Cantor, 2014). Conversely, Th2 cells are induced by IL-4 that antagonizes the Th1 polarization, and express IL-4, IL-5, IL-6, IL-10, and IL-13, which regulate innate immune responses, induce T-cell anergy and the loss of T-cell-mediated cytotoxicity, and modulate the B cell-dependent antibody production (Burkholder et al., 2014; Kim and Cantor, 2014). Overall, Th1 responses are supposed to be beneficial toward anti-tumour immunity, whereas Th2 responses are suggested to enhance pro-tumour responses (DeNardo and Coussens, 2007). In addition to Th1 and Th2 cells, several other subsets of CD4+ T cells have been involved in immune responses against tumour. In particular, Treg, which are controlled by the transcription factor FOXP3, differentiate in response to TGF-β

and generally suppress the function of other effector T cells and APC by cell-cell interactions and the release of TGF-β and IL-10 (Figure 7) (Burkholder et al., 2014; Kim and Cantor, 2014).

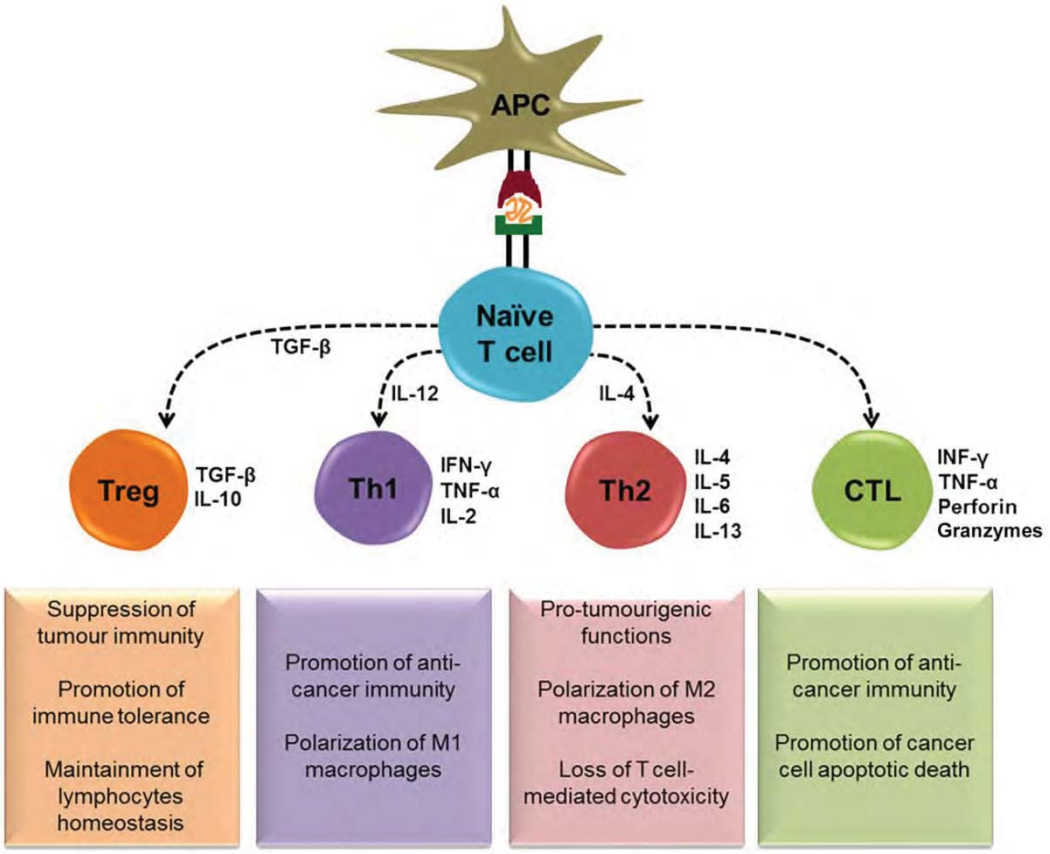

Figure 7. Different types of T lymphocytes in the breast tumour microenvironment. T helper subsets, Treg, and CTL differentiate from naïve lymphocytes (CD4+ and CD8+, respectively) following the encounter with the antigen and in the presence of specific environmental signals.

The presence of TIL in breast tumours has been associated with a favourable clinical outcome (Bottai et al., 2016a; Savas et al., 2016). Overall, TIL are more commonly found in triple-negative and HER2-positive breast cancers (Savas et al., 2016). Over the past few years, large prospective and retrospective studies have evaluated the prognostic and predictive value of TIL in breast cancer subtypes. Data from the Breast International Group (BIG) 02-98, Finland Herceptin (FinHER), National Epirubicin Adjuvant Trial (NEAT)/BR9601, Eastern Cooperative Oncology Group (ECOG) 2197, and ECOG 1199 trials demonstrated that patients with TNBC display a consistent linear relationship

between an increased number of TIL and improved outcome (Savas et al., 2016). A parallel association between TIL and outcome was reported for HER2-positive patients in the NeoALLTO study and in two French multicentric phase III trials (Dieci et al., 2015; Savas et al., 2016). These clinical findings have been explained by the high rates of cell proliferation and genomic instability of triple-negative and HER2-positive breast cancers. Indeed, the high CIN and mutational burden of these breast cancer subtypes have been suggested to potentially result in the generation of neoantigens, which can be recognized by TIL (Loi, 2013). However, breast cancer has not traditionally been considered as an immunogenic disease and the role of genomic instability in shaping the tumour immune response needs further investigations. The presence of TIL is also associated with better response to therapies (Savas et al., 2016). The analysis of TIL within the BIG 02-98, European Organisation for Research and Treatment of Cancer (EORTC) 10994/BIG 00-01, and in the Gepar series of trials revealed that the presence of lymphocytic infiltration is predictive of pCR following anthracycline-based chemotherapy, trastuzumab treatment, and the combined carboplatin-chemo-therapy in triple-negative and HER2-positive breast cancers (Savas et al., 2016).

Beside TIL overall, distinct immune cell subpopulations may have a specific biological significance. Indeed, cytotoxic CD8+ T cells have been shown to be an independent favourable prognostic factor and an immune gene signature enriched for CD8+ T cell-related genes has been associated with good prognosis in breast cancer, especially TNBC (Ali et al., 2014; Bottai et al., 2016a; Finak et al., 2008; Liu et al., 2012; Mahmoud et al., 2011). Although a tentative association between CD4+ or FOXP3+ T lymphocytes and poor prognosis has been suggested, the analysis of these TIL subsets has generated inconsistent results (Dushyanthen et al., 2015a).

In addition to the composition of the tumour immune microenvironment, other factors such as the localization and functionality of immune subpopulations may influence their biological actions. Noteworthy, the intraepithelial localization of CD8+ cells

mediated by integrins (*e.g.,* CD103) can influence their cytotoxic activity and impact tumour progression and clinical outcome (Djenidi et al., 2015; Le Floc'h et al., 2011; Webb et al., 2014). Furthermore, although TIL are able to identify and eliminate malignant cells, tumours have developed multiple mechanisms to maintain an immunosuppressive microenvironment (Topalian et al., 2015). During chronic inflammation or cancer, the prolonged exposure to antigen and other stimuli from the tumour microenvironment induce a state of T cell exhaustion, which is characterized by the inability of T cells to proliferate in the presence of the antigen, produce cytokines, and lyse target cells (Nguyen and Ohashi, 2015). T cell exhaustion is accompanied by the expression of various receptors that negatively regulate T cell function and reflect their functional status, including cytotoxic T lymphocyte-associated antigen 4 (CTLA-4), lymphocyte activation gene 3 protein (LAG-3), programmed cell death protein 1 (PD-1), and T cell immunoglobulin domain and mucin domain 3 (TIM-3) (Topalian et al., 2015). Many studies focused on the biological and clinical relevance of the PD-1/programmed cell death 1 ligand 1 (PD-L1) pathway. PD-1 is expressed only following activation on T cells, NK cells, B cells, and some myeloid cells to mediate the physiologic immune tolerance and balance immune response, attenuating T cell function, survival, and expansion (Nguyen and Ohashi, 2015). PD-1+ TIL were common in several types of cancer, including TNBC (Gatalica et al., 2014). PD-L1 is expressed on activated T cells, B cells, DC, macrophages, and on a wide range of cancer cells. In particular, PD-L1 protein has been reported to be expressed in nearly half of breast cancers, particularly TNBC and high-grade, proliferative tumours (Ghebeh et al., 2006; Schalper et al., 2014). The identification of these receptors has not only increased our understanding of the dynamics occurring within the tumour microenvironment, but has also revealed new treatment options for patients with breast cancer. Indeed, several clinical trials are currently evaluating the potential of immune checkpoints inhibitors for the treatment of breast cancer patients (Savas et al., 2016).

1.3.2 Tumour-associated macrophages

TAM are major players in the connection between inflammation and cancer, promoting cell proliferation, invasion, and metastatic spread, stimulating angiogenesis, regulating EMT, and inhibiting anti-tumour immune response mediated by T cell (Allavena et al., 2008; Mantovani et al., 2002; Williams et al., 2016). Mirroring the T helper differentiation, two distinct phenotypes of polarized macrophages have been reported (Figure 8). Microbial stimuli (*e.g.,* lipopolysaccharides [LPS]) and Th1 cytokines (*e.g.,* IFN-γ) polarize macrophages toward the M1 classically activated state, which is characterized by the release of inflammatory cytokines (*e.g.,* IL-12 and IL-23) and Th1 cell-attracting chemokines (*e.g.,* chemokine (C-X-C motif) ligand [CXCL] 9 and CXCL10), consequent activation of Th1 cells, and cytotoxic activity against neoplastic cells (Figure 8A) (Biswas and Mantovani, 2010). Conversely, the polarization toward an alternatively activated (M2) macrophage phenotype can be induced by CCL2, CXCL4, IL-4, IL-10, IL-13 and glucocorticoids (Figure 8) (Biswas and Mantovani, 2010). M2 macrophages show a high phagocytic activity, high expression of scavenging, mannose, and galactose receptors, low expression of IL-12, and high expression of CCL17, CCL18, CCL22, CCL24, IL-10, IL-1 decoy receptor, and IL-1 receptor antagonist (IL-1RA) (Biswas and Mantovani, 2010; Mantovani et al., 2002). Overall, these cells are involved in the Th2-mediated responses, diminish inflammation, have immunoregulatory functions, and promote tissue remodelling and tumour progression (Figure 8A).

Macrophage infiltrates have been associated with high grade, hormone receptor-negative tumours, basal-like subtype, and a poor clinical outcome in breast cancer (Bottai et al., 2016b; Campbell et al., 2011). Even though the contribution of different subsets of macrophages to the clinical progression of breast tumours has not been fully elucidated, the biological relevance of TAM can be explained by their ability to influence the balance between pro- and anti-tumour immunity and to closely interact with other components at the tumour site. Indeed, TAM, which generally resemble the M2 phenotype, help to

establish a permissive microenvironment capable of facilitating tumour invasion and migration through the promotion of angiogenesis, EMT, and the circumvention of anti-tumour immunity (Figure 8B) (Bottai et al., 2016b; Williams et al., 2016).

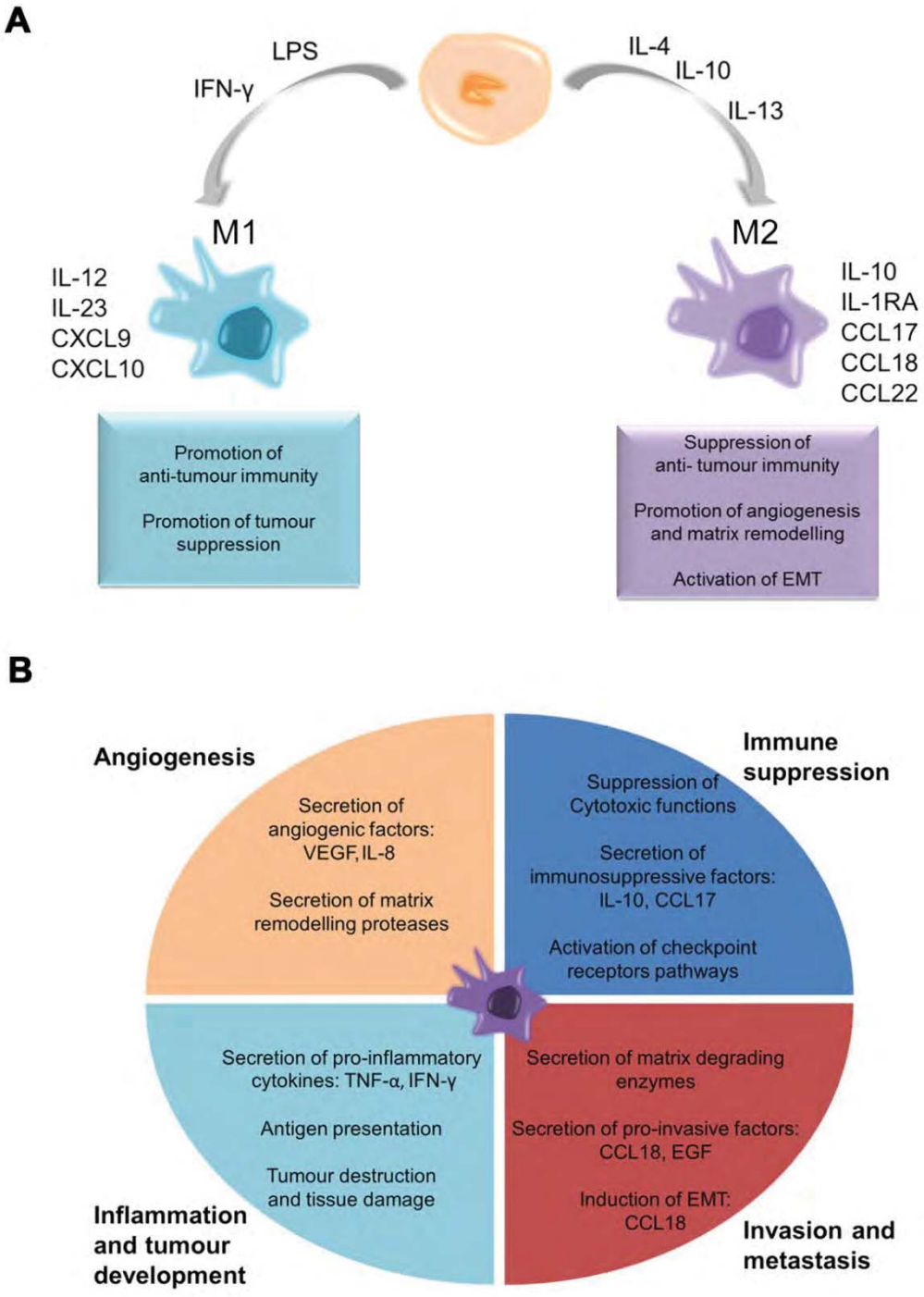

Figure 8. Polarization and functions of macrophages. A) When exposed to different cytokine milieu, monocytes differentiate into polarized macrophage subsets with distinct functions. B) The role of TAM in tumour development and progression.

In this regard, M2 macrophages are recognized as one of the major sources of the angiogenic, epithelial, and stromal growth factors, and also of matrix-remodelling enzymes that support neoplastic progression. Indeed, TAM secrete many pro-angiogenic signals, including CCL2, CXCL8, EGF, IL-1β, IL-8, matrix metalloproteinase (MMP)-9, platelet-derived growth factor (PDGF), TGF-β, TNF-α, and vascular endothelial growth factors VEGF, providing the vascular network required for cancer dissemination (Williams et al., 2016). Suppression of the anti-tumour immune response by TAM is also critical for disease progression. TAM-derived mediators such as CCL17, CCL22, IL-10, prostaglandin E_2 (PGE_2), and TGF-β contribute to the impairment of the cytotoxic function of effector T cells and NK cells and to the stimulation of Treg and Th2 responses (Biswas and Mantovani, 2010; Williams et al., 2016). Furthermore, the activation of PD-1 or CTLA-4, which are upregulated on activated T cells following the binding with their ligands (PD-L1/PD-L2 and CD80/CD86, respectively) expressed by TAM, results in T cell anergy, apoptosis, reduced cytotoxicity, and functional exhaustion (Williams et al., 2016).

Another important aspect that determines the ability of TAM to influence tumour progression is the direct interaction with malignant cells (Figure 9). Tumour cells provide multiple signals that modulate macrophages polarization and functions. Tumour-derived factors such as CCL2, CCL5, macrophage colony-stimulating factor 1 (CSF-1), granulocyte-macrophage colony-stimulating factor (GM-CSF), IL-6, IL-10, TGF-β, and TNF-α enhance the recruitment of monocytic precursors, promote an M2-like polarization, and drive the accumulation of TAM within the tumour mass (Mantovani et al., 2002). On the other hand, TAM promote tumour development and progression by providing factors that enhance the invasion of malignant cells. For instance, CSF-1 released by tumour cells stimulates macrophages to move and produce EGF, which in turn promotes the migration of tumour cells (Qian and Pollard, 2010). In human breast cancer, EGF is specifically expressed by macrophages, whereas the expression of CSF-1 is restricted to tumour cells and is associated with poor prognosis (Qian and Pollard, 2010). TAM also produce

CCL18, whose expression is associated with metastasis and reduced survival in breast cancer. CCL18 released by TAM induce EMT in breast cancer cells, promoting the invasiveness of cancer cells and breast cancer metastasis (Chen et al., 2011; Su et al., 2014a). In turn, mesenchymal-like breast cancer cells activate macrophages to a TAM-like phenotype by the release of GM-CSF, indicating the relevance of positive feedback loops between breast cancer cells and TAM (Su et al., 2014a). Moreover, TAM are a major source of other cytokines that are known mediators of cell migration and EMT, including osteonectin and TGF-β (Ostuni et al., 2015; Sangaletti et al., 2008; Williams et al., 2016). Due to their relevance in tumour progression, targeting tumourigenic factors and mechanisms promoted by TAM is emerging as a novel potential therapeutic strategy for aggressive cancer, including TNBC.

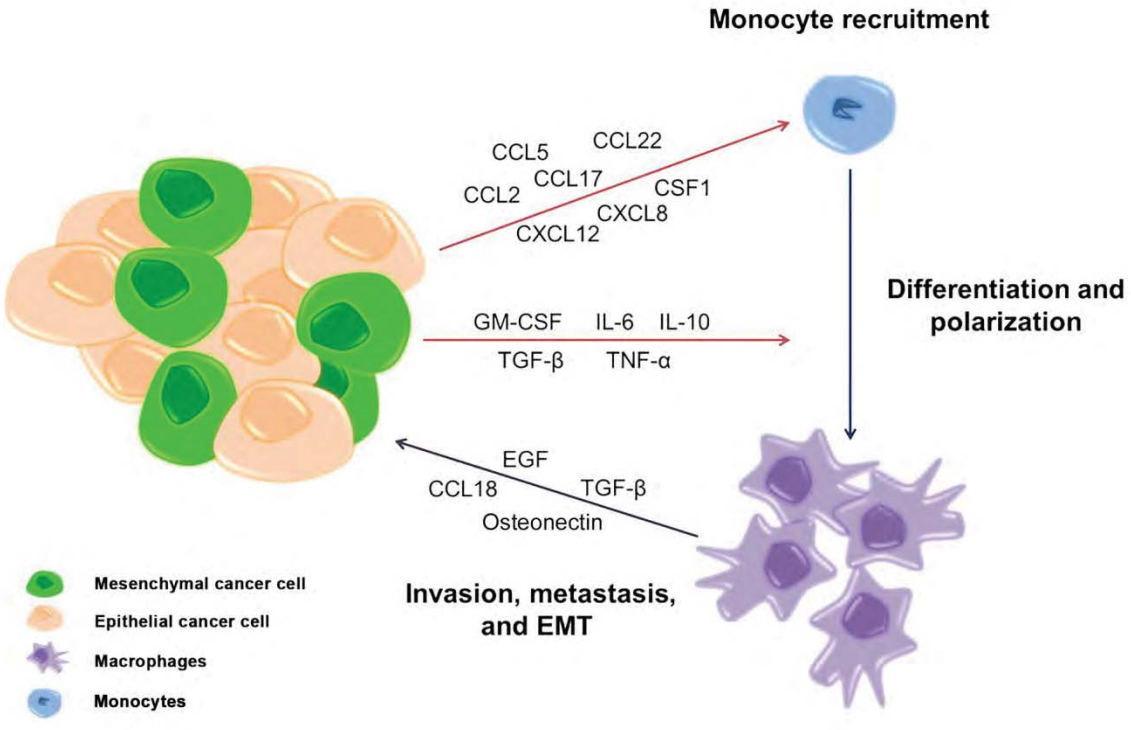

Figure 9. Cross-talk between tumour-associated macrophages and breast cancer cells. Tumour cells provide multiple signals that modulate macrophages polarization and functions. TAM promote tumour development and progression by providing factors that enhance invasion of malignant cells.

2. Aims

TNBC are usually characterized by an aggressive phenotype and associated with an increased risk of early distant recurrences and poor outcome. These characteristics and the lack of therapeutic targets represent an important clinical challenge. Indeed, conventional chemotherapy containing anthracyclines and taxanes remains the only treatment option with effect, even though the long-term results are not satisfactory. Numerous efforts have been made to identify novel targets in TNBC, but the molecular and clinical heterogeneity of this disease has led to limited success. In fact, TNBC encompass several subgroups characterized by distinct levels of chromosomal and genomic aberrations as well as different biological processes. In particular, the acquisition of hallmarks of cancer that allow tumour development and progression is enabled and sustained by genomic instability, EMT, and cancer-related immune responses, and broadly depend on the interactions between cancer cells and the tumour immune microenvironment.

Growing evidence suggests that infiltrating leukocytes are major determinants of the pathological and clinical behaviour of TNBC. In particular, the presence of TIL is now recognized as a consistent predictor of outcome and response to chemotherapy in TNBC. Noteworthy, the lymphocytic infiltrate is very heterogeneous, and a more detailed understanding of the tumour immune microenvironment is needed for the accurate selection of a proper immunomodulatory therapy. Furthermore, several lines of evidence indicate that the mutual interaction between cancer cells and TAM is a crucial bidirectional step supporting tumour aggressiveness, ultimately leading to cancer progression and metastatic spread. However, the biological and clinical role of specific macrophage subpopulations in TNBC as well as the relevance of this cross-talk are still poorly understood.

The aim of this study was to evaluate the relationship between these three major hallmarks of TNBC. In particular, we investigate the association of immune components

with TNBC molecular subtypes and different levels of CIN, to identify immunological characteristics of specific TNBC subsets that may be useful to direct treatment decision. We also assess the composition, localization, and functionality of specific immune cell subpopulations that may impact tumour progression and clinical outcome, and whose evaluation may help to identify TNBC patients eligible for immunomodulatory therapies. Furthermore, we aim to investigate the cross-talk between TNBC cells, particularly those with mesenchymal features, and TAM in order to clarify the potential mechanisms leading to tumour progression and resistance to chemotherapy, and to identify novel reliable prognostic markers and targetable signalling pathways, which may allow a better stratification of TNBC patients into different risk groups and the development of novel treatment strategies.

3. Materials and methods

3.1 Microarray data and gene expression normalization

Gene expression data from different publicly available cohorts of TNBC patients were retrieved from the National Center for Biotechnology Information's (NCBI) Gene Expression Omnibus (GEO; http://www.ncbi.nlm.nih.gov/geo) and the European Bioinformatics Institute's (EBI) ArrayExpress public repositories (https://www.ebi.ac.uk/arrayexpress). Only primary invasive TNBC and no metastases or local recurrences were included in this study. In addition, to avoid any effects of treatment on gene expression, patients untreated at the time of sample acquisition or treated with adjuvant chemotherapy were analysed separately. All gene expression data were generated with Affymetrix U133A and U133 Plus2 gene chips (Affymetrix; http://www.affymetrix.com). Raw intensity (CEL) files were processed in the R statistical environment using the affy Bioconductor package (http://www.bioconductor.org). Gene expression data were normalized using the Microarray Suite 5.0 (MAS5.0) algorithm (http://www.bioconductor.org), with the mean expression centred to 600 and log2 transformed, or the Robust Multi-array Average (RMA) algorithm. For genes targeted by multiple microarray probes, only the probe set with the highest Jetset score was selected (Li et al., 2011).

3.2 Subtype definition and molecular subtyping

To generate a homogeneous dataset the ER and HER2 status were determined for each patient using the probe sets 205225_at and 216836_s_at, respectively. Samples with normalized *ESR1* mRNA expression of greater than 10.18 were considered ER-positive cases, while those with HER2 mRNA expression of greater than 12.54 were considered HER2 amplified (Bianchini et al., 2010). To take into account the scaling factor existing between the U133A and U133 Plus2 platforms, normalized values of greater than 10.6 for

the probe set 205225_at were considered as ER-positive and values of greater than 13.04 for the probe set 216836_s_at were considered as HER2 positive for U133 Plus2 chips (Santarpia et al., 2013). The web-based algorithm TNBCtype (http://cbc.mc.vanderbilt.edu/tnbc) was used to classify TNBC molecular subtypes (Chen et al., 2012).

3.3 Construction of immune-related signatures

Based on a systematic literature review, we constructed ten comprehensive immune-related metagenes representing various cellular and signalling components of the tumour immune microenvironment: natural killer [NK], dendritic cells [DC], T cells [TC], B cells [BC], cytotoxic T cells [CT], interferon [IFN], nuclear factor-κB [NF-κB], macrophages [M], M1 macrophages [M1], and M2 macrophages [M2]. PubMed, Embase, and Web of Science databases were screened to identify published immune gene expression signatures related or unrelated to breast cancer. These immune metagenes were compared and filtered to exclude overlapping genes. Genes enclosed in published signatures capturing immune aspects that differed from those selected for this study were functionally annotated using the National Institutes of Health (NIH) DAVID database (https://david.ncifcrf.gov) and then specifically included in our metagenes (Huang da et al., 2009).

3.4 Analysis of the CIN70 signature

Affymetrix array data were pre-processed and normalized using the RMA algorithm in the R statistical environment with the Bioconductor affy package. CIN70 score for each sample was defined as the sum of the normalized expression of each gene enclosed in the signature in a given sample. CIN70 signature values were used as a surrogate marker of genomic instability and were dichotomized around the median to stratify patients according to their levels of CIN (Carter et al., 2006).

3.5 Patients' cohorts and tumour samples

Formalin-fixed, paraffin-embedded (FFPE) tissues were retrospectively collected from patients who underwent surgery at Humanitas Clinical and Research Institute (Rozzano – Milan, Italy) from 2006 to 2012. Additional TNBC specimens were collected from Humanitas Institutes (Rozzano, Catania, and Castellanza, Italy) and Semmelweis University Hospital (Budapest, Hungary). All patients had histologically confirmed invasive ductal TNBC and were treated with adjuvant anthracycline-based chemotherapy. ER, PR, and HER2 status were centrally assessed by IHC and/or FISH in nearly 90% of patients at Humanitas Clinical and Research Institute. The study was approved by the ethical committees of the Italian and Hungarian Institutions. The REporting of tumour MARKer Studies (REMARK) guidelines were followed in reporting results of this study (Altman et al., 2012).

3.6 Pathologic evaluation of tumour-infiltrating lymphocytes

Histopathologic analysis of stromal lymphocytic infiltration was performed on full face haematoxylin and eosin (HE)-stained sections according to Salgado et al (Salgado et al., 2015). Stromal TIL were defined as the percentage of tumour stroma containing infiltrating lymphocytes. Areas of adjacent normal breast, *in situ* carcinoma, necrosis, or fibrosis were not included in the evaluation.

3.7 Immunohistochemistry

FFPE sections (3 μm) from TNBC samples were deparaffinized with xylene, rehydrated with a graded ethanol series (100%, 95%, and 70%) to distilled water, according to standard immunohistochemical protocols. Specificity of staining was determined by IHC on a set of cultured cell pellet blocks, normal specimens, and diverse tumour tissues in the form of whole sections, processed using the same fixative and processing methods as TNBC samples tested in the study (Bordeaux et al., 2010; Vassilakopoulou et al., 2015).

Specificity was further determined by western blotting. The optimal concentration of each antibody was established performing serial titrations on serial FFPE sections. Antigen-retrieval conditions and detection methods were also optimized for each antibody to improve sensitivity and signal-to-noise ratio. Reproducibility of antibodies was assessed with IHC analysis of serial FFPE sections stained under the same conditions on different days (Vassilakopoulou et al., 2015).

Briefly, heat-induced antigen retrieval was performed by placing slides in Tris-EDTA (pH9), sodium citrate (pH6), or Diva (Biocare Medical) buffers using a water bath or a pressure cooker. Tissue sections were cooled in buffer for 20 min before the treatment with Peroxidase Blocking Reagent (Dako) for 10 min. Slides were then incubated with Background Sniper (Biocare Medical) for 20 min, and then with anti-AXL (1:100, R&D Systems), anti-CD4 (1:100, clone 4B12, Dako), anti-CD8 (1:100, clone C8/144B, Dako), anti-CD68 (1:200, clone KP1, Dako), anti-CD103 (1:500, clone EPR4166(2), Abcam), anti-CD163 (1:1000, clone 10D6, Novocastra), anti-E-cadherin (1:200, clone NCH-38, Dako), anti-FOXP3 (1:100, clone 236A/E7, Abcam), anti-LAG-3 (1:200, clone 17B4, LS Bio), and anti-PD-1 (1:100, clone NAT105, Abcam) primary antibodies. After washing with PBS, Envision systems (Dako), MACH 1 Universal HRP Polymer (Biocare Medical), or MACH4 Universal HRP Polymer (Biocare Medical), and diaminobenzidine (DAB; Biocare Medical) were used for chromogenic immunodetection, followed by counterstaining with haematoxylin. Negative control slides without primary antibody and positive controls for each marker were used for each immunostaining run. Full details on IHC protocols are provided in Table 3.

Table 3. Antibodies and immunostaining protocols

Antibody	Type	Clone	Source	Dilution	Positive controls	Antigen Retrieval	Detection system
AXL	Polyclonal	-	R&D Systems	1:100	Human liver	Citrate	MACH4
CD4	Monoclonal	4B12	Dako	1:100	Human tonsil	Tris-EDTA	Envision FLEX
CD8	Monoclonal	C8/144B	Dako	1:100	Human tonsil	Tris-EDTA	Envision FLEX
CD68	Monoclonal	KP1	Dako	1:200	Human tonsil	Tris-EDTA	MACH1
CD103	Monoclonal	EPR4166(2)	Abcam	1:500	Human colon	Tris-EDTA	MACH1
CD163	Monoclonal	10D6	Novocastra	1:1000	Placenta	Citrate	MACH4
E-cadherin	Monoclonal	NCH-38	Dako	1:200	Human colon	Tris-EDTA	Envision FLEX
FOXP3	Monoclonal	236A/E7	Abcam	1:200	Lymph node	Tris-EDTA	MACH1
LAG-3	Monoclonal	17B4	LS Bio	1:200	Lymph node	Citrate	MACH1
PD-1	Monoclonal	NAT105	Abcam	1:100	Lymph node	Diva buffer	MACH1

3.8 Evaluation of staining and scoring

Percentages of TIL were reported in increments of 10% (Adams et al., 2014; Loi et al., 2013). We defined the lymphocyte-predominant breast cancer (LPBC) as TNBC with ≥ 50% of infiltration of either tumour stroma or tumour nest (Adams et al., 2014; Loi et al., 2013). A binary cut-off ≥ 20% was also used to assess its potential to identify low-risk TNBC patients stratified by nodal status, as previously described (Loi et al., 2016).

IHC scoring was carried out as previously described (Balermpas et al., 2014; Bonde et al., 2012; Gjerdrum et al., 2010; Lee et al., 2008; Llosa et al., 2015; Medrek et al., 2012; Piras et al., 2005; Steidl et al., 2010; Taube et al., 2015). Briefly, each section was reviewed at low magnification. Positive lymphocytes in tumour stroma were counted in at least three high power fields (HPF; ×40; Olympus BX53, Olympus), which represent the spectrum of staining seen on the initial overview of the whole section, and displayed as average number of stained cells per HPF (Llosa et al., 2015). Patients were divided into two groups by the median value of CD4, CD8, and FOXP3 expression on TIL for statistical analyses. Cases where ≥ 5% of TIL expressed PD-1 or LAG-3 were considered positive (Taube et al., 2015). CD8 and CD103 markers were also evaluated as continuous variables and using different protein cut-offs. Briefly, patients with low and high density of immune infiltrates were defined using the 50^{th}- or 75^{th}-percentiles, and determining the optimal cut-off values by the X-tile software (http://medicine.yale.edu/lab/rimm/research/software.aspx) or receiver operating characteristic (ROC) analysis (Youden index). For each grouping scenario, we fitted Cox univariate and multivariate proportional hazards models to identify the cut-off that best stratified TNBC patients. Overall, the percentage of CD68+ and CD163+ cells in the whole tumour stroma was evaluated using a four-tiered system: 0 (no staining); 1 (few CD68+ or CD163+ macrophages for < 5%); 2 (moderate number of CD68+ or CD163+ macrophages for 5 – 25%); 3 (multiple CD68+ or CD163+ macrophages for ≥ 25%) (Balermpas et al., 2014; Bonde et al., 2012; Lee et al., 2008; Medrek et al., 2012; Piras et al., 2005; Steidl et

al., 2010). For statistical analyses, these categories were dichotomized into absent/moderate (0 – 2) or dense (3) macrophage infiltration. AXL staining was evaluated on whole sections and scored semi-quantitatively. Intensity was recorded as 0 (no staining), 1 (weak staining), 2 (moderate staining), or 3 (strong staining) and the proportion of positive tumour cells was defined as 0 < 1%; 1 = 1 – 9%; 2 = 10 – 49%; or 3 ≥ 50% (Gjerdrum et al., 2010). A composite staining index was calculated by multiplying the intensity by the percentage of positive cells and patients were stratified by low (0 – 4) or high (6 – 9) AXL expression for statistical analyses. The optimal cut-off point was determined by maximizing the sum of sensitivity and specificity. AXL expression was also evaluated as a continuous variable.

TIL and IHC were independently evaluated by two pathologists, who were blinded for patient characteristics and outcome. The mean value of the two assessments was used for the analyses. Agreement between the two pathologists was measured by calculating Cohen's kappa (κ) and the intraclass correlation coefficients (ICC). The inter-observer κ value for the categorical parameter LPBC was 0.63. The ICC for numerical variables were 0.74 for AXL, 0.82 for CD4, 0.84 for CD8, 0.63 for CD68, 0.80 for CD103, 0.69 for CD163, 0.76 for FOXP3, 0.78 for LAG-3, 0.79 for PD-1, and 0.79 for TIL

3.9 Multicolour immunofluorescence analysis and confocal microscopy

FFPE sections (3 μm) were deparaffinized in xylene and hydrated in graded alcohol. For CD103-PD-1 double immunofluorescence, after heat-induced antigen retrieval in Diva buffer (Biocare Medical), the samples were blocked with PBS containing 2% bovine serum albumin (BSA) and 2% goat serum. For AXL-CD163 double staining, samples were subjected to epitope retrieval using sodium citrate buffer and then blocked with PBS containing 2% BSA and 2% donkey serum. Sections were then incubated with anti-AXL (1:100, R&D Systems), anti-CD163 (1:500, clone 10D6, Novocastra), anti-CD103 (1:1500, clone EPR4166(2), Abcam), and anti-PD-1 (1:100, clone NAT105, Abcam)

primary antibodies for 1 hr at room temperature. Slides were then incubated with goat anti-mouse Alexa 594-conjugated, goat anti-rabbit Alexa-488-conjugated, donkey anti-goat Alexa 488-conjugated, and donkey anti-mouse Alexa-647-conjugated antibodies (Thermo Fisher Scientific). Slides were counterstained with DAPI, mounted with ProLong Gold (Thermo Fisher Scientific), and stored in the dark at 4 °C. Images were captured using an Olympus Fluoview FV1000 laser scanning confocal microscope (Olympus).

3.10 Expression analysis by quantitative reverse transcription PCR

We conducted a review of the literature using PubMed, Web of Science, and Embase databases from 2000 to 2016 using the search terms “breast cancer”, “epithelial-to-mesenchymal transition”, and “kinases”. Additional studies were identified through the references listed in review publications. Based on this comprehensive literature review, we selected the 30 most functionally relevant and well characterized kinases associated with EMT in breast cancer and evaluated their expression by quantitative real-time PCR (qRT-PCR). We also assessed the expression of EMT (*CDH1* and *VIM*) and basal (*EGFR*, *KRT5*, and *KRT6A*) markers as well as a panel of cytokines and chemokines in breast cancer cell lines. Briefly, total RNA was extracted from two 6 µm-thick sections of FFPE breast tumour samples using the High Pure FFPE RNA Micro Kit (Roche), according to manufacturer’s instructions. Total RNA from cells was extracted using Trizol (Qiagen). The concentration and quality of RNA were assessed with NanoDrop ND-1000 spectrophotometer (NanoDrop Technologies). The expression of selected genes was evaluated using TaqMan probes from Applied Biosystems, following the manufacturer's guidelines. Three replicates per sample were assayed for each gene. PCR amplification was carried out using a ViiA 7 Real-Time PCR system (Applied Biosystems), and glyceraldehyde-3-phosphate dehydrogenase (*GAPDH*) served as the normalizing control for relative quantification using the comparative CT method.

3.11 Cell cultures, treatments and preparation of tumour-conditioned media

Breast cancer cell lines (BT-474, BT-483, BT-549, HCC38, HCC70, HCC1143, Hs578T, MCF-7, MDA-MB-157, MDA-MB-453, MDA-MB-231, MDA-MB-361, MDA-MB-436, MDA-MB-468, and T47D) were obtained from the American Type Culture Collection (ATCC) and grown according to standard protocols at 37 °C with 5% CO_2. Paclitaxel, doxorubicin, and R428 (Selleck Chemicals) were dissolved in dimethyl sulfoxide (DMSO). Cells were treated with paclitaxel (25 nM), doxorubicin (1 μM), R428 (1 μM), or control vehicle. Once grown to sub-confluence, cells were serum starved and incubated with fresh medium for 24 hr. Conditioned media (CM) were collected and filtered at 0.2 μm.

3.12 Macrophages differentiation

Human monocytes were obtained from normal donor buffy coat by two-step gradient centrifugation with Ficoll and Percoll (GE-Healthcare), as previously described (Solinas et al., 2010). Briefly, blood was washed with saline and then centrifuged on Ficoll. Peripheral blood mononuclear cells (PBMC) were suspended in iso-osmotic complete RPMI 1640 (Lonza) and layered on a 46% Percoll solution. Monocytes were recovered and resuspended in complete RPMI 1640. Residual lymphocytes were removed by plastic adherence. Purified monocytes were cultivated for 6 days in RPMI 1640 with 5% fetal bovine serum (FBS) and 50 ng/ml of recombinant human macrophage colony-stimulating factor (M-CSF; Peprotech). M1 macrophages were polarized by culturing overnight the M-CSF-treated cells with LPS (100 ng/ml; Peprotech) and IFN-γ (100 ng/ml; Peprotech). M2 macrophages were obtained using IL-4 (20 ng/ml; Peprotech). CM were collected and filtered at 0.2 μm. Freshly isolated human monocytes were also cultured in the absence or presence of 30% CM from HCC38, MCF-7, MDA-MB-231, MDA-MB-436, or MDA-MB-468 for 6 days (Solinas et al., 2010; Su et al., 2014a).

3.13 Flow cytometry

Macrophages were treated as indicated in the text and analysed by flow cytometry on a FACSCanto II flow cytometer (BD Biosciences). Human FcRs were blocked using 1% human serum in PBS. Cells were washed and resuspended in FACS buffer (0.5% BSA, 0.05% NaN3 in PBS) and incubated for 20 min at 4 °C with phycoerythrin (PE)-mouse anti-human CD163 (clone GHI/61; BD Bioscience), Allophycocyanin (APC)-mouse anti-human CD206 (clone 19.2; BD Bioscience), or appropriate IgG1 κ isotype controls (BD Bioscience). Data were analysed with the FACSDiva software (BD Bioscience).

3.14 Enzyme-linked immunosorbent assay

The levels of CCL18, IL-10, IL-12, and growth arrest-specific 6 (Gas6) in macrophage supernatants were measured by commercially available enzyme-linked immunosorbent assay (ELISA) kits according to manufacturer's instructions (R&D Systems). All experiments were performed with three wells for each condition and repeated four times.

3.15 Cell viability assay

Viable cells were identified using the 3-[4,5-dimethylthiazol-2-yl]-2,5-diphenyltetrazolium bromide assay (MTT; Sigma Aldrich). Briefly, 3 x 10^3 MDA-MB-231 cells were plated in 96-well plates in DMEM supplemented with 10% FBS. Cells were allowed to attach overnight and then treated as indicated in the text. After 72 hr, the MTT reagent (5 mg/ml) was added to each well, followed by incubation for 4 hr at 37 °C. The MTT crystals were solubilized in DMSO. The absorbance was read at 560 nm with an iMark plate reader (Bio-Rad). All treatments were performed in triplicate and cell viability was expressed as a percentage of the control (mean ± standard deviation [SD]).

3.16 Wound healing assay

For the wound healing assay, breast cancer cells were seeded in 6-well plates and grown at 37 °C in DMEM with 10% FBS. At 90% confluence, a scratch was produced using a pipette tip. Cells were then incubated with control medium or M2 macrophages-CM for 24 hr in the absence or presence of R428. Cell migration was captured immediately after stimulation (0 hr time point) and following 24 hr to monitor the closure of the wounded area. Image analysis was conducted with ImageJ software.

3.17 Western blotting

Cells were washed with ice-cold PBS and scraped into ice-cold RIPA lysis buffer (Thermo Fisher Scientific) supplemented with protease and phosphatase inhibitor cocktails (Thermo Fisher Scientific). Lysates were cleared by centrifugation at 13,000 rpm for 10 min at 4 °C, then supernatants were removed and assayed for protein concentration using the Pierce BCA Protein Assay Kit (Thermo Fisher Scientific). Sixty micrograms of total lysate was resolved on SDS-PAGE gels and transferred to PVDF membranes (Bio-Rad). Membranes were blocked for 1 hr in 5% non-fat dry milk in Tris-buffered saline (TBS)-Tween and then hybridized using primary antibodies in 5% non-fat dry milk in TBS-Tween. Anti-phospho-AXL (Tyr779) and anti-AXL antibodies were purchased from R&D Systems. Anti-phospho-AKT (Ser473), anti-AKT, anti-phospho-ERK1/2 (Thr202/Tyr204), anti-ERK1/2, anti-phospho-SRC (Tyr416), anti-SRC, and anti-β-actin antibodies were from Cell Signaling Technology. Anti-rabbit horseradish peroxidase (HRP)-conjugated secondary antibodies (Cell Signaling Technology) were diluted in 5% non-fat dry milk in TBS-Tween. Protein-antibody complexes were detected by chemiluminescence with Clarity Western ECL Substrate (Bio-Rad). Chemiluminescence imaging was performed on a Bio-Rad ChemiDoc MP Imager (Bio-Rad).

3.18 Statistical analysis

Clinicopathological associations were tested using Fisher's exact test and Mann-Whitney *U* test for categorical and continuous data, respectively. Differences between two groups were determined using the Student's *t* test, the Mann-Whitney *U* test, or the Kruskal-Wallis test. Spearman's rank and Pearson's linear correlation tests were used to evaluate the correlation between variables. Co-expression and enrichment analyses were performed using the Search-based Exploration of Expression Compendium (SEEK; http://seek.princeton.edu) (Aure et al., 2013). Pathway analysis was performed using Ingenuity Pathway Analysis software (IPA; Qiagen). Patients who developed distant tumour recurrence within 36 months after primary surgery were considered positive for tumour relapse, whereas patients who remained free of recurrence for the same time frame were defined as non-relapsing tumours. Relapse-free survival (RFS) was defined as the time from surgery until the detection of distant recurrence. Overall survival (OS) was defined as the time from surgery to date of death. Patients who were alive (for OS) or recurrence-free (for RFS) were censored at date of last follow-up. Survival analyses were performed by the Kaplan-Meier method, log-rank test (Mantel-Cox), and Cox univariate proportional hazard model using categorical or continuous variables. Forest plots were used to visualize the results of Cox univariate analysis for RFS and OS. Multivariate Cox proportional hazard regression analysis was adjusted for relevant clinical covariates, including age at diagnosis, histological grade, lymph node status, tumour size, and tumour stage. The likelihood ratio (LR) test was performed to compare the different prognostic models. Changes in the LR values ($\Delta LR\chi^2$) were used to quantitatively measure the relative amount of prognostic information of one model compared with another. All tests were two-sided and the level of statistical significance was set at $P \leq 0.05$. *P*-values were corrected using the Bonferroni or the Benjamini-Hochberg methods as indicated in the text. Statistical analyses were performed using GraphPad Prism version 5, StatsDirect version 3, Epi Info version 7, and R software version 3.2.3 (https://www.r-project.org).

4. Results

4.1 Landscape of the immune microenvironment in triple-negative breast cancer

4.1.1 Immune metagenes are differentially expressed in triple-negative breast cancers characterized by varying levels of chromosomal instability

Gene expression data from forty-two data sets (E-MTAB-365, E-TABM-43, GSE11121, GSE12276, GSE1456, GSE16391, GSE16446, GSE16716, GSE17705, GSE18728, GSE19615, GSE20194, GSE20271, GSE2034, GSE20685, GSE20711, GSE21653, GSE22093, GSE23988, GSE25066, GSE2603, GSE26971, GSE29044, GSE2990, GSE31448, GSE31519, GSE32646, GSE3494, GSE36771, GSE37946, GSE41998, GSE42568, GSE43358, GSE43365, GSE45255, GSE4611, GSE46184, GSE48390, GSE50948, GSE5327, GSE65194, and GSE7390), including a total of 862 non-redundant TNBC samples, were collected. To explore the potential link between the tumour immune microenvironment and the levels of CIN in TNBC we evaluated the expression of ten gene signatures that represent distinct immune components. As a surrogate marker of CIN, we used the CIN70 signature, which is defined as the sum of the normalized expression value of each gene enclosed in the signature in a given sample (Carter et al., 2006). TNBC patients were stratified into two groups based on the median expression of the CIN70 signature. In agreement with the published literature, the vast majority of TNBC showed a high level of CIN (83%) (Figure 10). Interestingly, several immune modules were differentially expressed between CIN-high and CIN-low tumours (Figure 11). Specifically, CT, NK, DC, M, and NF-κB signatures were overexpressed in TNBC with low levels of CIN (Figure 11). Considering the heterogeneity of CIN within TNBC, we evaluated the distribution of genomic instability among the three main TNBC molecular subgroups – basal-like [BL1/2], immunomodulatory [IM], and mesenchymal/mesenchymal stem-like [MS]. Overall, our cohort included 34.0% of BL1/2, 26.7% of IM, and 39.3% of MS TNBC. Noteworthy, the CIN-high group was similarly composed by BL1/2 (39%) and MS

(35%) tumours, while TNBC with low CIN levels were consistently enriched for MS cancers (61%) (Figure 10).

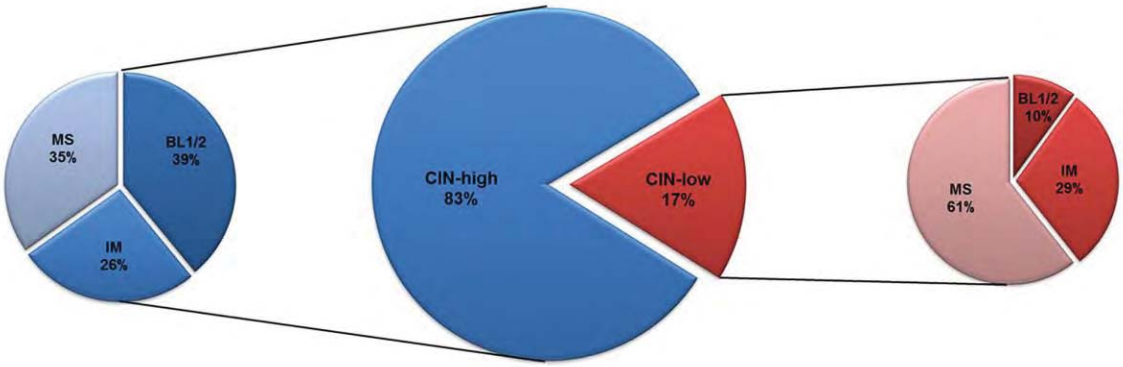

Figure 10. Distribution of chromosomal instability levels and intrinsic subtypes of triple-negative breast cancer. CIN70 scores were dichotomized around the median to stratify patients according to their levels of CIN. The majority of TNBC shows a high level of CIN. Molecular subtypes of TNBC, which are defined accordingly to the Lehmann's classification, are differentially distributed between CIN-high and CIN-low groups (Lehmann et al., 2011).

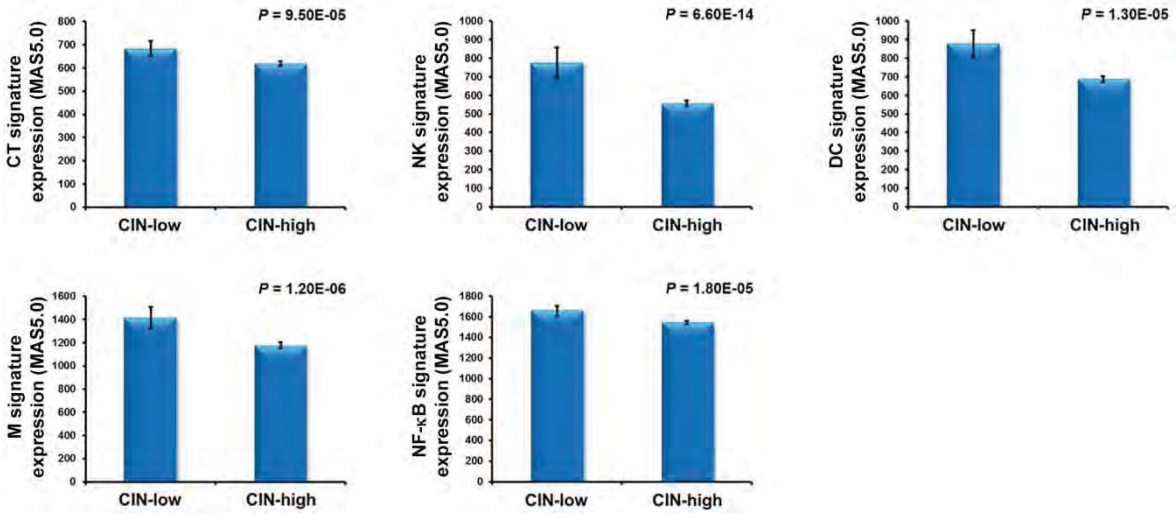

Figure 11. Expression of immune signatures in triple-negative breast cancers with different levels of chromosomal instability. TNBC patients were stratified into CIN-high and CIN-low groups based on the median expression of the CIN70 signature. Immune signatures related to CT cells, NK cells, DC, macrophages, and NF-κB are overexpressed in TNBC with low levels of CIN. *P*-values were obtained using the Mann-Whitney *U* test. The 95% confidence intervals are shown.

4.1.2 Immune metagenes are specifically enriched in different molecular subtypes of triple-negative breast cancer

To further explore the composition of the tumour immune microenvironment we evaluated the expression of the ten immune gene signatures in TNBC molecular subtypes. We found that TNBC molecular subgroups and specific microenvironmental immune signatures were consistently correlated. As expected, the IM subtype was enriched for almost all the immune modules (Figure 12). In particular, TC, BC, CT, IFN, NF-κB, and M signatures were overexpressed in the IM subtype (Figure 12A). Conversely, the gene expression signatures related to NK cells was enriched in the MS TNBC subtype (Figure 12B). The expression of genes related to DC did not differ between molecular subtypes (Figure 12C).

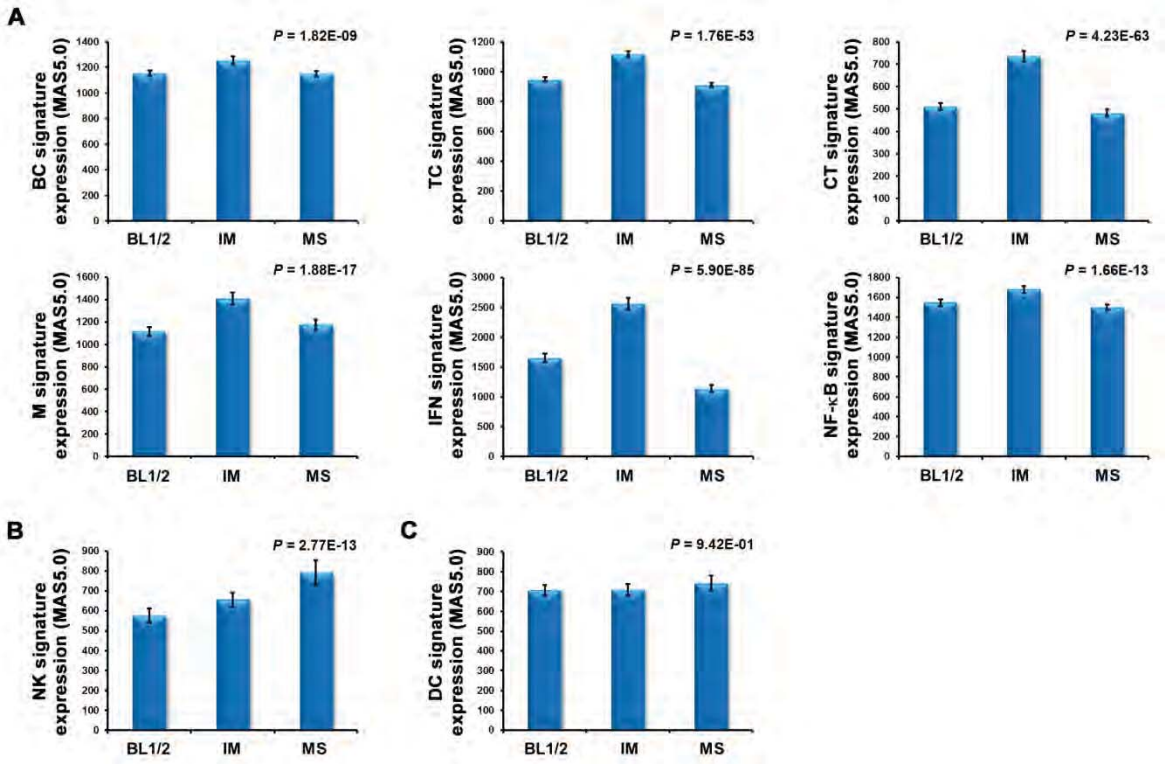

Figure 12. Expression of immune signatures in triple-negative breast cancer molecular subtypes. A) Immune signatures related to B cells, T cells, cytotoxic cells, macrophages, interferon, and NF-κB are overexpressed in the IM subtype. B) The MS TNBC subtype is enriched for the immune signature related to NK cells. C) The gene module reflecting the presence of DC is not significantly differentially expressed between TNBC molecular subtypes. Differences in signatures expression between groups were calculated using the Kruskal-Wallis test. The 95% confidence intervals are shown.

Given the plasticity and heterogeneity of macrophages, we developed two different signatures reflecting the polarization of anti-tumour M1 or pro-tumour M2 macrophages (Bottai et al., 2016b). Interestingly, while the M1 signature was overexpressed in the IM molecular subtype, the M2 macrophages-related metagene was enriched in the MS subgroup of TNBC, suggesting a potential relationship between macrophages and TNBC with mesenchymal-like properties (Figure 13).

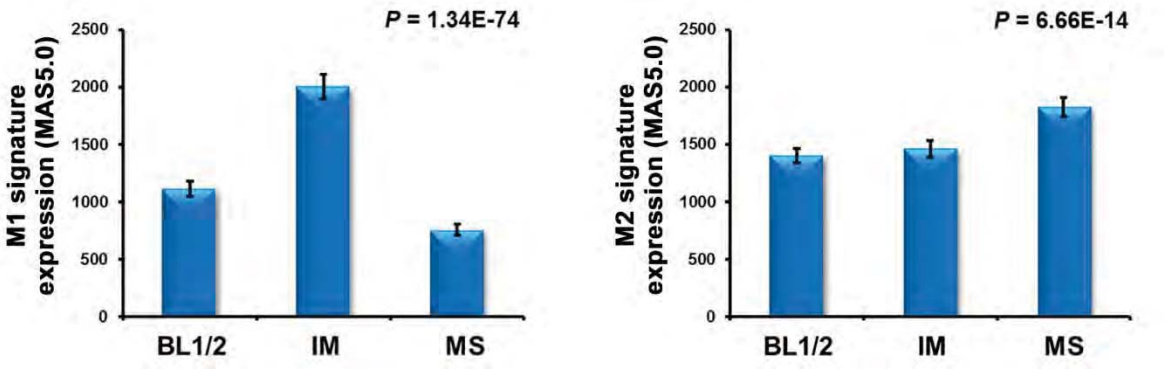

Figure 13. Macrophage subsets are specifically associated with triple-negative breast cancer molecular subtypes. The immune signature related to anti-tumour M1 macrophages is overexpressed in the IM molecular subtype, while the M2 macrophages-related metagene is enriched in the MS subgroup of TNBC. Differences in signatures expression between groups were calculated using the Kruskal-Wallis test. The 95% confidence intervals are shown.

4.2 Composition and functionality of lymphocytic infiltration and checkpoint receptors in triple-negative breast cancer

4.2.1 Phenotypic profiling of tumour-infiltrating lymphocytes in triple-negative breast cancer

We analysed samples from 259 patients with invasive ductal TNBC treated with adjuvant anthracycline-based chemotherapy. Clinical characteristics of patients are presented in Table 4. The majority of TNBC samples had lymphocytic infiltration in tumour stroma. Approximately 75% of TNBC had at least 10% of stromal TIL (range 10% to 80%), while only 25% showed a virtual absence of lymphocytes (range 0% to 1%). LPBC (TIL ≥ 50%) phenotype was found in 10.8% of TNBC.

We further explored the nature of immune infiltrates by performing IHC for the main lymphocyte subsets. Phenotypic characterization of lymphocyte components showed that the presence of elevated TIL was positively associated with the density of CD4+ ($r = 0.347$) and FOXP3+ ($r = 0.327$) lymphocytes, and the highest correlation was found with CD8+ T cells ($r = 0.511$; Figure 14A). These results were confirmed by analysing an additional cohort of TNBC patients ($n = 104$; Figure 14B and Table 4). Representative images of TNBC cases with different degrees of TIL and lymphocyte subpopulations are depicted in Figure 14C and D.

Table 4. Patient characteristics

Clinical and pathological information	Discovery cohort	Validation cohort
Patients (*n*)	259	104
Median age: years (IQR)	50 (46 – 68)	53 (47 – 68)
Median tumour size: mm (IQR)	20 (14.5 – 35)	20 (15 – 45)
T stage		
T1	135 (52.1%)	52 (50.0%)
T2	94 (36.3%)	30 (28.8%)
T3	21 (8.1%)	17 (16.4%)
T4	9 (3.5%)	5 (4.8%)
TNM Stage		
I	78 (30.1%)	28 (26.9%)
II	99 (38.2%)	40 (38.5%)
III	82 (31.7%)	36 (34.6%)
Node status		
Negative	125 (48.3%)	53 (51.0%)
Positive	134 (51.7%)	51 (49.0%)
Histological grade		
grade 1	3 (1.2%)	1 (1.0%)
grade 2	52 (20.1%)	39 (37.5%)
grade 3	204 (78.7%)	64 (61.5%)
Lymphovascular invasion		
Absent	113 (43.6%)	-
Present	78 (30.1%)	-
Unknown	68 (26.3%)	104 (100%)
Recurrence within 36 months		
Yes	65 (25.1%)	14 (13.5%)
No	194 (74.9%)	90 (86.5%)
TIL		
Median (range)	10 (0 – 75)	10 (0 – 75)
IQR	2 – 25	1 – 25
TIL scores		
0	64 (24.7%)	27 (26.0%)
10	102 (39.4%)	28 (26.9%)
20	21 (8.1%)	14 (13.5%)
30	29 (11.1%)	19 (18.3%)
40	15 (5.8%)	6 (5.8%)
50	10 (3.9%)	2 (1.9%)
60	10 (3.9%)	5 (4.8%)
70	2 (0.8%)	1 (1.0%)
80	6 (2.3%)	2 (1.9%)
90	0 (0.0%)	0 (0.0%)
100	0 (0.0%)	0 (0.0%)

Abbreviations: N, number; IQR, Interquartile range; TIL, tumour-infiltrating lymphocytes.

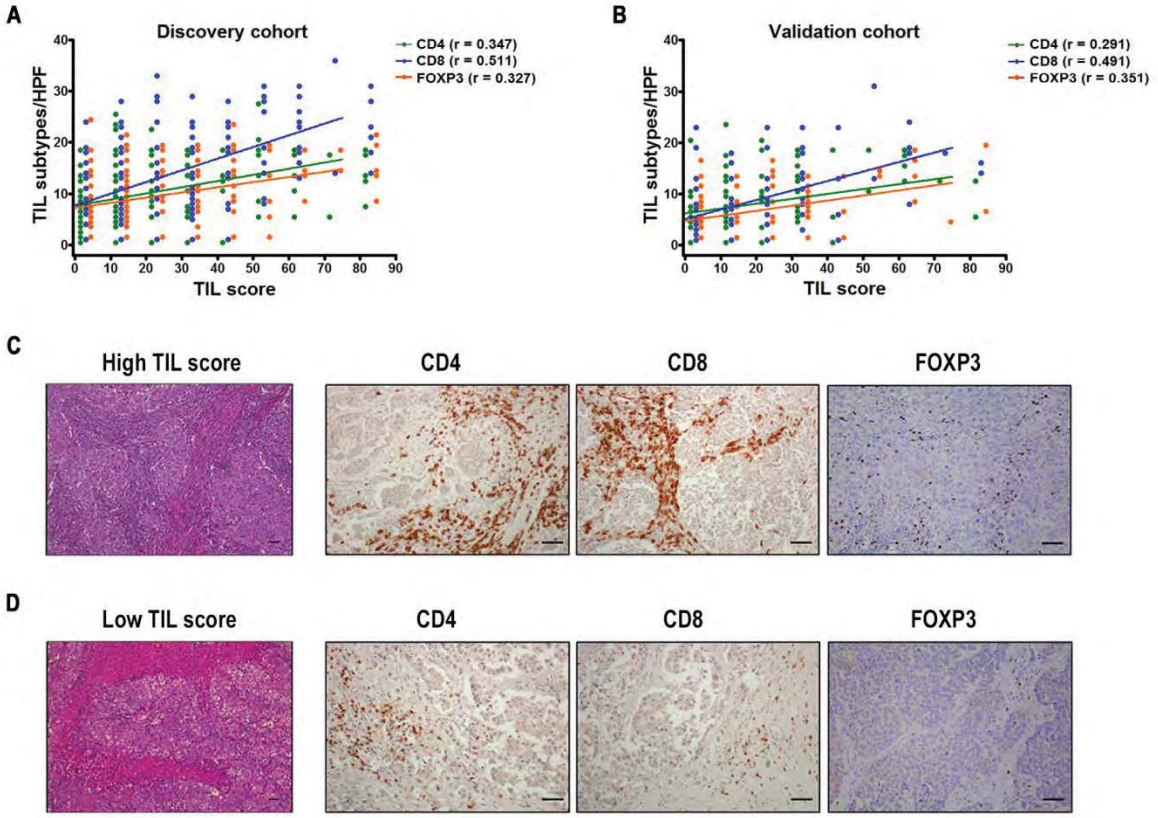

Figure 14. Distribution of tumour-infiltrating lymphocytes and immune cell subpopulations in triple-negative breast cancer. Immunophenotypic characterization of lymphocyte components shows that the presence of elevated TIL positively correlate with the density of CD4+, CD8+, and FOXP3+ lymphocytes in TNBC of the discovery (A) and the validation (B) cohorts. Pearson's correlation coefficients (r) for each cells subpopulation are shown. Cell density was scored by determining the average number of stained cells in three distinct HPF. Representative images of HE sections from TNBC samples with high (C) and low (D) TIL scores. Representative immunohistochemical staining of CD4, CD8, and FOXP3 in serial sections of TNBC specimens with high (C) and low (D) lymphocytic infiltration. Scale bars represent 50 μm.

4.2.2 Association of tumour-infiltrating lymphocytes with clinicopathological parameters and survival in triple-negative breast cancer

A lower stromal TIL content was associated with larger tumour size (P = 1.80E-02; Table 5). There were no other significant associations between the variables examined and the presence of TIL or different immune cell subsets in the discovery cohort (n = 259; Table 5). The data were confirmed in the validation cohort of TNBC (n = 104; Table 6).

Table 5. Associations between tumour-infiltrating lymphocytes and clinicopathological features in triple-negative breast cancer (n = 259)

		Continuous TIL[a]			CD4[b]			CD8[b]			FOXP3[b]		
Patient characteristics	***n***	**Median (range)**	**IQR**	***P***	**High (%)**	**Low (%)**	***P***	**High (%)**	**Low (%)**	***P***	**High (%)**	**Low (%)**	***P***
Age at diagnosis													
< 50	135	10 (0 – 75)	2 – 25	0.765	60 (44.4)	75 (55.6)	0.098	58 (43.0)	77 (57.0)	0.386	55 (40.7)	80 (59.3)	0.900
≥ 50	124	10 (0 – 75)	1 – 23.5		42 (33.9)	82 (66.1)		60 (48.4)	64 (51.6)		52 (46.0)	72 (54.0)	
LN status													
Negative	125	8 (0 – 72)	2 – 25	0.223	47 (37.6)	78 (62.4)	0.612	62 (49.6)	63 (50.4)	0.215	52 (41.6)	73 (58.4)	1.000
Positive	134	10 (0 – 75)	1 – 20		55 (41.0)	79 (59.0)		56 (41.8)	78 (58.2)		55 (41.0)	79 (59.0)	
Histological grade													
G1-2	55	10 (0 – 72)	2 – 25	0.413	21 (38.2)	34 (61.8)	0.878	25 (45.5)	30 (54.5)	1.000	17 (30.9)	38 (69.1)	0.090
G3	204	10 (0 – 75)	0 – 23.5		81(39.7)	123 (60.3)		93 (45.6)	111 (54.4)		90 (44.1)	114 (55.9)	
pTNM staging													
I-II	177	10 (0 – 72)	2 – 25	0.338	74 (41.8)	103 (58.2)	0.275	85 (48.0)	92 (52.0)	0.284	76 (42.9)	101 (57.1)	0.498
III	82	10 (0 – 75)	1 – 20		28 (34.1)	54 (65.9)		33 (40.2)	49 (59.8)		31 (37.8)	51 (62.2)	
Tumour size (mm)													
≤ 20	138	10 (0 – 75)	2 – 25	**0.018**	55 (39.9)	83 (60.1)	0.899	71 (51.4)	67 (48.6)	0.060	58 (42.0)	80 (58.0)	0.800
> 20	120	8 (0 – 72)	1 – 13.5		46 (38.3)	74 (61.7)		47 (39.2)	73 (60.8)		48 (40.0)	72 (60.0)	
LVI													
Absent	113	8 (0 – 75)	2 – 23.5	0.860	47 (41.6)	66 (58.4)	1.000	60 (53.1)	53 (46.9)	0.056	58 (51.3)	55 (48.7)	0.186
Present	78	10 (0 – 72)	1 – 17.5		33 (42.3)	45 (57.7)		30 (38.5)	48 (61.5)		32 (41.0)	46 (59.0)	

[a]Mann-Whitney U test P-values. TIL scores were used as a continuous variable for each 10% increment.

[b]Fisher's exact test P-values. Median values were used as cut-offs for CD4, CD8, and FOXP3.

Significant P-values are given in bold. Abbreviations: N, number; IQR, Interquartile range; LN, lymph node; LVI, lymphovascular invasion; TIL, tumour-infiltrating lymphocyte.

Table 6. Associations between tumour-infiltrating lymphocytes and clinicopathological features in triple-negative breast cancer (n = 104)

		Continuous TIL[a]			CD4[b]			CD8[b]			FOXP3[b]		
Patient characteristics	***n***	**Median (range)**	**IQR**	***P***	**High (%)**	**Low (%)**	***P***	**High (%)**	**Low (%)**	***P***	**High (%)**	**Low (%)**	***P***
Age at diagnosis													
< 50	51	12 (0 – 72)	1 – 30	0.507	16 (31.4)	35 (68.6)	0.266	16 (31.4)	35 (68.6)	0.831	8 (15.7)	43 (84.3)	0.458
≥ 50	53	10 (0 – 75)	2 – 23.5		11 (20.8)	42 (79.2)		15 (28.3)	38 (71.7)		12 (22.6)	41 (77.4)	
LN status													
Negative	53	10 (0 – 75)	1 – 25	0.860	15 (28.3)	38 (71.7)	0.657	20 (37.7)	33 (62.3)	0.088	10 (18.9)	43 (81.1)	1.000
Positive	51	10 (0 – 62)	2 – 25		12 (23.5)	39 (76.5)		11 (21.6)	40 (78.4)		10 (19.6)	41 (80.4)	
Histological grade													
G1-2	40	10 (0 – 75)	1 – 21.7	0.288	13 (32.5)	27 (67.5)	0.256	14 (35.0)	26 (65.0)	0.385	8 (20.0)	32 (80.0)	1.000
G3	64	11 (0 – 62)	2 – 28.7		14 (21.9)	50 (78.1)		17 (26.6)	47 (73.4)		12 (18.8)	52 (81.2)	
pTNM staging													
I-II	68	10 (0 – 75)	1 – 28.7	0.978	18 (26.5)	50 (73.5)	1.000	22 (32.4)	46 (67.6)	0.504	12 (17.6)	56 (82.4)	0.607
III	36	10 (0 – 60)	2.7 – 25		9 (25.0)	27 (75.0)		9 (25.0)	27 (75.0)		8 (22.2)	28 (77.8)	
Tumour size (mm)													
≤ 20	54	13.5 (0 – 72)	1.7 – 30	**0.039**	18 (33.3)	36 (66.7)	0.116	20 (37.0)	34 (63.0)	0.133	14 (25.9)	40 (74.1)	0.085
> 20	50	5 (0 – 75)	1 – 20.2		9 (18.0)	41 (82.0)		11 (22.0)	39 (78.0)		6 (12.0)	44 (88.0)	

[a]Mann-Whitney *U* test *P*-values. TIL scores were used as a continuous variable for each 10% increment.

[b]Fisher's exact test *P*-values. Median values were used as cut-offs for CD4, CD8, and FOXP3.

Significant *P*-values are given in bold. Abbreviations: N, number; IQR, Interquartile range; LN, lymph node; LVI, lymphovascular invasion; TIL, tumour-infiltrating lymphocytes.

The association between LPBC, continuous TIL scores, and single immune components with RFS and OS in TNBC patients was evaluated by Cox proportional hazard regression analyses (Figure 15, Figure 16, and Table 7). TIL assessed as a binary variable (LPBC *v* non-LPBC) were associated with both RFS (Hazard ratio (HR) = 0.22; 95% Confidence interval (CI), 0.05 – 0.88; *P* = 3.28E-02) and OS (HR = 0.29; 95% CI, 0.09 – 0.93; *P* = 3.73E-02) in TNBC in univariate analysis (Figure 15 and Figure 16A), but lost their prognostic value in multivariate analysis (Table 7). However, continuous TIL scores had a significant prognostic value for RFS (HR = 0.92; 95% CI, 0.82 – 0.98; *P* < 1.00E-04) and OS (HR = 0.92; 95% CI, 0.89 – 0.95; *P* < 1.00E-04) in TNBC (Figure 15 and Figure 16B).

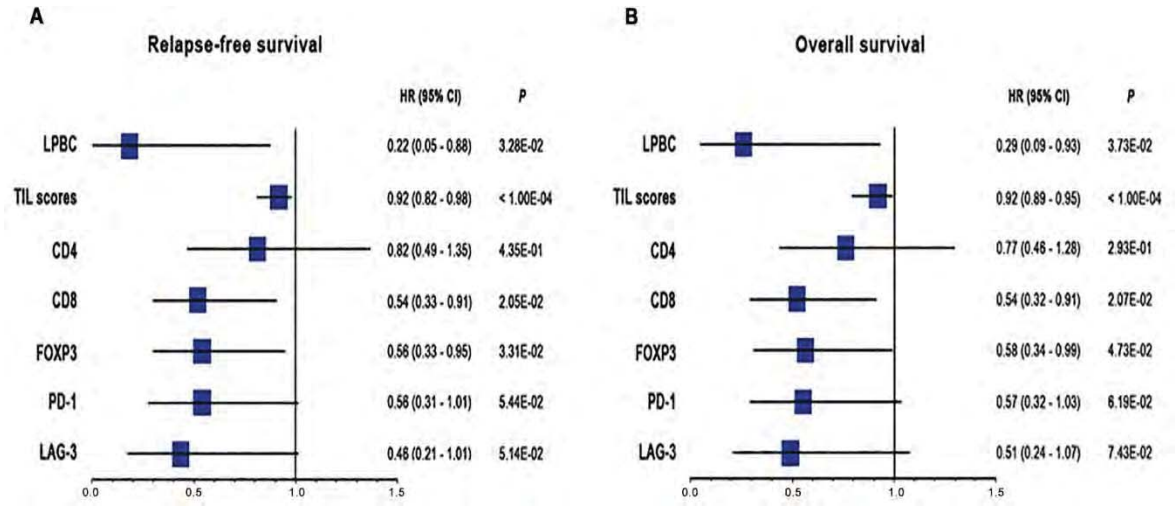

Figure 15. Univariate Cox regression analysis of tumour-infiltrating lymphocytes, immune markers and checkpoint receptors for relapse-free survival and overall survival in triple-negative breast cancer (*n* = 259). Forest plot of hazard ratios (HR) with 95% confidence interval (CI) for RFS (A) and OS (B) of LPBC (cut-off value ≥ 50%), TIL scores (used as a continuous variable for each 10% increment), immune markers (CD4, CD8, and FOXP3; median values were used as cut-offs), and immune checkpoints (PD-1, and LAG-3; a cut-off value ≥ 5% was used). *P*-values and HR (95% CI in parentheses) are shown.

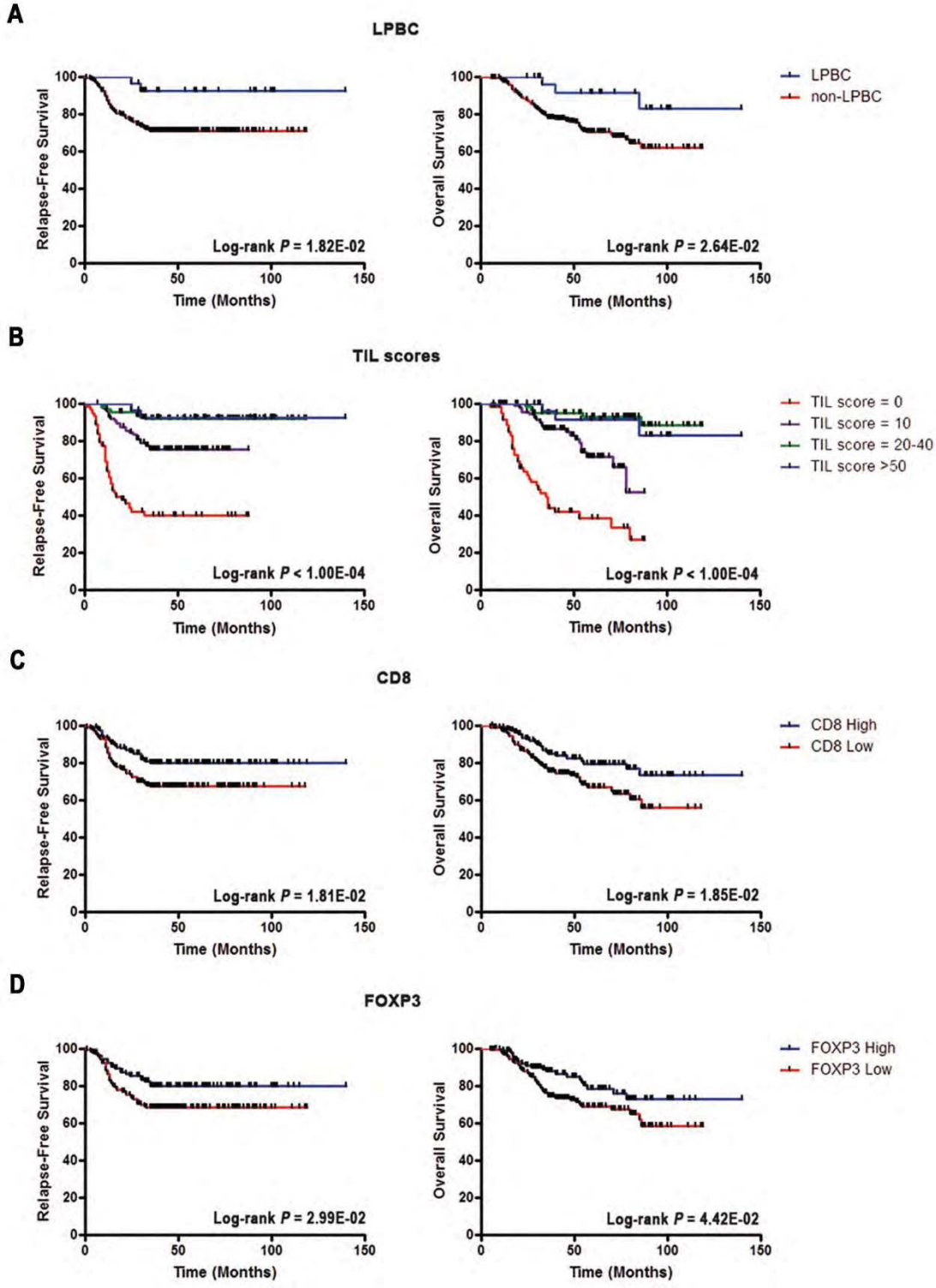

Figure 16. **Prognostic value of stromal tumour-infiltrating lymphocytes and immune cell subpopulations in triple-negative breast cancer (*n* = 259).** Kaplan-Meier curves of RFS and OS for (A) binary LPBC (cut-off value ≥ 50%), (B) continuous stromal TIL (grouped as 0 [range 0% to 1%] *v* 10 [range 2% to 10%] *v* 20 to 40 [range 11% to 40%] *v* 50 to 80 [range 41% to 80%]), (C) CD8 (median value); D) FOXP3 (median value). Curves were compared using log-rank test.

Table 7. Multivariate Cox regression analysis of tumour-infiltrating lymphocytes and immune markers for relapse-free survival and overall survival in triple-negative breast cancer (*n* = 259)

	Relapse-Free Survival			Overall Survival		
Variable	**HR**	**95% CI**	***P*-value**	**HR**	**95% CI**	***P*-value**
LPBC	0.24	0.06 – 1.00	5.10E-02	0.32	0.10 – 1.03	5.60E-02
Age	1.09	0.66 – 1.80	7.28E-01	1.13	0.68 – 1.87	6.27E-01
Histological grade	1.66	0.78 – 3.53	1.91E-01	1.85	0.87 – 3.94	1.09E-01
Nodal status	3.44	1.72 – 6.88	**5.00E-04**	3.19	1.59 – 6.39	**1.00E-03**
Tumour size	1.21	0.74 – 1.99	4.48E-01	1.27	0.77 – 2.09	3.48E-01
Tumour stage	1.34	0.76 – 2.35	3.12E-01	1.38	0.78 – 2.43	2.69E-01
TIL[a]	0.93	0.89 – 0.96	**1.00E-04**	0.93	0.90 – 0.96	**1.00E-04**
Age	0.97	0.58 – 1.61	8.97E-01	1.02	0.61 – 1.71	9.32E-01
Histological grade	1.34	0.63 – 2.87	4.48E-01	1.76	0.83 – 3.75	1.40E-01
Nodal status	2.91	1.43 – 5.90	**3.10E-03**	2.59	1.27 – 5.28	**8.70E-03**
Tumour size	1.11	0.68 – 1.83	6.70E-01	1.15	0.70 – 1.90	5.73E-01
Tumour stage	1.46	0.82 – 2.62	2.00E-01	1.45	0.80 – 2.63	2.19E-01
CD8[b]	0.58	0.34 – 0.97	**3.72E-02**	0.58	0.34 – 0.97	**3.88E-02**
Age	1.12	0.68 – 1.85	6.66E-01	1.16	0.70 – 1.93	5.58E-01
Histological grade	1.71	0.80 – 3.65	1.67E-01	1.91	0.90 – 4.08	9.34E-02
Nodal status	3.46	1.73 – 6.90	**4.00E-04**	3.23	1.62 – 6.45	**9.00E-04**
Tumour size	1.20	0.73 – 1.97	4.80E-01	1.26	0.76 – 2.07	3.70E-01
Tumour stage	1.35	0.76 – 2.37	3.01E-01	1.35	0.76 – 2.40	2.99E-01
FOXP3[b]	0.52	0.31 – 0.89	**1.71E-02**	0.55	0.32 – 0.94	**2.90E-02**
Age	1.10	0.67 – 1.83	6.98E-01	1.16	0.70 – 1.92	5.70E-01
Histological grade	1.81	0.84 – 3.87	1.28E-01	2.01	0.94 – 4.30	7.27E-02
Nodal status	3.54	1.79 – 7.00	**3.00E-04**	3.30	1.67 – 6.53	**6.00E-04**
Tumour size	1.23	0.75 – 2.03	4.05E-01	1.30	0.79 – 2.13	3.06E-01
Tumour stage	1.37	0.79 – 2.41	2.65E-01	1.38	0.78 – 2.42	2.66E-01

Multivariate analysis adjusted for age (≥ 50 *v* < 50), histological grade (III *v* I-II), nodal status (1 *v* 0), tumour size (> 20 mm *v* ≤ 20 mm), and tumour stage (III *v* I-II). Significant *P*-values are given in bold.

[a]Analysed as a continuous variable for each 10% increment.

[b]Median values were used as cut-offs.

Abbreviations: CI, confidence interval; HR, hazard ratio; LPBC, lymphocyte-predominant breast cancer; TIL, tumour-infiltrating lymphocytes.

Cox multivariate analysis confirmed that TIL scores were independently associated with RFS (HR = 0.93; 95% CI, 0.89 – 0.96; *P* = 1.00E-04) and OS (HR = 0.93; 95% CI, 0.90 – 0.95; *P* = 1.00E-04) in TNBC (Table 7). Furthermore, continuous TIL scores added significant prognostic information for RFS ($\Delta LR\chi 2$ = 31.35; *P* < 1.00E-04) and OS ($\Delta LR\chi 2$ = 28.23; *P* < 1.00E-04) beyond that provided by standard clinicopathological parameters (Table 8).

Table 8. Comparisons of added prognostic information

	Relapse-free survival		**Overall survival**	
Variable	**$\Delta LR\chi^{2a}$**	***P*-value**	**$\Delta LR\chi^{2a}$**	***P*-value**
CP + TIL score *v* CP	31.35	**< 1.00E-04**	28.23	**< 1.00E-04**
CP + LPBC *v* CP	5.20	**2.26E-02**	4.97	**2.58E-02**
CP + TIL score + CD8 *v* CP + TIL score	0.43	5.12E-01	0.50	4.79E-01
CP + TIL score + FOXP3 *v* CP + TIL score	1.02	3.12E-01	0.99	3.20E-01
CP + TIL score + CD8 + FOXP3 *v* CP + TIL score	1.82	4.02E-01	1.70	4.27E-01

[a]Changes in the LR values ($\Delta LR\chi 2$) were used to quantitatively measure the relative amount of prognostic information of one model compared with another. Significant *P*-values from the LR test are given in bold.
Abbreviations: CP, clinicopathological variables (age, histological grade, nodal status, tumour size, and tumour stage); LPBC, lymphocyte-predominant breast cancer; LR, likelihood ratio; TIL, tumour-infiltrating lymphocytes.

Given that recent data suggested that stromal TIL value ≥ 20% in early-stage TNBC could identify patients with good outcome across nodal categories, we performed a Kaplan-Meier analysis to evaluate the prognostic value of this cut-off in TNBC stratified by nodal status (lymph node-negative and lymph node-positive) (Loi et al., 2016). Overall, we found that patients with high levels of TIL (≥ 20%) had a better outcome compared with those with low TIL (< 20%) in both nodal categories (Figure 17).

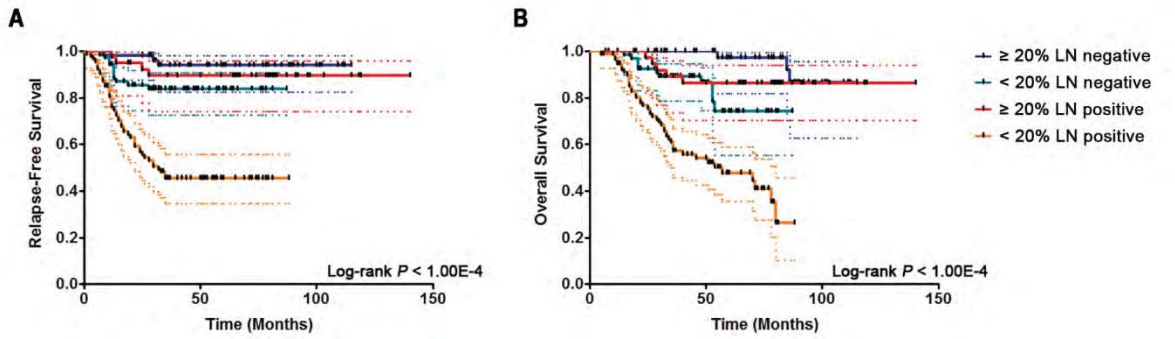

Figure 17. Prognostic value of the binary tumour-infiltrating lymphocytes cut-off ≥ 20% in triple-negative breast cancer patients stratified by nodal status. (A) Kaplan-Meier curves of RFS for binary 20% cut-off (≥ 20% *v* < 20%) in TNBC patients of the discovery cohort stratified according to lymph node (LN) status (positive *v* negative) (*P* = 6.64E-02 in LN-negative TNBC patients; *P* < 1.00E-04 in LN-positive TNBC patients). (B) Kaplan-Meier curves of OS for binary 20% cut-off (≥ 20% *v* < 20%) in TNBC patients of the discovery cohort stratified according to LN status (positive *v* negative) (*P* = 2.00E-03 in LN-negative TNBC patients; *P* < 1.00E-04 in LN-positive TNBC patients). Curves were compared using log-rank test. The dashed lines represent the 95% confidence intervals.

Among lymphocyte subsets, the density of CD4+ cells was not significantly prognostic in TNBC (Figure 15), while CD8+ lymphocytes were consistently associated with prolonged RFS and OS in both univariate (HR = 0.54; 95% CI, 0.33 – 0.91; *P* = 2.05E-02 for RFS; HR = 0.54; 95% CI, 0.32 – 0.91; *P* = 2.07E-02 for OS) and multivariate analysis (HR = 0.58; 95% CI, 0.34 – 0.97; *P* = 3.72E-02 for RFS; HR = 0.58; 95% CI, 0.34 – 0.97; *P* = 3.88E-02 for OS), indicating that cytotoxic CD8+ T lymphocytes are the main effectors of anti-tumour immune responses (Figure 15, Figure 16C, and Table 7). Furthermore, high FOXP3+ cells were also significantly associated with better survival in univariate (HR = 0.56; 95% CI, 0.33 – 0.95; *P* = 3.31E-02 for RFS; HR = 0.58; 95% CI, 0.34 – 0.99; *P* = 4.73E-02 for OS) and multivariate analysis (HR = 0.52; 95% CI, 0.31 – 0.89; *P* = 1.71E-02 for RFS; HR = 0.55; 95% CI, 0.32 – 0.94; *P* = 2.90E-02 for OS; Figure 15, Figure 16D, and Table 7). However, FOXP3+ cells were consistently associated with the density of CD8+ lymphocytes (r = 0.716), and the presence of FOXP3+ TIL was prognostically insignificant in TNBC cases stratified by the presence or absence of CD8+ cells (Table 9). Interestingly, we found that the infiltration of FOXP3+ cells tended to be

associated with reduced survival in TNBC cases with low content of CD8+ lymphocytes (Table 9), suggesting that the prognostic value of FOXP3+ cells is highly dependent on the concurrent presence of CTL. Noteworthy, neither CD8+ nor FOXP3+ cells added consistent prognostic value for RFS ($\Delta LR\chi2 = 0.43$; $P = 5.12E\text{-}01$ for CD8; $\Delta LR\chi2 = 1.02$; $P = 3.12E\text{-}01$ for FOXP3) and OS ($\Delta LR\chi2 = 0.50$; $P = 4.79E\text{-}01$ for CD8; $\Delta LR\chi2 = 0.99$; $P = 3.20E\text{-}01$ for FOXP3) beyond that provided by TIL score in multivariate model (Table 8), suggesting that the evaluation of single immune components may not be as informative as the global evaluation of stromal TIL.

Table 9. Univariate Cox regression analysis of FOXP3 for relapse-free survival and overall survival in triple-negative breast cancer ($n = 259$) stratified by CD8+ tumour-infiltrating lymphocytes status

	TNBC with high CD8+ TIL			**TNBC with low CD8+ TIL**		
Variable	**HR**	**95% CI**	***P*-value**	**HR**	**95% CI**	***P*-value**
			Relapse-Free Survival			
FOXP3	0.49	0.21 – 1.16	1.04E-01	1.04	0.47 – 2.35	9.14E-01
			Overall Survival			
FOXP3	0.49	0.21 – 1.15	1.03E-01	1.20	0.53 – 2.72	6.58E-01

Median values were used as cut-offs for CD8 and FOXP3.
Abbreviations: CI, confidence interval; HR, hazard ratio; TNBC, triple-negative breast cancer; TIL, tumour-infiltrating lymphocytes

4.2.3 Evaluation of the clinical relevance of immune checkpoints in triple-negative breast cancer

To assess the functional status of TIL in TNBC we analysed the expression of the checkpoint receptors PD-1 and LAG-3 by IHC. We first evaluated the specificity and the reproducibility of the two antibodies through western blot on human cells and IHC on cells pellet blocks. (Figure 18). Furthermore, we also performed IHC on set of normal and tumour FFPE tissues processed using the same fixative and processing methods as TNBC specimens tested in the study (Figure 19).

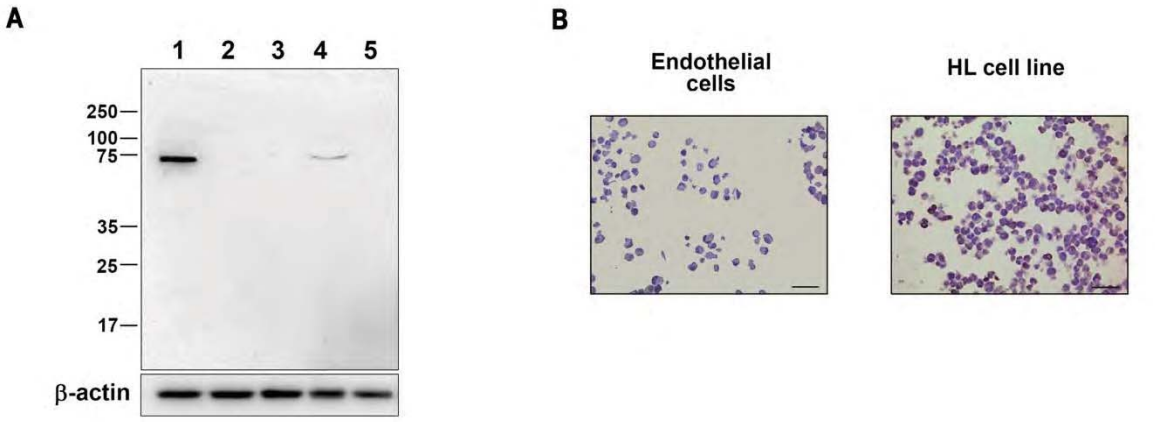

Figure 18. Analytical validation of antibodies using cells. A) Representative western blot analysis of Hodgkin Lymphoma HDLM2 cells (lane 1), HUVEC endothelial cells (lane 2), MCF7 breast cancer cells (lane 3), activated CD8+ lymphocytes sorted from human PBMC by FACS analysis (lane 4), and PBMC (lane 5) using the anti-LAG-3 antibody. Anti-β-actin antibody was used as a loading control. A single band is detected in lines 1 and 4, demonstrating the specificity of the antibody. B) Antibodies were tested on FFPE HDLM2 and HUVEC cells pellet blocks.

After antibodies validation, we found that PD-1+ and LAG-3+ TIL were present in approximately 30% and 18% of TNBC, respectively (Figure 20). Concurrent expression of both immune checkpoints was observed in 15.4% of TNBC cases. We found that the expression of both PD-1 and LAG-3 positively correlated with the presence of TIL ($r = 0.511$; $r = 0.576$, respectively), particularly with CD8+ cells ($r = 0.568$; $r = 0.490$, respectively; Figure 21A). We confirmed that PD-1 and LAG-3 were concurrently expressed in 13.5% of patients and that their expression was positively associated with TIL ($r = 0.438$; $r = 0.537$, respectively), and with CD8+ cells ($r = 0.495$; $r = 0.467$, respectively) in the validation cohort (Figure 21B). Even though a trend for longer RFS was observed in univariate analysis, the presence of both PD-1+ and LAG-3+ TIL showed no significant prognostic value in the discovery dataset (Figure 15).

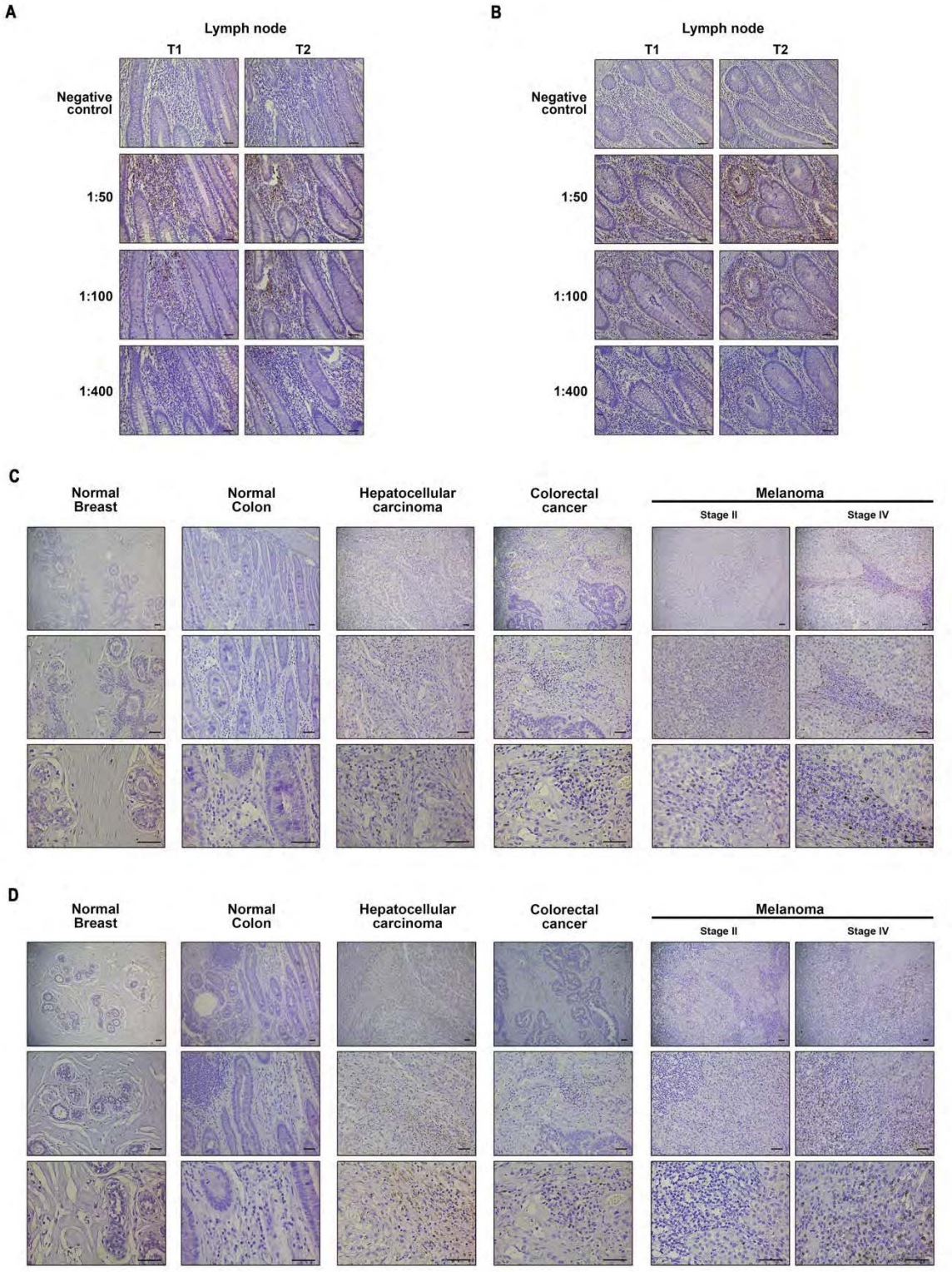

Figure 19. Immunohistochemical validation of antibodies on normal and tumour tissues. Representative images of IHC on serial FFPE lymph node sections stained with anti-PD-1 (A) and anti-LAG-3 (B) antibodies at different dilutions on different days (T1 and T2). Negative controls without primary antibody are also shown. Analytic validation of PD-1 (C) and LAG-3 (D) antibodies was also performed on a set of normal and tumour tissues, in the form of whole tissue sections processed using the same fixative and processing methods as TNBC specimens tested in the study. Scale bars represent 50 μm.

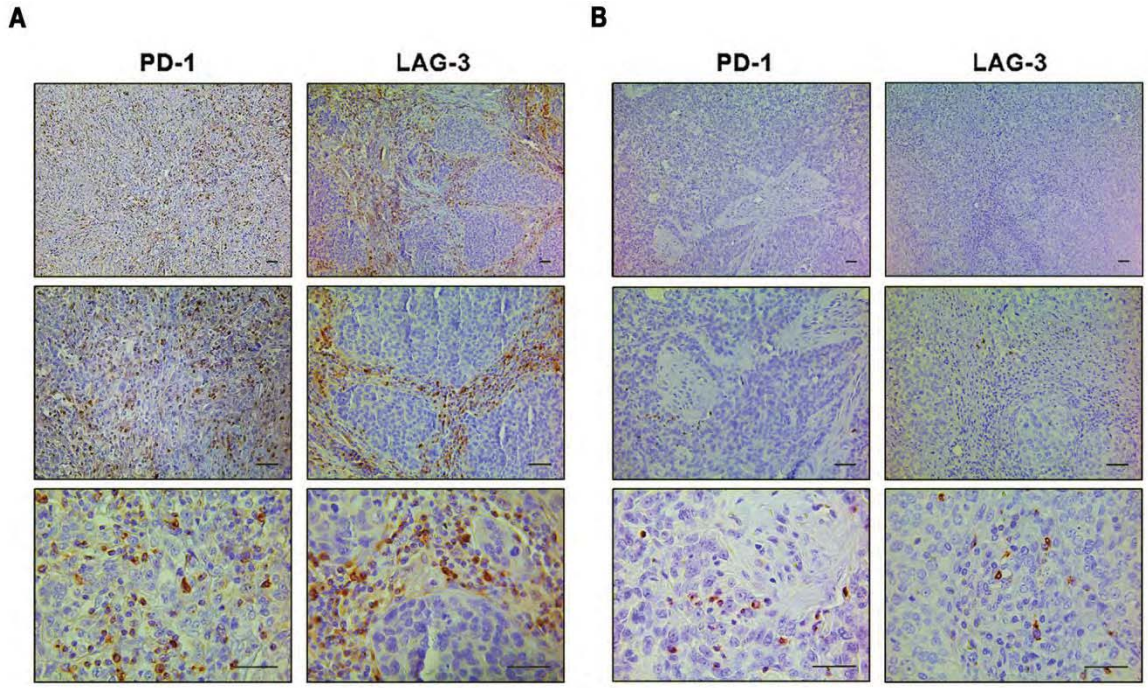

Figure 20. PD-1 and LAG-3 expression in triple-negative breast cancer. Representative immunohistochemical staining of PD-1 and LAG-3 at different magnification in serial sections of TNBC specimens with high (A) and low (B) lymphocytic infiltration. Scale bars represent 50 μm.

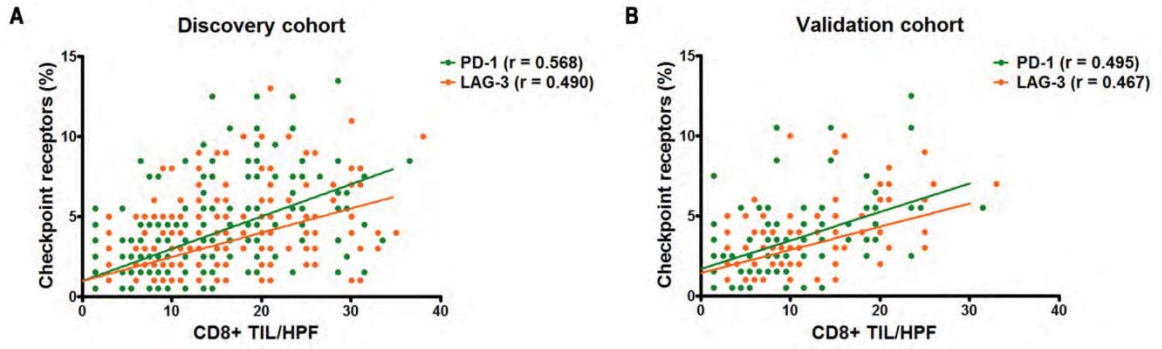

Figure 21. Correlation between the expression of PD-1 and LAG-3 and the presence of CD8+ cells in triple-negative breast cancer. The density of CD8+ T lymphocytes positively correlates with the expression of the checkpoint receptors PD-1 and LAG-3 in TNBC of the discovery (A) and the validation (B) cohorts. Pearson's correlation coefficients (r) for each cells subpopulation are shown. Cell density was scored by determining the average number of stained cells in three distinct HPF.

4.3 Functional status, tumour localization, and clinical relevance of cytotoxic tumour-infiltrating lymphocytes in triple-negative breast cancer

4.3.1 Expression of CD8 and CD103 in human triple-negative breast cancer

To evaluate the clinical relevance of CD8+ TIL based on their tumour localization, we analysed samples from 230 patients with invasive ductal TNBC treated with adjuvant anthracycline-based chemotherapy (Table 10).

Table 10. Patient characteristics

Clinical and pathological information	**Discovery cohort**	**Validation cohort**
Patients (*n*)	230	100
Median age: years (IQR)	50 (45 – 68)	52 (47 – 68)
Median tumour size: mm (IQR)	20 (14 – 35)	19.5 (15 – 40)
TNM Stage		
I	70 (30.4%)	27 (27.0%)
II	86 (37.4%)	40 (40.0%)
III	74 (32.2%)	33 (33.0%)
Node status		
Negative	108 (47.0%)	59 (59.0%)
Positive	122 (53.0%)	41 (41.0%)
Histological grade		
grade 1	2 (0.9%)	1 (1.0%)
grade 2	40 (17.4%)	39 (39.0%)
grade 3	188 (81.7%)	60 (60.0%)
Recurrence within 36 months		
Yes	65 (28.3%)	14 (14.0%)
No	165 (71.7%)	86 (86.0%)

Abbreviations: N, number; IQR, Interquartile range.

Overall, CD8+ cells were more numerous than CD103+ cells, with a mean (+/-SD) of 24 cells/HPF (+/-17) and 14 cells/HPF (+/-12), respectively (Figure 22A). CD8+ TIL were enriched within the stroma (mean stromal = 13 +/-10; mean intraepithelial = 11 +/-7), while CD103+ cells were predominantly localized to intraepithelial areas (mean stromal = 6 +/-7; mean intraepithelial = 9 +/-7; $P < 1.00E-04$) (Figure 22B).

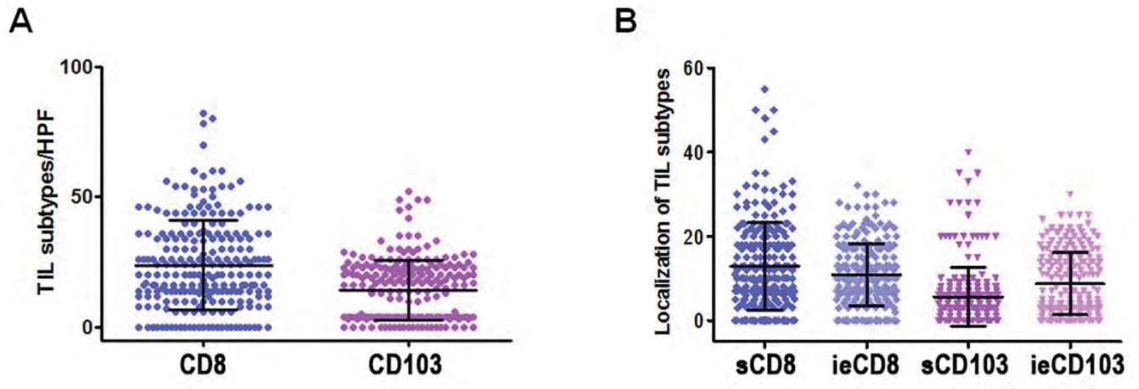

Figure 22. **CD8+ and CD103+ tumour-infiltrating lymphocytes density and localization in triple-negative breast cancer (*n* = 230).** A) Overall distribution of CD8+ and CD103+ TIL in TNBC. (B) Distribution of CD8+ and CD103+ in stromal (sCD8 and sCD103) and intraepithelial (ieCD8 and ieCD103) areas of TNBC.

We then analysed the relationship between CD8+ and CD103+ TIL in TNBC. IHC and Spearman's correlation analysis showed that intraepithelial CD8+ cells frequently expressed the integrin CD103 and that there was a strong positive association between CD103+ and CD8+ TIL in TNBC (overall Spearman's coefficient [rs] = 0.739, stromal rs = 0.612, intraepithelial rs = 0.691; $P < 1.00E-04$; Figure 23A and B).

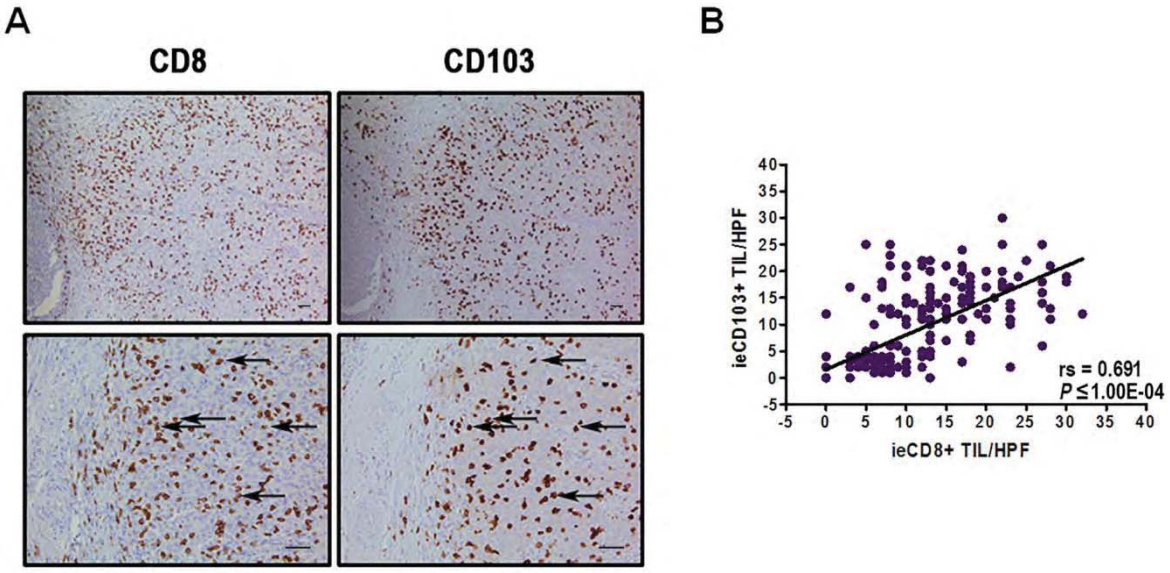

Figure 23. Relationship between CD8+ and CD103+ tumour-infiltrating lymphocytes in triple-negative breast cancer. (A) Representative IHC staining of CD8 and CD103 in serial sections of TNBC samples showing that intraepithelial CCD8+ cells frequently expressed the integrin CD103. Scale bars represent 50 µm. (B) Spearman's rank correlation analysis between intraepithelial CD8+ and CD103+ TIL in TNBC of the discovery cohort (rs = 0.691; $P \leq 1.00E-4$).

Although the binding of CD103 to its ligand E-cadherin has been suggested to be responsible for the retention of active lymphocytes within epithelial tissues, we found no correlation between the presence of CD103+ lymphocytes and the expression of E-cadherin in TNBC (Figure 24).

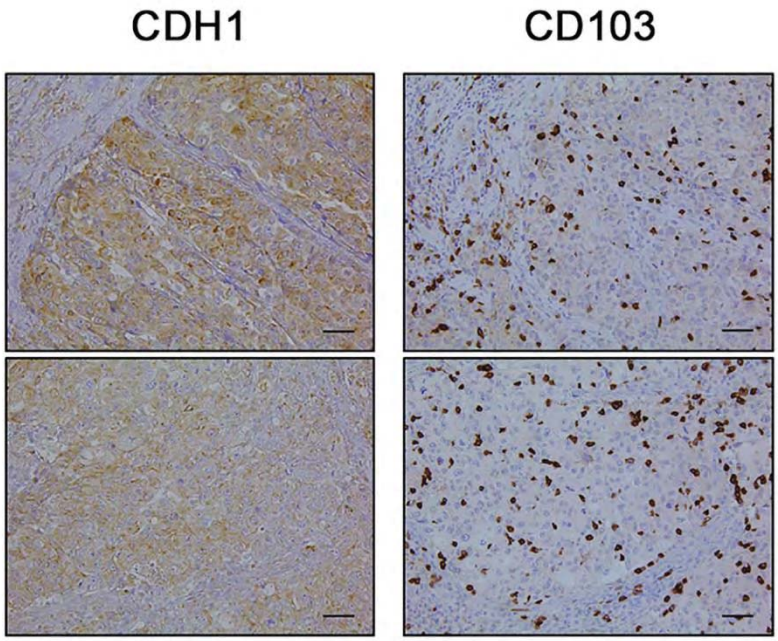

Figure 24. Absence of correlation between CD103+ lymphocytes and E-cadherin expression in triple-negative breast cancer. Representative images showing the lack of correlation between the presence of CD103+ lymphocytes and the expression of E-cadherin in TNBC. Scale bars represent 50 μm.

4.3.2 Association of CD8+ and CD103+ lymphocytes with clinicopathological parameters in triple-negative breast cancer

We next evaluated the association between the presence of CD8+ and CD103+ TIL and clinicopathological characteristics, including age at diagnosis, lymph node status, histological grade, tumour stage, and tumour size in TNBC. There were no consistent associations between the variables examined and the presence of CD8+ or CD103+ TIL in the discovery cohort of 230 TNBC (Table 11). These results were confirmed in an additional cohort of 100 primary TNBC (Table 10 and Table 12).

Table 11. Associations between CD8+ and CD103+ tumour-infiltrating lymphocytes and clinicopathological features in triple-negative breast cancer (n = 230)

		CD8[a]						CD103[a]					
		Overall		Stromal		Intraepithelial		Overall		Stromal		Intraepithelial	
Patient characteristics	***n***	**Median (IQR)**	***P*[b]**	**Median (IQR)**	***P*[b]**	**Median (IQR)**	***P*[b]**	**Median (IQR)**	***P*[b]**	**Median (IQR)**	***P*[b]**	**Median (IQR)**	***P*[b]**
Age at diagnosis													
< 50	120	20 (12.5 – 34)	0.740	10 (6 – 18)	0.751	9 (6 – 15)	0.528	16 (4 – 23)	0.225	4 (1 – 8)	0.486	8.5 (6 – 15)	0.649
≥ 50	110	20 (10 – 36)		10 (5 – 21)		10 (6 – 17)		14 (4 – 22)		3 (2 – 7)		10 (5 – 17)	
Nodal status													
Negative	108	20 (12 – 36)	0.625	10 (6 – 20)	0.466	9.5 (5 – 17)	0.860	15 (4 – 23)	0.626	3.5 (1 – 7)	0.909	5 (3 – 15)	0.519
Positive	122	20 (12 – 34)		10 (6 – 18)		10 (6 – 15.5)		15.5 (4 – 23)		3 (2 – 7)		7 (2 – 15)	
Histological grade													
G1-2	42	17.5 (10 – 29)	0.286	8.5 (5 – 16)	0.354	8 (5 – 13.5)	0.245	5 (4 – 21)	0.259	2 (1 – 6)	0.131	4 (3 – 13)	0.598
G3	188	20 (12 – 36)		10 (6 – 18)		10 (6 – 17)		16 (4 – 23)		4 (2 – 7)		7 (2 – 15)	
pTNM staging													
I-II	156	20 (10 – 36)	0.963	10 (5 – 20)	0.819	10 (5 – 18)	0.753	15.5 (4 – 23)	0.659	3 (2 – 7)	0.650	5 (2 – 15)	0.905
III	74	20 (14 – 34)		10 (7 – 17)		10 (7 – 17)		14 (4 – 23)		3 (1 – 6)		7.5 (2 – 15)	
Tumour size (mm)													
≤ 20	123	24 (14 – 36)	0.077	12 (7 – 21)	0.065	10 (6 – 18)	0.105	17 (4 – 23)	0.146	4 (2 – 7)	0.051	7 (2 – 15)	0.337
> 20	107	16 (12 – 30)		8 (6 – 17)		8 (6 – 13)		12 (4 – 23)		2 (1 – 6)		4 (2 – 14)	

[a]Analysed as a continuous variable.

[b]Mann-Whitney *U* test *P*-values.

Abbreviations: N, number; IQR, Interquartile range.

Table 12. Associations between CD8+ and CD103+ tumour-infiltrating lymphocytes and clinicopathological features in triple-negative breast cancer (n = 100)

		CD8[a]						CD103[a]					
		Overall		Stromal		Intraepithelial		Overall		Stromal		Intraepithelial	
Patient characteristics	***n***	**Median (IQR)**	***P*[b]**	**Median (IQR)**	***P*[b]**	**Median (IQR)**	***P*[b]**	**Median (IQR)**	***P*[b]**	**Median (IQR)**	***P*[b]**	**Median (IQR)**	***P*[b]**
Age at diagnosis													
< 50	45	20 (14 – 45.5)	0.558	8 (6.5 – 24.5)	0.992	10 (7 – 19)	0.487	6 (4 – 19)	0.191	3 (2 – 7.5)	0.184	3 (2 – 14)	0.173
≥ 50	55	23 (12 – 36)		10 (7 – 20)		10 (5 – 20)		14 (4 – 21)		6 (2 – 8)		5 (3 – 15)	
Nodal status													
Negative	59	26 (14 – 42)	0.125	10 (7 – 22)	0.486	15 (7 – 20)	0.054	14 (4 – 23)	0.418	5 (2 – 8)	0.634	6 (2 – 15)	0.640
Positive	41	18 (11 – 36)		8 (5.5 – 19.5)		8 (5 – 19)		10 (4 – 19.5)		4 (1.5 – 7.5)		4 (2 – 14.5)	
Histological grade													
G1-2	40	20 (14 – 41)	0.773	8 (7 – 21)	0.857	15 (5.5 – 20)	0.494	12.5 (4 – 19.5)	0.974	5 (2 – 8)	0.527	5 (2 – 15)	0.838
G3	60	20 (13 – 40.5)		10 (6 – 22)		10 (6 – 19)		10.5 (4 – 23)		4 (2 – 8)		4 (2 – 15)	
pTNM staging													
I-II	67	20 (12 – 39)	0.618	8 (5 – 21)	0.270	10 (5 – 19)	0.735	12 (4 – 20)	0.317	4 (2 – 8)	0.614	4 (2 – 15)	0.162
III	33	19 (14 – 41.5)		11 (7 – 22)		10 (7 – 20)		12 (4 – 24)		6 (2 –7.5)		5 (3 – 15)	
Tumour size (mm)													
≤ 20	56	24 (13 – 42)	0.474	10.5 (7 – 22)	0.279	11.5 (6 – 20)	0.656	13.5 (4 – 23)	0.571	4.5 (2 – 8)	0.532	5 (2 – 15)	0.499
> 20	44	19.5 (13 – 33)		8 (5 – 16.5)		10 (7 – 19)		11 (4 – 20)		4.5 (2 – 8)		4 (2 – 13)	

[a]Analysed as a continuous variable

[b]Mann-Whitney *U* test *P*-values.

Abbreviations: N, number; IQR, interquartile range.

4.3.3 Prognostic value of CD8+ and CD103+ lymphocytes in triple-negative breast cancer

Overall, both CD8+ and CD103+ TIL as continuous variables were associated with better RFS (HR = 0.97; 95% CI, 0.95 – 0.98; *P* = 2.00E-04 for CD8; HR = 0.98; 95% CI, 0.95 – 0.99; *P* = 3.43E-02 for CD103) and OS (HR = 0.97; 95% CI, 0.95 – 0.99; *P* = 2.00E-04 for CD8; HR = 0.98; 95% CI, 0.95 – 0.99; *P* = 4.86E-02 for CD103) in TNBC in univariate analysis (Figure 25). Both TIL subsets retained their prognostic value in multivariate analysis for RFS (HR = 0.97; 95% CI, 0.95 – 0.98; *P* = 2.00E-04 for CD8; HR = 0.97; 95% CI, 0.95 – 0.99; *P* = 2.64E-02 for CD103) and OS (HR = 0.97; 95% CI, 0.95 – 0.98; *P* = 1.00E-04 for CD8; HR = 0.98; 95% CI, 0.95 – 0.99; *P* = 3.73E-02) in TNBC (Table 13).

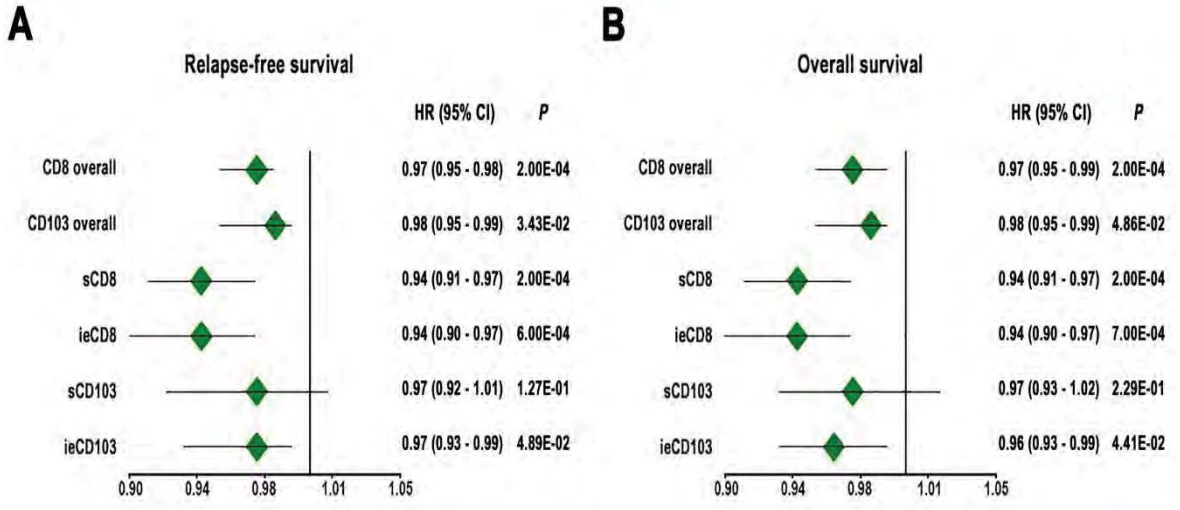

Figure 25. **Univariate Cox regression analysis of CD8+ and CD103+ tumour-infiltrating lymphocytes for relapse-free survival and overall survival in triple-negative breast cancer (*n* = 230).** Forest plot of hazard ratios (HR) with 95% confidence interval (CI) of RFS (A) and OS (B) for CD8+ and CD103+ lymphocytes overall and according to their stromal or intraepithelial localization. The presence of CD8+ and CD103+ cells was analysed as a continuous variable. *P*-values and HR (95% CI in parentheses) are shown.

Table 13. Multivariate Cox regression analysis of CD8+ and CD103+ tumour-infiltrating lymphocytes for relapse-free survival and overall survival in triple-negative breast cancer (*n* = 230)

	Relapse-free survival			Overall survival		
Variable	**HR**	**95% CI**	***P*-value**	**HR**	**95% CI**	***P*-value**
CD8 overall[a]	0.97	0.95 – 0.98	**2.00E-04**	0.97	0.95 – 0.98	**1.00E-04**
Age	1.04	0.63 – 1.72	8.77E-01	1.10	0.66 – 1.82	7.24E-01
Grade	1.57	0.74 – 3.35	2.41E-01	1.94	0.91 – 4.12	8.66E-02
Nodal status	2.90	1.46 – 5.75	**2.30E-03**	2.76	1.39 – 5.47	**3.60E-03**
Tumour size	1.08	0.65 – 1.78	7.68E-01	1.13	0.68 – 1.87	6.32E-01
Tumour stage	1.49	0.84 – 2.65	1.71E-01	1.46	0.82 – 2.62	2.02E-01
CD103 overall[a]	0.97	0.95 – 0.99	**2.64E-02**	0.98	0.95 – 0.99	**3.73E-02**
Age	1.02	0.62 – 1.69	9.24E-01	1.04	0.63 – 1.72	8.75E-01
Grade	1.47	0.69 – 3.13	3.21E-01	1.74	0.82 – 3.70	1.53E-01
Nodal status	3.10	1.57 – 6.14	**1.10E-03**	2.93	1.48 – 5.81	**2.00E-03**
Tumour size	1.20	0.73 – 1.97	4.77E-01	1.23	0.75 – 2.02	4.17E-01
Tumour stage	1.40	0.79 – 2.47	2.47E-01	1.36	0.76 – 2.42	2.97E-01
sCD8[a]	0.94	0.91 – 0.97	**2.00E-04**	0.94	0.91 – 0.97	**1.00E-04**
Age	1.06	0.64 – 1.75	8.18E-01	1.12	0.67 – 1.86	6.64E-01
Grade	1.60	0.75 – 3.41	2.27E-01	1.97	0.92 – 4.19	8.00E-02
Nodal status	2.89	1.46 – 5.71	**2.30E-03**	2.76	1.39 – 5.46	**3.60E-03**
Tumour size	1.08	0.65 – 1.77	7.76E-01	1.12	0.68 – 1.86	6.47E-01
Tumour stage	1.47	0.83 – 2.61	1.85E-01	1.44	0.81 – 2.57	2.20E-01
ieCD8[a]	0.93	0.90 – 0.97	**5.00E-04**	0.94	0.90 – 0.97	**4.00E-04**
Age	1.02	0.62 – 1.70	9.26E-01	1.07	0.64 – 1.78	7.93E-01
Grade	1.53	0.72 – 3.26	2.69E-01	1.87	0.88 – 3.97	1.04E-01
Nodal status	2.92	1.47 – 5.79	**2.10E-03**	2.75	1.39 – 5.46	**3.80E-03**
Tumour size	1.10	0.67 – 1.82	7.05E-01	1.16	0.70 – 1.91	5.68E-01
Tumour stage	1.52	0.85 – 2.70	1.57E-01	1.49	0.83 – 2.67	1.84E-01
ieCD103[a]	0.96	0.93 – 0.99	**3.41E-02**	0.96	0.93 – 0.99	**3.18E-02**
Age	1.03	0.62 – 1.70	9.12E-01	1.05	0.63 – 1.74	8.53E-01
Grade	1.44	0.68 – 3.07	3.45E-01	1.69	0.80 – 3.60	1.71E-01
Nodal status	3.02	1.53 – 5.96	**1.50E-03**	2.86	1.45 – 5.66	**2.50E-03**
Tumour size	1.21	0.74 – 1.99	4.44E-01	1.25	0.76 – 2.05	3.87E-01
Tumour stage	1.46	0.83 – 2.58	1.94E-01	1.42	0.80 – 2.52	2.36E-01

[a]Analysed as a continuous variable.

Multivariate analysis adjusted for age (≥ 50 *v* < 50), histological grade (III *v* I-II), nodal status (1 *v* 0), tumour size (> 20 mm *v* ≤ 20 mm), and tumour stage (III *v* I-II). Significant *P*-values are given in bold.

Abbreviations: CI, confidence interval; HR, hazard ratio; ieCD8/CD103, intraepithelial CD8/CD103, sCD8/CD103, stromal CD8/CD103

When assessing the relevance of TIL according to their localization, we found an association with good outcome for CD8+ cells in both stromal (HR = 0.94; 95% CI, 0.91 –

0.97; *P* = 2.00E-04 for RFS; HR = 0.94; 95% CI, 0.91 – 0.97; *P* = 2.00E-04 for OS) and intraepithelial (HR = 0.94; 95% CI, 0.90 – 0.97; *P* = 6.00E-04 for RFS; HR = 0.94; 95% CI, 0.90 – 0.97; *P* = 7.00E-04 for OS) areas, whereas only intraepithelial CD103+ TIL were predictive of better RFS (HR = 0.97; 95% CI, 0.93 – 0.99; *P* = 4.89E-02) and OS (HR = 0.96; 95% CI, 0.93 – 0.99; *P* = 4.41E-02) (Figure 25). The prognostic value of CD8+ cells in both stromal (HR = 0.94; 95% CI, 0.91 – 0.97; *P* = 2.00E-04 for RFS; HR = 0.94; 95% CI, 0.91 – 0.97; *P* = 1.00E-04 for OS) and intraepithelial (HR = 0.93; 95% CI, 0.90 – 0.97; *P* = 5.00E-04 for RFS; HR = 0.94; 95% CI, 0.90 – 0.97; *P* = 4.00E-04 for OS) areas as well as of intraepithelial CD103+ TIL (HR = 0.96; 95% CI, 0.93 – 0.99; *P* = 3.41E-02 for RFS; HR = 0.96; 95% CI, 0.93 – 0.99; *P* = 3.18E-02 for OS) was confirmed in multivariate analysis (Table 13). These findings were supported by the results from univariate and multivariate Cox regression analyses in the validation cohort (Table 14).

Table 14. Cox regression analysis of CD8+ and CD103+ tumour-infiltrating lymphocytes for relapse-free survival and overall survival in triple-negative breast cancer (*n* = 100)

	Univariate analysis			**Multivariate analysis**		
	HR	**95% CI**	***P*-value**	**HR**	**95% CI**	***P*-value**
			Relapse-free survival			
CD8 overall[a]	0.82	0.74 – 0.91	**2.00E-04**	0.82	0.73 – 0.92	**9.00E-04**
sCD8[a]	0.63	0.50 – 0.80	**2.00E-04**	0.61	0.46 – 0.81	**7.00E-04**
ieCD8[a]	0.75	0.64 – 0.89	**7.00E-04**	0.75	0.62 – 0.90	**1.90E-03**
CD103 overall[a]	0.91	0.84 – 0.98	**1.97E-02**	0.91	0.83 – 0.99	**2.16E-02**
sCD103[a]	0.87	0.74 – 1.02	9.10E-02	-	-	-
ieCD103[a]	0.86	0.76 – 0.98	**2.22E-02**	0.86	0.75 – 0.98	**2.35E-02**
			Overall survival			
CD8 overall[a]	0.88	0.82 – 0.94	**4.00E-04**	0.88	0.82 – 0.95	**6.00E-04**
sCD8[a]	0.79	0.67 – 0.92	**3.10E-03**	0.79	0.67 – 0.93	**4.50E-03**
ieCD8[a]	0.80	0.71 – 0.90	**2.00E-04**	0.80	0.71 – 0.90	**4.00E-04**
CD103 overall[a]	0.91	0.85 – 0.98	**1.13E-02**	0.91	0.84 – 0.98	**9.80E-03**
sCD103[a]	0.88	0.76 – 1.01	6.83E-01	-	-	-
ieCD103[a]	0.87	0.78 – 0.97	**1.23E-02**	0.86	0.77 – 0.97	**1.20E-02**

[a]Analysed as a continuous variable.

Multivariate analysis adjusted for age (≥ 50 *v* < 50), histological grade (III *v* I-II), nodal status (1 *v* 0), tumour size (> 20 mm *v* ≤ 20 mm), and tumour stage (III *v* I-II). Significant *P*-values are given in bold.

Abbreviations: CI, confidence interval; HR, hazard ratio; ieCD8/CD103, intraepithelial CD8/CD103, sCD8/CD103, stromal CD8/CD103

4.3.4 Association between the concurrent presence of intraepithelial CD8+ and CD103+ tumour-infiltrating lymphocytes and the outcome of triple-negative breast cancer patients

Considering the relevance of both TIL subsets in the intraepithelial compartment, we evaluated different protein cut-offs to properly identify TNBC patients (n = 230) with high or low CD8+ and CD103+ TIL density in this tumour area. As the Youden index and the output of the X-Tile software were comparable, we defined the combined X-Tile/ROC cut-off. Following univariate and multivariate Cox regression analyses, we selected the upper quartile for intraepithelial CD8+ TIL and the cut-off identified by the X-Tile/ROC analyses for intraepithelial CD103+ cells as the best predictors of patients' outcome (Table 15).

Table 15. Univariate and multivariate Cox regression analysis of intraepithelial CD8+ and CD103+ tumour-infiltrating lymphocytes cut-offs in triple-negative breast cancer (n = 230)

	Univariate analysis			**Multivariate analysis**		
	HR	**95% CI**	***P*-value**	**HR**	**95% CI**	***P*-value**
Relapse-free survival						
CD8						
50th percentile	0.55	0.33 – 0.90	**1.86E-02**	0.53	0.32 – 0.88	**1.39E-02**
75th percentile	0.38	0.18 – 0.79	**1.02E-02**	0.35	0.16 – 0.73	**5.50E-03**
X-Tile/ROC	0.40	0.21 – 0.79	**8.00E-03**	0.39	0.20 – 0.78	**7.30E-03**
CD103						
50th percentile	0.87	0.53 – 1.41	5.62E-01	-	-	-
75th percentile	0.57	0.30 – 1.09	8.76E-02	-	-	-
X-Tile/ROC	0.42	0.24 – 0.72	**1.70E-03**	0.46	0.26 – 0.80	**5.80E-03**
Overall survival						
CD8						
50th percentile	0.55	0.33 – 0.91	**1.94E-02**	0.52	0.31 – 0.88	**1.35E-02**
75th percentile	0.37	0.18 – 0.77	**8.30E-03**	0.33	0.15 – 0.69	**3.50E-03**
X-Tile/ROC	0.46	0.24 – 0.88	**1.82E-02**	0.44	0.22 – 0.84	**1.32E-02**
CD103						
50th percentile	0.83	0.50 – 1.35	4.45E-01	-	-	-
75th percentile	0.56	0.29 – 1.11	9.70E-01	-	-	-
X-Tile/ROC	0.42	0.24 – 0.72	**1.60E-03**	0.45	0.26 – 0.78	**4.20E-03**

Significant *P*-values are given in bold.

Abbreviations: CI, confidence interval; HR, hazard ratio; ROC, receiver operating characteristic.

Univariate analysis showed that the concurrent presence of high CD8+ and CD103+ TIL was consistently associated with prolonged RFS (HR = 0.23; 95% CI, 0.10 – 0.54; *P* = 7.00E-04) and OS (HR = 0.24; 95% CI, 0.10 – 0.55; *P* = 8.00E-04) compared with tumours with mixed or reduced levels of both TIL subpopulations (Figure 26 and Table 16). Multivariate analysis demonstrated that the concomitant massive intraepithelial infiltration of CD8+ and CD103+ TIL was predictive of RFS (HR = 0.27; 95% CI, 0.11 – 0.63; *P* = 2.40E-03) and OS (HR = 0.28; 95% CI, 0.12 – 0.64; *P* =2.90E-03) in TNBC (Table 16). The ability of the selected cut-offs to discriminate patients' outcomes and the prognostic value of CD8+ and CD103+ TIL were confirmed in the validation cohort (Figure 26 and Table 17).

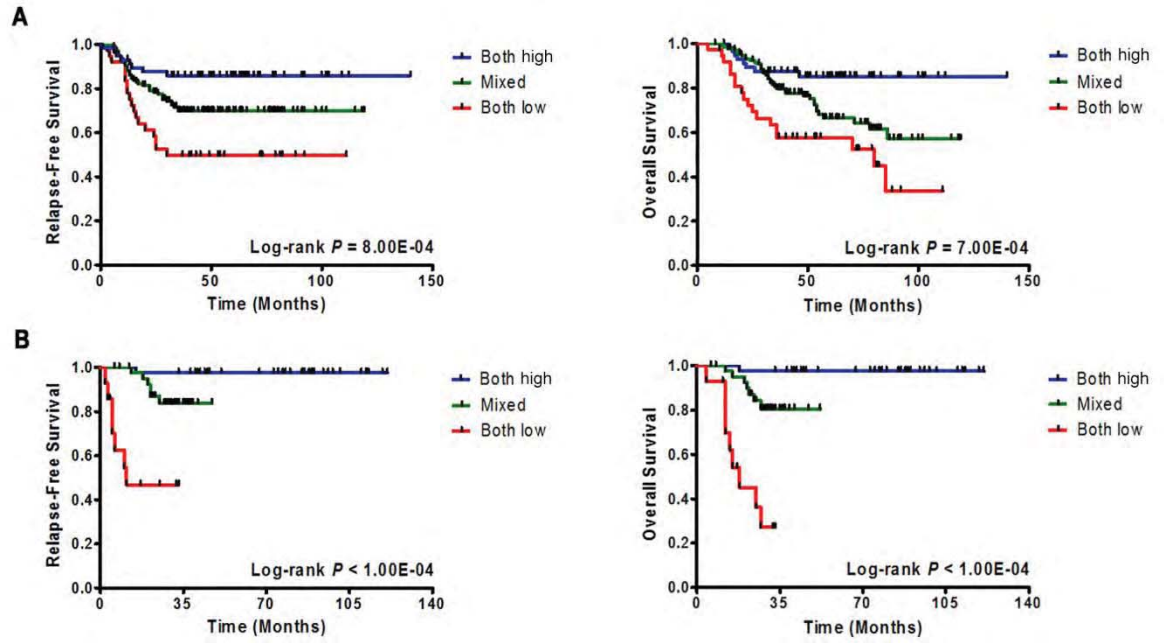

Figure 26. Prognostic value of the concurrent presence of intraepithelial CD8+ and CD103+ tumour-infiltrating lymphocytes in triple-negative breast cancer. (A) Kaplan-Meier curves of RFS and OS in TNBC of the discovery cohort (*n* = 230) stratified according to the expression status of intraepithelial CD8+ and CD103+ TIL. (B) Kaplan-Meier of RFS and OS in TNBC of the validation cohort (*n* = 100) stratified according to the expression status of intraepithelial CD8+ and CD103+ TIL. The upper quartile for intraepithelial CD8+ TIL and the cut-off identified by the X-Tile/ROC analyses for intraepithelial CD103+ cells were used. Curves were compared using log-rank test.

Table 16. Univariate and multivariate Cox regression analysis of the concurrent presence of intraepithelial CD8+ and CD103+ tumour-infiltrating lymphocytes for relapse-free survival and overall survival in triple-negative breast cancer (*n* = 230)

	Relapse-free survival			Overall survival		
Variable	**HR**	**95% CI**	***P*-value**	**HR**	**95% CI**	***P*-value**
			Univariate analysis			
CD8+/CD103+[a]	0.23	0.10 – 0.54	**7.00E-04**	0.24	0.10 – 0.55	**8.00E-04**
			Multivariate analysis			
CD8+/CD103+[a]	0.27	0.11 – 0.63	**2.40E-03**	0.28	0.12 – 0.64	**2.90E-03**
Age	1.27	0.56 – 2.86	5.69E-01	1.47	0.65 – 3.35	3.58E-01
Grade	0.38	0.10 – 1.48	1.64E-01	0.50	0.13 – 1.88	3.02E-01
Nodal status	7.31	2.02 – 26.43	**2.40E-03**	7.43	2.13 – 25.90	**1.60E-03**
Tumour size	1.15	0.51 – 2.60	7.29E-01	1.16	0.51 – 2.63	7.31E-01
Tumour stage	0.70	0.29 – 1.66	4.15E-01	0.59	0.24 – 1.43	2.42E-01

[a]Analysed as a categorical variable. The upper quartile for intraepithelial CD8+ TIL and the cut-off identified by the X-Tile/ROC analyses for intraepithelial CD103+ cells were used.
Multivariate analysis adjusted for age (≥ 50 *v* < 50), histological grade (III *v* I-II), nodal status (1 *v* 0), tumour size (> 20 mm *v* ≤ 20 mm), and tumour stage (III *v* I-II). Significant *P*-values are given in bold.
Abbreviations: CI, confidence interval; HR, hazard ratio

Table 17. Univariate and multivariate Cox regression analysis of intraepithelial CD8+ and CD103+ tumour-infiltrating lymphocytes using the selected cut-offs in the validation cohort (*n* = 100)

	Univariate analysis			Multivariate analysis		
	HR	**95% CI**	***P*-value**	**HR**	**95% CI**	***P*-value**
			Relapse-free survival			
CD8[a]	0.08	0.01 – 0.64	**1.71E-02**	0.10	0.01 – 0.81	**3.04E-02**
CD103[a]	0.14	0.05 – 0.41	**3.00E-04**	0.09	0.03 – 0.29	**1.00E-04**
CD8+/CD103+[a]	0.03	0.01 – 0.25	**1.20E-03**	0.02	0.01 – 0.19	**1.10E-03**
			Overall survival			
CD8[a]	0.07	0.01 – 0.48	**7.30E-03**	0.07	0.01 – 0.50	**8.80E-03**
CD103[a]	0.14	0.05 – 0.36	**1.00E-04**	0.10	0.04 – 0.31	**1.00E-04**
CD8+/CD103+[a]	0.02	0.01 – 0.16	**2.00E-04**	0.01	0.001 – 0.10	**4.00E-04**

[a]Analysed as a categorical variable. The upper quartile for intraepithelial CD8+ TIL and the cut-off identified by the X-Tile/ROC analyses for intraepithelial CD103+ cells were used.
Multivariate analysis adjusted for age (≥ 50 *v* < 50), histological grade (III *v* I-II), nodal status (1 *v* 0), tumour size (> 20 mm *v* ≤ 20 mm), and tumour stage (III *v* I-II). Significant *P*-values are given in bold.
Abbreviations: CI, confidence interval; HR, hazard ratio.

4.3.5 Co-expression of PD-1 and CD103 by tumour-infiltrating lymphocytes in triple-negative breast cancer

To evaluate the hypothesis that the prolonged CD103-mediated intraepithelial retention of CD8+ TIL might result in T cell exhaustion, we analysed the functional status of CD103+ TIL by IHC. We found a consistent correlation between the expression of intraepithelial CD103 and PD-1 in TNBC tissues (rs = 0.515, $P < 1.00E-04$; Figure 27A and B). Double immunofluorescence analysis revealed that PD-1 and CD103 were frequently co-expressed on intraepithelial TIL in TNBC (Figure 28). Furthermore, although PD-1 was not associated with patients' outcome, survival analysis demonstrated that double-positive CD103/PD-1 cells were predictive of good outcome in TNBC (HR = 0.34; 95% CI, 0.16 – 0.71; log-rank $P = 3.90E-03$ for RFS; HR = 0.39; 95% CI, 0.19 – 0.79; log-rank $P = 8.90E-03$ for OS; Figure 29). The association between the density of CD103+/PD-1+ cells and favourable outcome in TNBC was confirmed in the validation dataset (Figure 30).

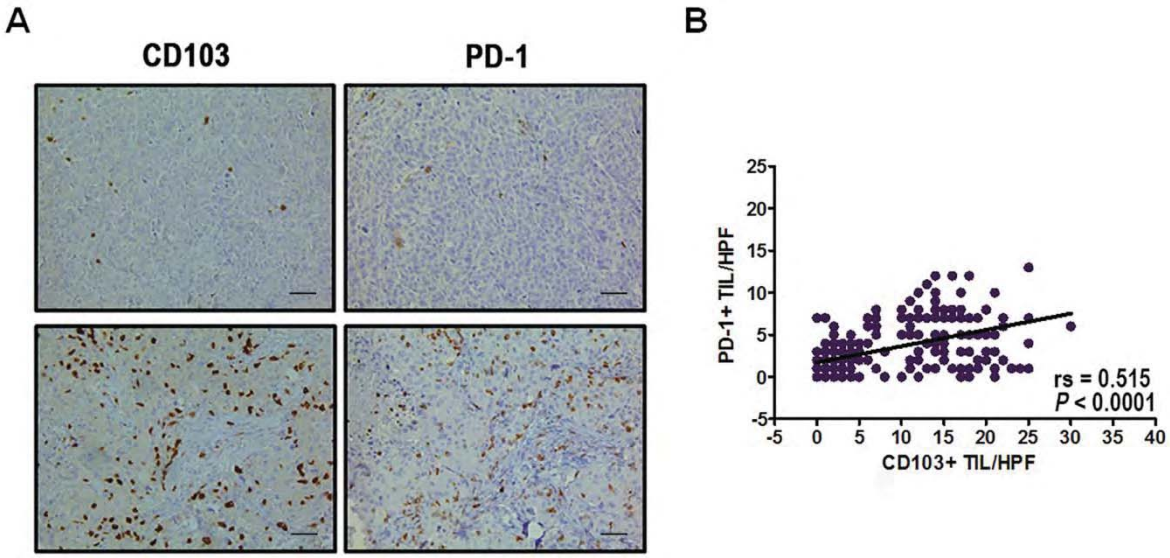

Figure 27. **Correlation between CD103+ and PD-1+ tumour-infiltrating lymphocytes in triple-negative breast cancer**. (A) Representative images of serial sections of TNBC specimens with low (upper panel) and high (lower panel) content of CD103+ and PD-1+ TIL. (B) Spearman's rank correlation analysis between CD103 and PD-1 proteins expression in TNBC of the discovery cohort (rs = 0.515; $P < 1.00E-04$). Scale bars represent 50 μm.

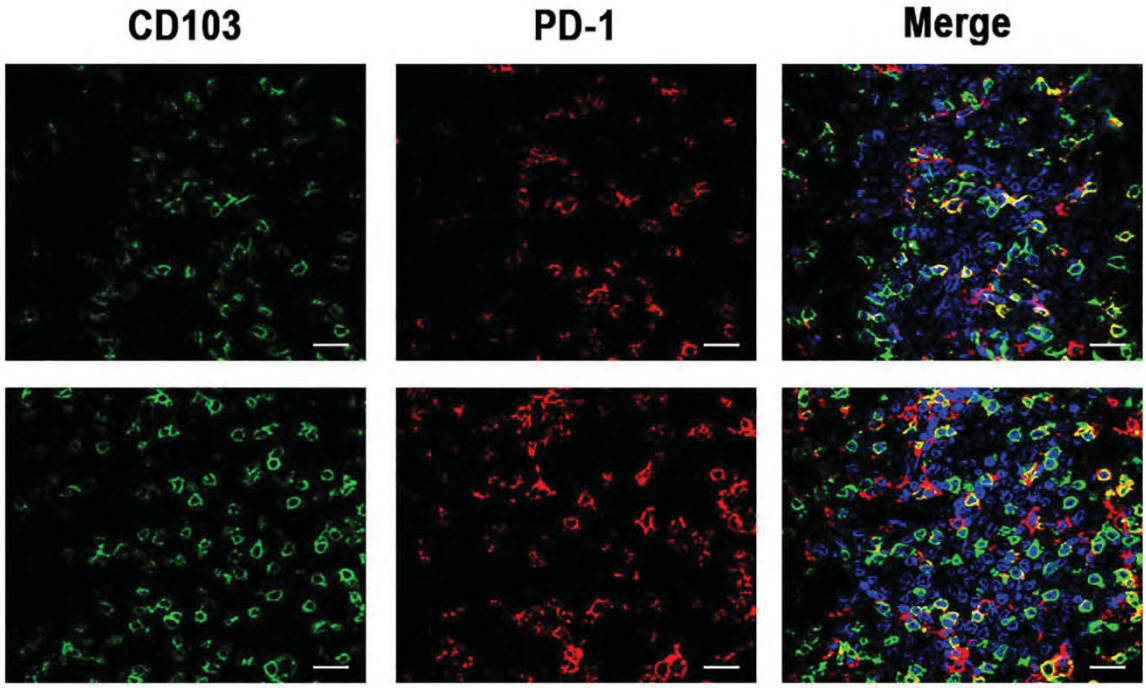

Figure 28. **Co-expression of CD103 and PD-1 on intraepithelial tumour-infiltrating lymphocytes in triple-negative breast cancer**. Representative pictures of double immunofluorescence staining and confocal microscopy showing that PD-1 and CD103 are co-expressed on intraepithelial TIL in TNBC. Scale bars represent 20 µm.

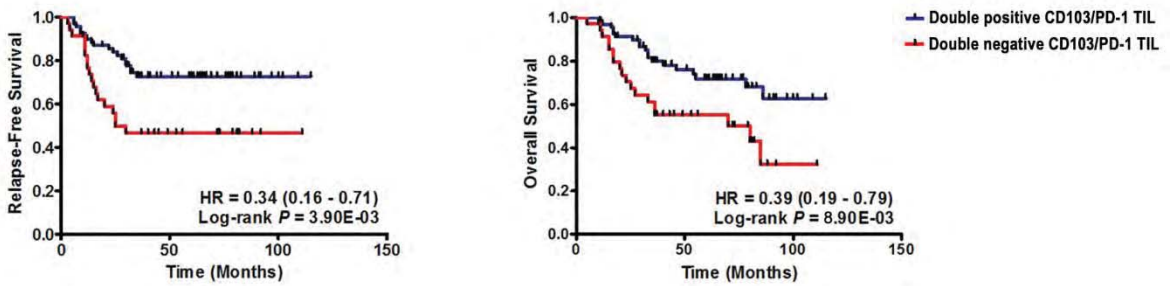

Figure 29. **Association of double-positive CD103/PD-1 tumour-infiltrating lymphocytes with the outcome of triple-negative breast cancer patients (*n* = 230)**. Kaplan-Meier curves of RFS and OS for double-positive CD103/PD-1 cells in TNBC. High CD103 infiltration was defined according to the X-Tile/ROC cut-off. For PD-1, a cut-off value ≥ 5% was used. Curves were compared using log-rank test. *P*-values and hazard ratios (HR) (95% confidence interval in parentheses) are shown.

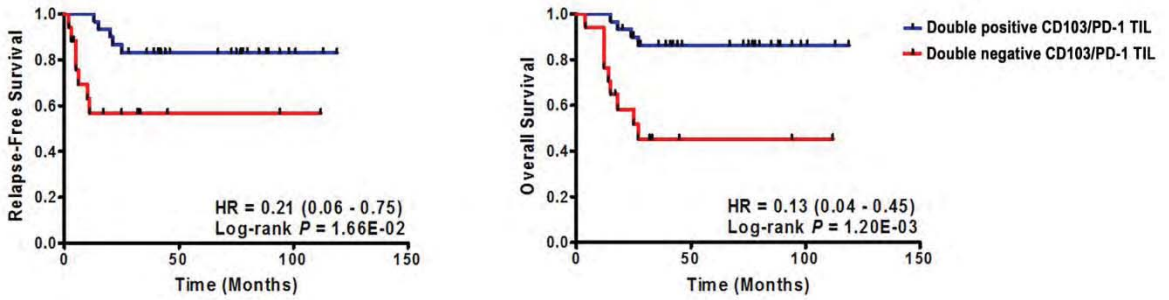

Figure 30. Prognostic value of intraepithelial CD103+/PD-1+ tumour-infiltrating lymphocytes in triple-negative breast cancer of the validation cohort. Kaplan-Meier curves of RFS and OS in TNBC with double-positive and double-negative CD103+/PD-1+ TIL in the validation cohort (*n* = 100). High CD103 infiltration was defined according to the X-Tile/ROC cut-off. For PD-1, a cut-off value ≥ 5% was used. *P*-values and hazard ratios (HR) (95% confidence interval in parentheses) are shown.

4.4 Epithelial-to-mesenchymal transition and tumour-associated inflammation in triple-negative breast cancer

4.4.1 Tumour-associated macrophages in triple-negative breast cancer

We analysed samples from 203 patients with invasive ductal TNBC treated with adjuvant anthracycline-based chemotherapy. Clinical characteristics of patients are presented in Table 18. Approximately 42% of TNBC samples had a dense infiltration of CD68+ macrophages.

4.4.2 The receptor tyrosine kinase AXL is associated with macrophage infiltration in triple-negative breast cancer

To evaluate the link between EMT and the presence of TAM, we selected 30 relevant EMT-related kinases and correlated their expression with the expression of CD68 in TNBC (Table 19). *AXL* was the most significant kinase correlated with the frequency of CD68+ TAM in TNBC (rs = 0.405; Bonferroni-adjusted *P* = 7.00E-03; Figure 31A and Table 19). We confirmed this positive correlation at the protein level (rs = 0.342; *P* < 1.00E-04; Figure 31B) and by analysing gene expression data from 3 publicly available TNBC datasets (*n* = 311) (rs = 0.360; *P* < 1.00E-04; Figure 31C and Table 18).

Table 18. Patient characteristics

Clinical and pathological information	Discovery cohorts			
	Internal cohort	Affymetrix data sets		
		Hatziz	IGR	MAQC-II
Patients (*n*)	203	198	29	84
Median age, years (IQR)	50 (46 – 68)	48.2 (25 – 75)	49 (33 – 67)	50 (29 – 75)
Median tumour size, mm (IQR)	19 (15 – 32)	-	60 (20 – 175)	-
T stage				
T1	51.2%	6.6%	3.5%	13.1%
T2	36.4%	47.0%	31.0%	38.1%
T3	8.0%	32.8%	65.5%	22.6%
T4	3.9%	13.1%	0.0%	21.4%
Unknown	0.5%	0.5%	0.0%	4.8%
TNM Stage				
I-II	67.0%	52.5%	58.6%	45.2%
III	33.0%	46.5%	41.4%	50.0%
Unknown	0.0%	1.0%	0.0%	4.8%
Node status				
Negative	46.3%	27.3%	34.5%	19.0%
Positive	53.7%	72.7%	65.5%	79.8%
Unknown	0.0%	0.0%	0.0%	1.2%
Histological grade				
grade 1	1.0%	0.5%	0.0%	0.0%
grade 2	22.7%	12.7%	13.8%	17.9%
grade 3	76.3%	78.2%	75.9%	72.6%
Unknown		8.6%	10.3%	9.5%
LVI				
Absent	32.0%	-	-	-
Present	18.7%	-	-	-
Unknown	49.3%	-	-	-
Recurrence				
Yes	19.7%	-	-	-
No	80.3%	-	-	-
Site of first metastasis				
Bone	17.0%	-	-	-
Visceral	53.2%	-	-	-
Unknown	29.8%			
Death of breast cancer				
Yes	19.7%	-	-	-
No	78.3%	-	-	-
Unknown	2.0%	-	-	-
Series accession no		GSE25066	GSE22093	GSE20194

Table 18. (continued)

Clinical and pathological information	Validation cohorts	
	Affymetrix data sets	**Internal cohort**
Patients (*n*)	137	95
Median age, years (IQR)	-	51 (46 – 66)
Median tumour size, mm (IQR)	-	20 (9.5 – 30)
T stage		
T1	-	45.3%
T2	-	41.0%
T3	-	8.4%
T4	-	5.3%
Unknown	-	0.0%
TNM Stage		
I-II	-	58.9%
III	-	41.1%
Unknown	-	0.0%
Node status		
Negative	32.8%	45.3%
Positive	32.8%	54.7%
Unknown	34.4%	0.0%
Histological grade		
grade 1	2.2%	2.1%
grade 2	8.0%	20.0%
grade 3	65.7%	77.9%
Unknown	24.1%	
LVI		
Absent	-	44.2%
Present	-	34.7%
Unknown	-	21.1%
Recurrence		
Yes	29.9%	18.9%
No	70.1%	81.1%
Site of first metastasis		
Bone	-	19.0%
Visceral	-	61.9%
Unknown	-	19.1%
Death of breast cancer		
Yes	-	20.0%
No	-	80.0%
Unknown	-	0.0%
Series accession no	GSE3494, GSE4611, GSE5327, GSE1456, GSE19615, GSE21653, GSE31519, GSE37946, GSE45255	

Abbreviations: N, number; IQR, interquartile range; LVI, lymphovascular invasion

Table 19. Correlations between CD68 protein expression and gene expression of the 30 most relevant EMT-associated kinases in triple-negative breast cancer (n = 203).

	CD68 protein expression		
EMT-associated kinases	**Spearman correlation coefficient**	***P*-value[a]**	***P*-value[b]**
AKT1	0.173	**1.37E-02**	3.43E-01
AKT2	-0.086	2.24E-01	2.47E+00
AXL	0.405	**< 1.00E-04**	**7.10E-03**
DDR1	0.048	4.98E-01	3.85E+00
DDR2	0.131	6.25E-02	1.06E+00
EGFR	0.03	6.67E-01	3.85E+00
ERK1	-0.125	7.55E-02	1.13E+00
ERK2	0.171	**1.47E-02**	3.53E-01
FAK	0.177	**1.18E-02**	3.19E-01
FGFR1	0.183	**9.00E-03**	2.52E-01
FGFR2	0.162	**2.08E-02**	4.38E-01
FGFR3	0.13	6.36E-02	1.06E+00
FYN	0.154	**2.81E-02**	5.32E-01
GSK3B	-0.005	9.47E-01	3.85E+00
IGF1R	0.006	9.34E-01	3.85E+00
IKKA	0.156	**2.59E-02**	5.18E-01
IKKB	0.163	**1.99E-02**	4.38E-01
LYN	0.174	**1.32E-02**	3.43E-01
MET	0.052	4.63E-01	3.85E+00
PDGFRA	-0.091	1.97E-01	2.36E+00
PDGFRB	-0.026	7.15E-01	3.85E+00
PTK2B	-0.064	3.65E-01	3.65E+00
SRC	0.056	4.28E-01	3.85E+00
SYK	-0.097	1.67E-01	2.16E+00
TGFBR1	-0.03	6.71E-01	3.85E+00
TGFBR2	0.168	**1.69E-02**	3.89E-01
VEGFR1	0.043	5.43E-01	3.85E+00
VEGFR2	0.111	1.17E-01	1.63E+00
VEGFR3	0.207	**3.10E-03**	8.99E-02
YES1	0.154	**2.80E-02**	5.32E-01

[a]Spearman's rank correlation *P*-values.

[b]*P*-values corrected for multiple-testing error by the Bonferroni method. Significant *P*-values are given in bold.

Abbreviations: EMT, epithelial-to-mesenchymal transition.

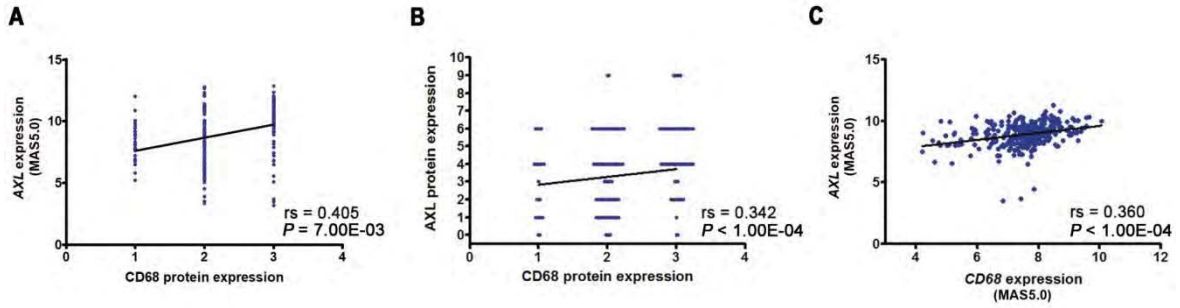

Figure 31. AXL expression correlates with CD68 expression in triple-negative breast cancer. A) Spearman's rank correlation analysis between *AXL* gene expression and CD68 protein in the internal cohort of 203 TNBC (rs = 0.405; Bonferroni-adjusted *P* = 7.00E-03). B) A scatter diagram showing the positive Spearman's correlation between immunohistochemical staining of AXL and CD68 proteins in TNBC (*n* = 203) (rs = 0.342; *P* < 1.00E-04). C) Spearman's rank correlation analysis between the expression of *AXL* and *CD68* performed on gene expression data from publicly available TNBC datasets (*n* = 311) (rs = 0.360; *P* < 1.00E-04).

Considering the potential association between *AXL* expression and tumour immune response, we evaluated the clinical significance of global macrophage content in the internal cohort of TNBC. We found a higher infiltration of CD68+ macrophages in TNBC patients who experienced distant recurrence within 36 months after surgery compared with non-recurrent patients (55.3% *v* 38.5%, *P* = 4.50E-02; Figure 32A and Table 20). No statistically significant association between the presence of CD68+ macrophages and other clinicopathological parameters was, however, identified (Table 20). Furthermore, Kaplan-Meier analysis showed no prognostic relevance of CD68+ macrophage counts in terms of RFS and OS in TNBC (Figure 32B).

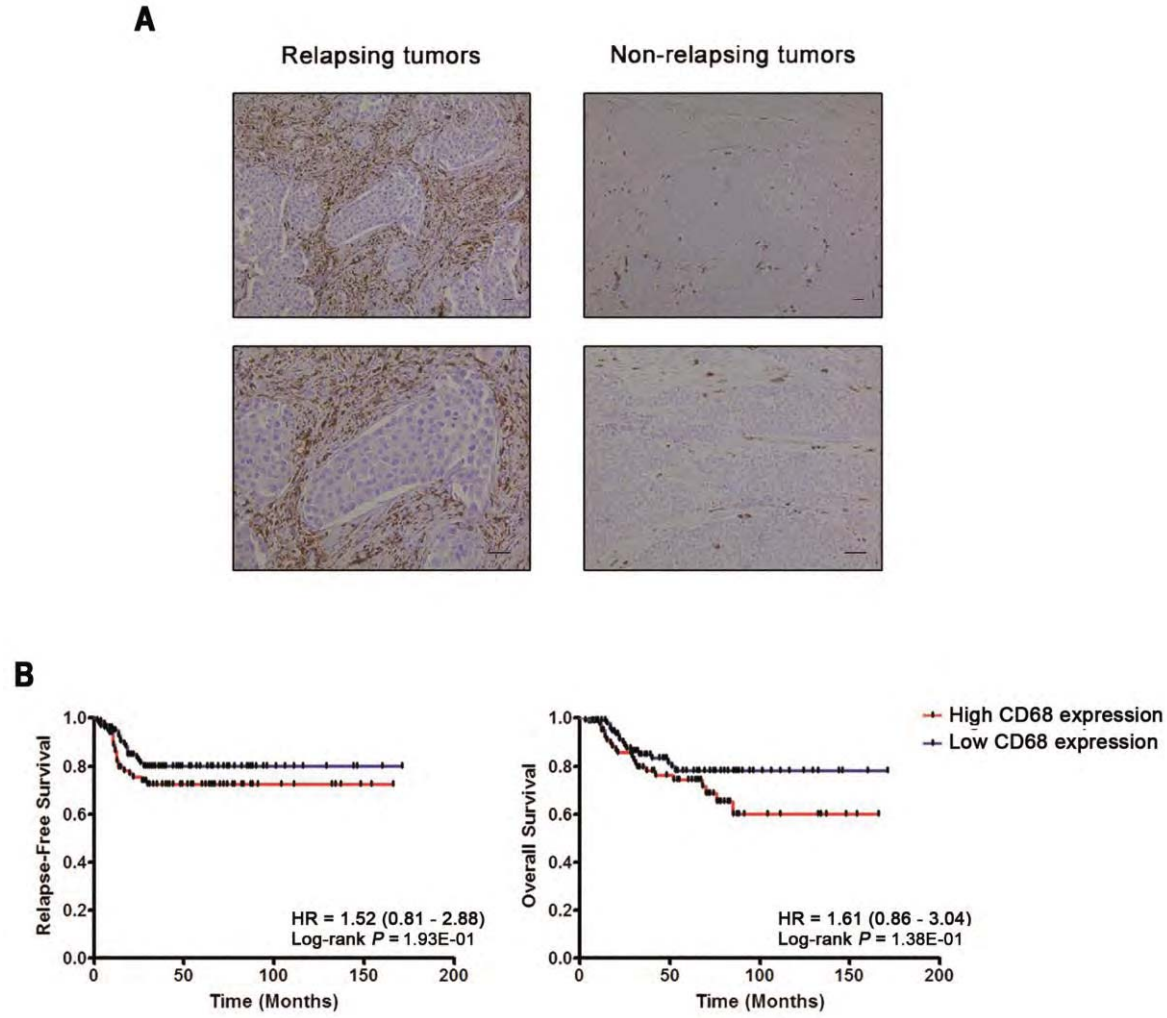

Figure 32. High infiltration of CD68+ cells is associated with relapse but not with survival in triple-negative breast cancer. A) Representative immunohistochemical staining of CD68 in tumour samples from TNBC patients with distant recurrence (left panel) and without recurrence (right panel). Scale bars represent 50 µm. B) Kaplan-Meier analysis for RFS (left panel) and OS (right panel) according to the content of CD68+ macrophages in tumour stroma. TNBC patients (*n* = 203) were stratified by absent/moderate (0 - 2) or dense (3) macrophage infiltration. Curves were compared using log-rank test. *P*-values and hazard ratios (HR) (95% confidence interval in parentheses) are shown.

Table 20. Associations between CD68, CD163 and AXL proteins expression and clinicopathological features in triple-negative breast cancer (n = 203)

		CD68[a]			CD163[a]			AXL[b]		
Patient characteristics	***n***	**High (%)**	**Low (%)**	***P*-value**	**High (%)**	**Low (%)**	***P*-value**	**High (%)**	**Low (%)**	***P*-value**
Age at diagnosis										
< 50	102	39 (38.2)	63 (61.8)	0.257	44 (43.1)	58 (56.9)	0.888	37 (36.3)	65 (63.7)	0.666
≥ 50	101	47 (46.5)	54 (53.5)		45 (44.6)	56 (55.4)		40 (39.6)	61 (60.4)	
Lymph node status										
Negative	96	35 (36.5)	61 (63.5)	0.119	37 (38.5)	59 (58.3)	0.159	29 (30.2)	67 (69.8)	**0.042**
Positive	107	51 (47.7)	56 (52.3)		52 (48.6)	55 (51.4)		48 (44.9)	59(55.1)	
Histological grade										
G1-2	48	21 (43.7)	27 (56.3)	0.868	26 (54.2)	22 (45.8)	0.134	21 (43.7)	27 (56.3)	0.395
G3	155	65 (41.9)	90 (58.1)		63 (40.6)	92 (59.4)		56 (36.1)	99 (63.9)	
TNM staging										
I-II	136	55 (40.4)	81 (59.6)	0.453	58 (42.7)	78 (57.3)	0.654	50 (36.8)	86 (63.2)	0.647
III	67	31 (46.3)	36 (53.7)		31 (46.3)	36 (53.7)		27 (40.3)	40 (59.7)	
Tumour size (mm)										
≤ 20	105	42 (40.0)	63 (60.0)	0.478	47 (44.8)	58 (55.2)	0.888	39 (37.1)	66 (62.9)	0.774
> 20	97	44 (45.4)	53 (54.6)		42 (43.3)	55 (56.7)		38 (39.2)	59 (60.8)	
Lymphovascular invasion										
Absent	65	29 (44.6)	36 (55.4)	0.406	29 (44.6)	36 (55.4)	0.839	24 (36.9)	41 (63.1)	0.835
Present	38	13 (34.2)	25 (65.8)		16 (42.1)	22 (57.9)		15 (39.5)	23 (60.5)	
Recurrence										
Yes	47	26 (55.3)	21 (44.7)	**0.045**	28 (59.6)	19 (40.4)	**0.018**	31 (66.0)	16 (34.0)	**< 0.0001**
No	156	60 (38.5)	96 (61.5)		61 (39.1)	95 (60.9)		46 (29.5)	110 (70.5)	
First site of distant metastasis										
Bone	8	2 (25.0)	6 (75.0)	0.101	4 (50.0)	4 (50.0)	0.695	3 (37.5)	5 (62.5)	**0.036**
Visceral	25	16 (64.0)	9 (36.0)		15 (60.0)	10 (40.0)		20 (80.0)	5 (20.0)	

[a]Triple-negative breast cancer patients were stratified by absent/moderate (0 - 2) or dense (3) CD68+ or CD163+ macrophage infiltration.

[b]Triple-negative breast cancer patients were stratified by low (0 – 4) or high (6 – 9) AXL expression.

Significant *P*-values are given in bold. Abbreviations: N, number; IQR, interquartile range.

4.4.3 AXL correlates with M2-polarized tumour macrophages in triple-negative breast cancer

To evaluate the potential role of AXL in the regulation of cancer-related inflammation in TNBC, we analysed co-regulated genes and pathways using the SEEK platform and the IPA software. This analysis demonstrated that, beyond its well-known role in EMT, AXL was strongly co-expressed with genes involved in several immune functions (Figure 33), confirming AXL as a key player of a gene network that influences both EMT and tumour-associated inflammation in TNBC.

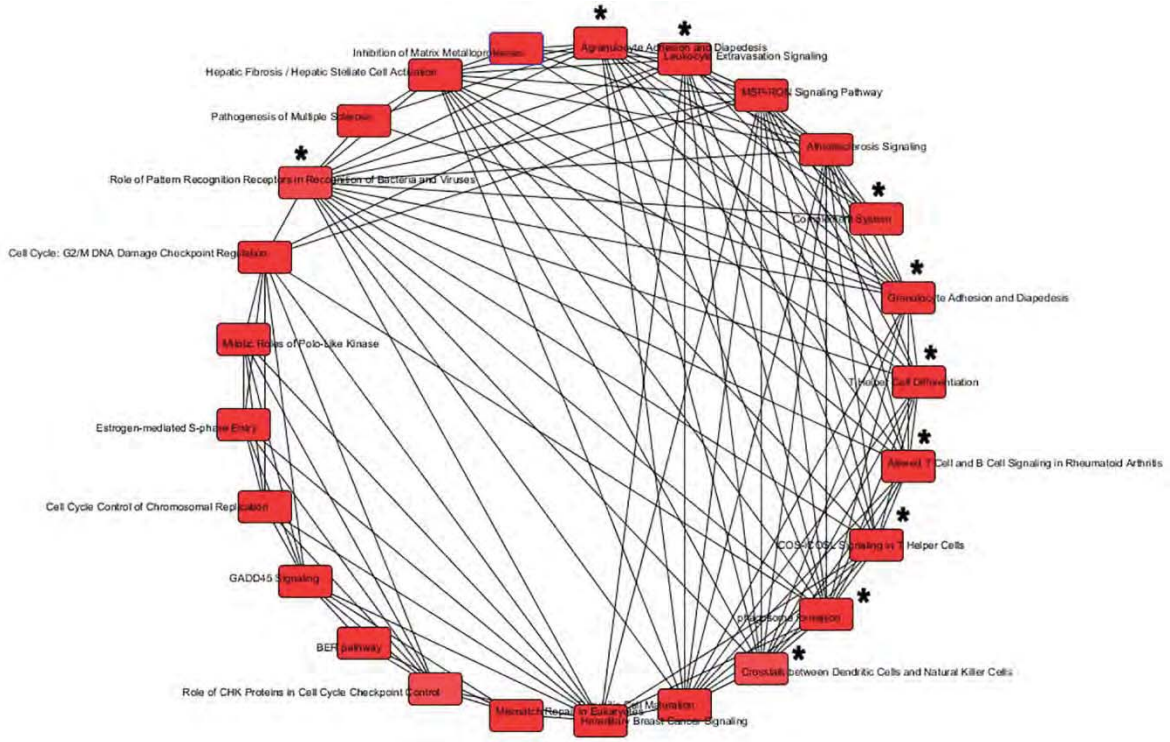

Figure 33. **Co-expression of AXL and genes involved in tumour immune response.** Pathway analysis of genes co-expressed with AXL in TNBC. Co-regulated genes were identified using the SEEK platform and pathway analysis was performed with Ingenuity Pathway Analysis (IPA) software. *P*-values for pathway enrichment were adjusted for multiple testing using the Benjamini-Hochberg correction. Immune pathways are indicated with an asterisk.

Given the plasticity and heterogeneity of macrophages, we next investigated the role of AXL in shaping the inflammatory tumour microenvironment in TNBC. Two distinct immune gene modules reflecting the polarization of anti-tumour M1 or pro-tumour

M2 macrophages were assembled based on a literature review and analysed using SEEK. We found that AXL showed no relationship with M1-polarized macrophages in TNBC, whereas it was consistently co-expressed with genes enclosed in the M2-related module (co-expression score = 1.013; P = 1.30E-02; Figure 34), suggesting that AXL expressed by tumour cells may be involved in the switch toward an M2 phenotype, thus sustaining the pro-tumour activity of TAM.

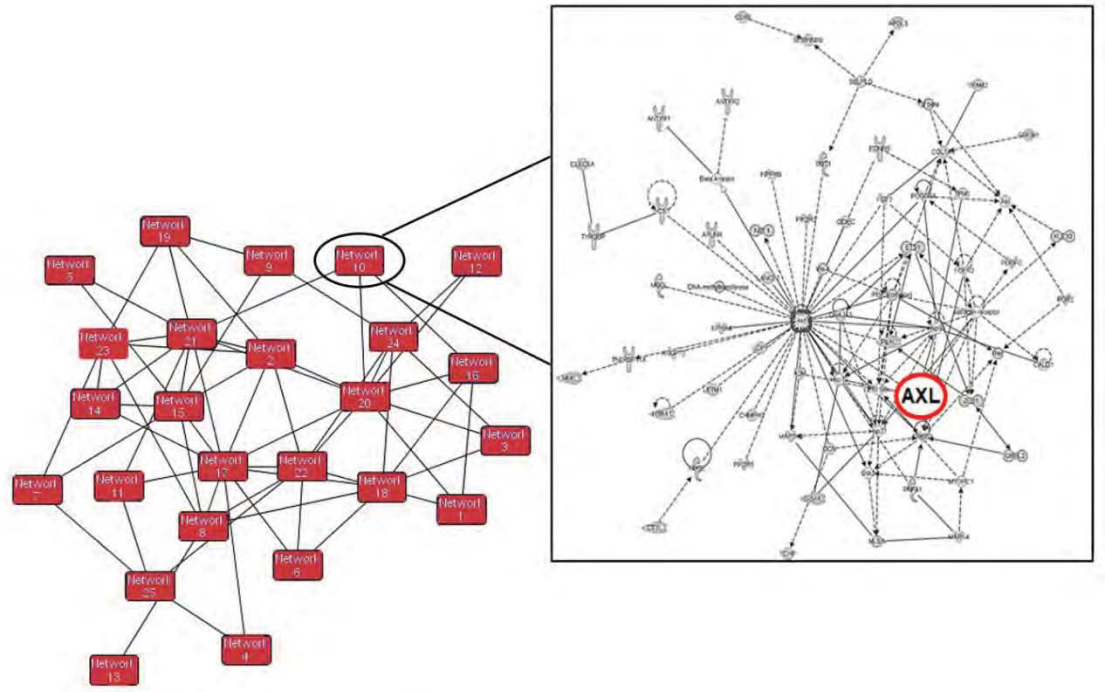

Network 1 Cellular Development, Hematological System Development and Function, Hematopoiesis
Network 2 Cell Death and Survival, Cell Cycle, DNA Replication, Recombination, and Repair
Network 3 Cardiovascular Disease, Developmental Disorder, Hematological Disease
Network 4 Cellular Movement, Cell Morphology, Cellular Growth and Proliferation
Network 5 Lipid Metabolism, Molecular Transport, Small Molecule Biochemistry
Network 6 Cellular Movement, Cardiovascular System Development and Function, Organismal Development
Network 7 Cellular Function and Maintenance, Cellular Growth and Proliferation, Hematological System Development and Function
Network 8 Cellular Movement, Immune Cell Trafficking, Cellular Function and Maintenance
Network 9 Cancer, Organismal Injury and Abnormalities, Cell Death and Survival
Network 10 Cellular Movement, Cell Death and Survival, Cellular Development
Network 11 Cellular Movement, Cell Morphology, Cellular Assembly and Organization
Network 12 Cancer, Connective Tissue Disorders, Developmental Disorder
Network 13 Developmental Disorder, Hereditary Disorder, Metabolic Disease
Network 14 Cell-To-Cell Signaling and Interaction, Hematological System Development and Function, Immune Cell Trafficking
Network 15 Cellular Movement, Hematological System Development and Function, Immune Cell Trafficking
Network 16 Hereditary Disorder, Neurological Disease, Organismal Injury and Abnormalities
Network 17 Gene Expression, Cancer, Cell Death and Survival
Network 18 Cell Death and Survival, Cellular Movement, Cancer
Network 19 Cell Death and Survival, Post-Translational Modification, Protein Degradation
Network 20 Cellular Growth and Proliferation, Cell Cycle, Cellular Development
Network 21 RNA Post-Transcriptional Modification, Developmental Disorder, Neurological Disease
Network 22 Gene Expression, Cell Cycle, Cell Morphology
Network 23 Cellular Function and Maintenance, Hematological System Development and Function, Lymphoid Tissue Structure and Development
Network 24 Cardiovascular System Development and Function, Cellular Assembly and Organization, DNA Replication, Recombination, and Repair
Network 25 Cellular Movement, Cancer, Organismal Injury and Abnormalities

Figure 34. AXL is involved in a gene network regulating M2 macrophages. The image represents the top networks identified with Ingenuity Pathway Analysis (IPA) software for the genes significantly co-expressed (P < 0.01) with the immune module reflecting the polarization of M2 macrophages. As evidenced in the right panel, *AXL* is present in the signalling network associated with the M2-related module.

To confirm these observations, we analysed the expression of AXL and the M2 macrophage marker CD163 in the testing cohort of TNBC patients, identifying a positive correlation between AXL and the infiltration of CD163+ cells (rs = 0.503; P < 1.00E-04; Figure 35A). Furthermore, TNBC patients who experienced distant relapse had a significant higher expression of both AXL and CD163 compared with patients without recurrence (P < 1.00E-04 and P = 1.80E-02, respectively; Figure 35B, and Table 20).

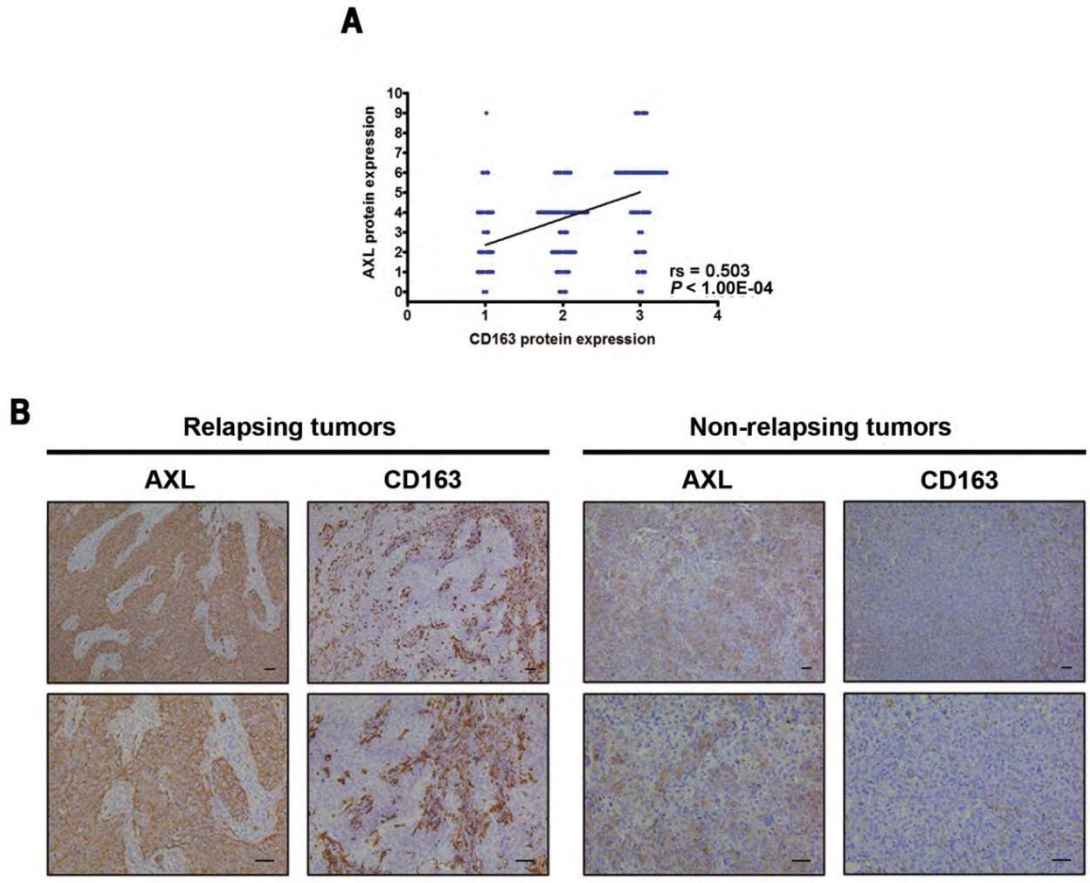

Figure 35. AXL expression correlates with the infiltration of CD163+ cells in triple-negative breast cancer. A) A scatter diagram showing a positive Spearman's correlation between immunohistochemical staining of AXL and CD163 in TNBC (n = 203; rs = 0.5031; P < 1.00E-04). B) Representative immunohistochemical staining of AXL and CD163 in serial sections of samples from TNBC patients with recurrence (left panel) and without recurrence (right panel). Scale bars represent 50 μm.

High levels of AXL expression were also associated with lymph node positivity (P = 4.20E-02) and interestingly with metastasis to visceral organs as the first sites of distant recurrence (P = 3.60E-02) (Table 20). Furthermore, double immunofluorescence staining

for AXL and CD163, clearly demonstrated the specific localization of macrophages in direct contact with AXL-expressing tumour cells (Figure 36).

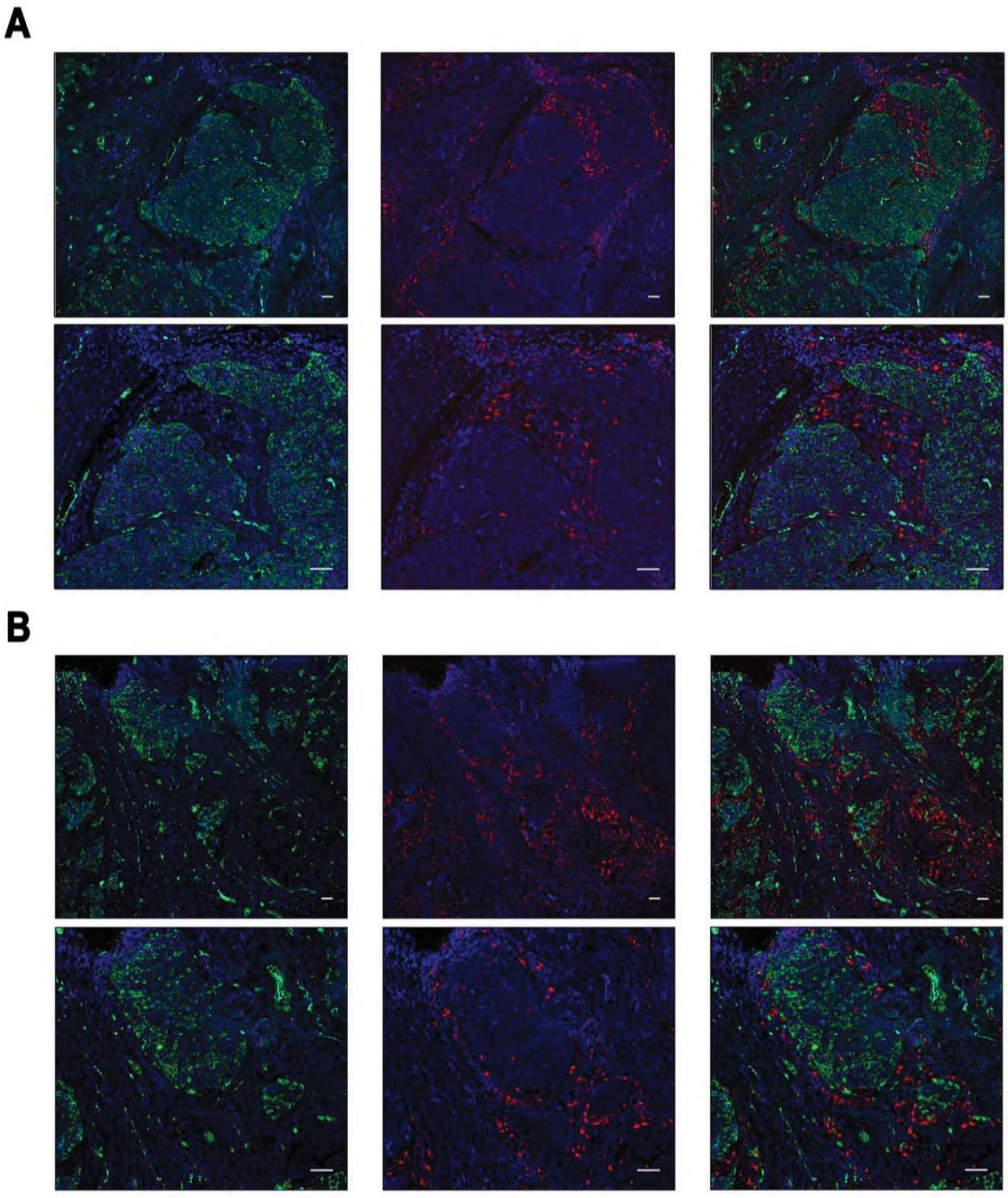

Figure 36. CD163+ macrophages are in direct contact with AXL-expressing tumour cells. A, B) Representative pictures of double immunofluorescent staining and confocal microscopy of two different TNBC samples showing that AXL-expressing cancer cells (green) are in close contact with adjacent stromal TAM (red). Scale bars represent 50 μm.

4.4.4 AXL is an independent prognostic marker in triple-negative breast cancer

To assess the prognostic value of AXL and CD163 in TNBC patients, we performed Kaplan-Meier and Cox univariate regression analyses in the internal cohort of TNBC (Figure 37 and Table 21). We found that patients with high levels of AXL protein expression had significant shorter RFS and OS (HR = 3.44; 95% CI, 1.78 – 6.65; log-rank *P* = 2.00E-04 for RFS; HR = 3.38; 95% CI, 1.75 – 6.50; log-rank *P* = 3.00E-04 for OS; Figure 37A and Table 21), whereas CD163 was associated with RFS only (HR = 2.03; 95% CI, 1.08 – 3.83; log-rank *P* = 2.90E-02; Figure 37B and Table 21).

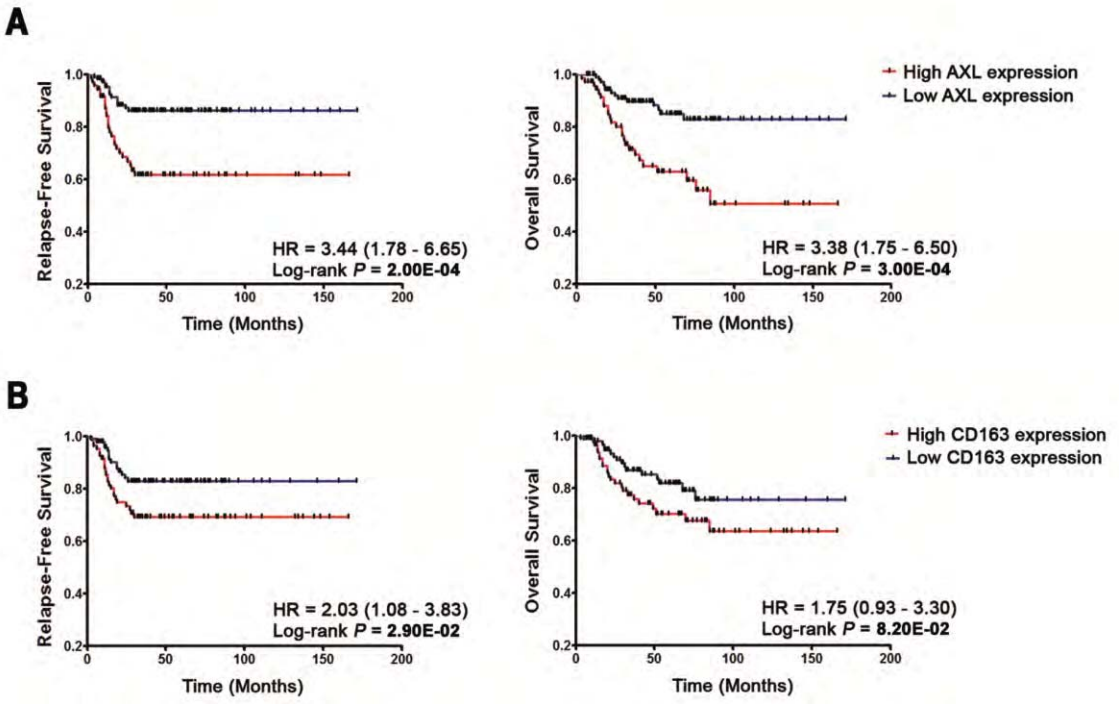

Figure 37. AXL is associated with survival in triple-negative breast cancer. A) Kaplan-Meier analysis for RFS (left panel) and OS (right panel) according to AXL scoring. TNBC patients (*n* = 203) were stratified by low (0-4) or high (6-9) AXL expression. B) Kaplan-Meier analysis for RFS (left panel) and OS (right panel) according to the content of CD163+ cells in tumour stroma. TNBC patients were stratified by absent/moderate (0-2) or dense (3) CD163+ macrophage infiltration. Curves were compared using log-rank test. *P*-values and hazard ratios (HR) (95% confidence interval in parentheses) are shown.

Table 21. Univariate Cox regression analysis of AXL and CD163 for relapse-free survival and overall survival in triple-negative breast cancer (*n* = 203).

	Relapse-Free Survival			Overall Survival		
Variable	**HR**	**95% CI**	***P*-value**	**HR**	**95% CI**	***P*-value**
AXL[a]	3.19	1.66 – 6.14	**5.00E-04**	3.16	1.64 – 6.08	**6.00E-04**
CD163[b]	2.02	1.06 – 3.85	**3.29E-02**	1.75	0.92 – 3.31	8.65E-02

[a]Triple-negative breast cancer patients were were stratified by low (0 – 4) or high (6 – 9) AXL expression.
[b]Triple-negative breast cancer patients were stratified by absent/moderate (0 - 2) or dense (3) CD68+ or CD163+ macrophage infiltration.
Significant *P*-values are given in bold. Abbreviations: CI, confidence interval; HR, hazard ratio.

Cox multivariate analysis demonstrated that only AXL expression remained an independent prognostic factor in TNBC patients, while CD163 only retained a positive trend for reduced RFS (Table 22). Multivariate analysis performed in an additional independent cohort of 95 TNBC, and analysing AXL as a continuous variable, confirmed the prognostic significance of AXL for both RFS and OS (Table 23 and Table 24).

Table 22. Multivariate Cox regression analysis of AXL and CD163 for relapse-free survival and overall survival in triple-negative breast cancer (*n* = 203).

	Relapse-Free Survival			Overall Survival		
Variable	**HR**	**95% CI**	***P*-value**	**HR**	**95% CI**	***P*-value**
AXL[a]	2.84	1.45 – 5.55	**2.20E-03**	3.09	1.58 – 6.06	**1.00E-03**
Age	0.88	0.46 – 1.69	7.11E-01	1.08	0.57 – 2.07	8.09E-01
Grade	1.68	0.69 – 4.11	2.53E-01	2.06	0.84 – 5.09	1.16E-01
Nodal status	2.53	1.01 – 6.31	**4.72E-02**	2.62	1.05 – 6.55	**3.98E-02**
Tumour size	1.33	0.69 – 2.58	3.97E-01	1.17	0.61 – 2.25	6.30E-01
Tumour stage	1.72	0.81 – 3.66	1.60E-01	1.67	0.78 – 3.57	1.88E-01
CD163[b]	1.85	0.96 – 3.55	6.58E-02	1.63	0.85 – 3.12	1.40E-01
Age	0.95	0.50 – 1.80	8.72E-01	1.16	0.61 – 2.20	6.45E-01
Grade	1.68	0.68 – 4.13	2.60E-01	1.90	0.77 – 4.73	1.65E-01
Nodal status	2.90	1.18 – 7.13	**2.02E-02**	3.08	1.25 – 7.59	**1.43E-02**
Tumour size	1.36	0.70 – 2.65	3.60E-01	1.19	0.62 – 2.30	5.99E-01
Tumour stage	1.54	0.74 – 3.22	2.48E-01	1.41	0.67 – 2.94	3.66E-01

[a]Triple-negative breast cancer patients were were stratified by low (0 – 4) or high (6 – 9) AXL expression.
[b]Triple-negative breast cancer patients were stratified by absent/moderate (0 - 2) or dense (3) CD68+ or CD163+macrophage infiltration.
Multivariate analysis adjusted for age (≥50 *v* <50), histological grade (G3 *v* G1-2), nodal status (1 *v* 0), tumour size (> 20 mm *v* ≤ 20 mm), and tumour stage (III *v* I-II). Significant *P*-values are given in bold.
Abbreviations: CI, confidence interval; HR, hazard ratio.

Table 23. Multivariate Cox regression analysis of AXL for relapse-free survival and overall survival in the validation cohort of triple-negative breast cancer (*n* = 95)

	Relapse-Free Survival			Overall Survival		
Variable	**HR**	**95% CI**	***P*-value**	**HR**	**95% CI**	***P*-value**
AXL[a]	6.05	1.93 – 18.72	**1.80E-03**	6.09	2.12 – 17.54	**8.00E-04**
Age	0.87	0.32 – 2.36	7.86E-01	0.89	0.35 – 2.25	8.01E-01
Grade	1.54	0.42 – 5.57	5.12E-01	2.01	0.55 – 7.32	2.90E-01
Nodal status	5.96	1.16 – 30.57	**3.20E-02**	3.99	1.05 – 15.19	**4.20E-02**
Tumour size	1.69	0.63 – 4.54	2.96E-01	1.43	0.53 – 3.85	4.76E-01
Tumour stage	1.12	0.36 – 3.51	8.44E-01	1.01	0.31 – 3.21	9.93E-01

[a]Triple-negative breast cancer patients were were stratified by low (0 – 4) or high (6 – 9) AXL expression. Significant *P*-values are given in bold. Abbreviations: CI, confidence interval; HR, hazard ratio.

Table 24. Multivariate Cox regression analysis of AXL evaluated as a continuous variable for relapse-free survival and overall survival in the discovery (*n* = 203) and validation (*n* = 95) cohorts of triple-negative breast cancer.

	Relapse-Free Survival			Overall Survival		
Variable	**HR**	**95% CI**	***P*-value**	**HR**	**95% CI**	***P*-value**
			Discovery cohort			
AXL	1.25	1.07 – 1.46	**3.39E-03**	1.32	1.13 – 1.53	**5.00E-04**
Age	0.95	0.50 – 1.82	8.81E-01	1.09	0.57 – 2.07	8.05E-01
Grade	1.60	0.65 – 3.90	3.04E-01	1.93	0.78 – 4.74	1.54E-01
Nodal status	2.67	1.07 – 6.67	**3.49E-02**	1.37	0.61 – 3.08	4.42E-01
Tumour size	1.51	0.78 – 2.91	2.18E-01	1.14	0.60 – 2.17	6.91E-01
Tumour stage	1.71	0.80 – 3.68	1.66E-01	1.22	0.52 – 2.87	6.49E-01
			Validation cohort			
AXL	1.42	1.12 – 1.81	**4.44E-03**	1.44	1.13 – 1.83	**3.00E-03**
Age	1.20	0.44 – 3.30	7.23E-01	1.24	0.47 – 3.26	6.65E-01
Grade	1.54	0.42 – 5.62	5.14E-01	1.91	0.53 – 6.97	3.25E-01
Nodal status	5.65	1.06 – 30.24	**4.30E-02**	3.44	0.88 – 13.42	7.58E-02
Tumour size	1.47	0.51 – 4.27	4.78E-01	1.20	0.43 – 3.35	7.34E-01
Tumour stage	0.97	0.32 – 2.93	9.52E-01	0.88	0.29 – 2.65	8.23E-01

Multivariate analysis adjusted for age (≥50 *v* <50), histological grade (G3 *v* G1-2), nodal status (1 *v* 0), tumour size (> 20 mm *v* ≤ 20 mm), and tumour stage (III *v* I-II). Significant *P*-values are given in bold. Abbreviations: CI, confidence interval; HR, hazard ratio.

We next assessed the prognostic value of *AXL* by analysing the gene expression data from 137 TNBC patients treated with adjuvant chemotherapy (Table 18). *AXL* expression was consistently associated with reduced RFS (HR = 2.3; 95% CI, 1.20 – 4.30; log-rank *P* = 8.00E-03; Figure 38A), and did not correlate with the expression of the proliferation marker *MKI67* (Pearson's coefficient [r] = 0.014; Figure 38B), suggesting a role of AXL towards cellular dedifferentiation.

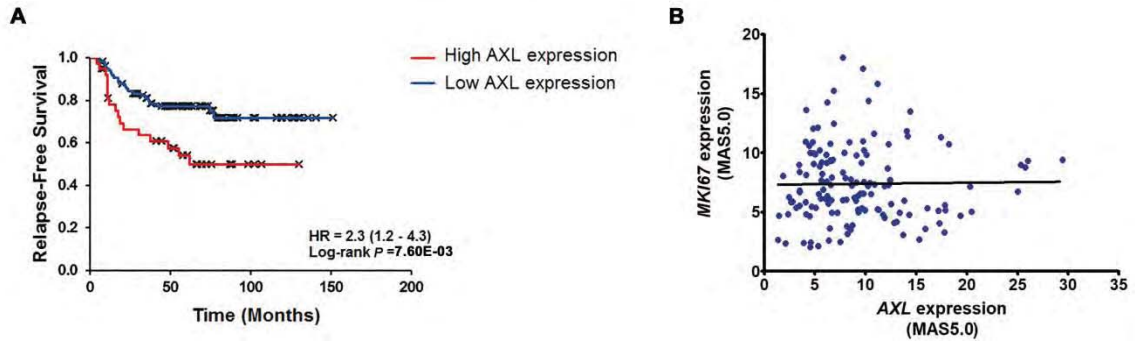

Figure 38. *AXL* expression is predictive of relapse-free survival independently of proliferation in adjuvant chemotherapy-treated triple-negative breast cancers. A) Kaplan-Meier analysis for RFS according to *AXL* expression in 137 TNBC treated with adjuvant chemotherapy. The median expression value of *AXL* was used as cut-off. B) Pearson's correlation analysis showing that *AXL* expression does not correlate with the expression of *MKI67* (r = 0.014). *P*-values and hazard ratios (HR) (95% confidence interval in parentheses) are shown.

4.4.5 AXL-overexpressing breast cancer cells and M2-like macrophages reciprocally interact in vitro

To characterize the expression of *AXL in vitro* we analysed the expression of *AXL*, EMT (*CDH1* and *VIM*), and basal (*EGFR*, *KRT5*, and *KRT6A*) markers in 15 breast cancer cell lines by qRT-PCR. *AXL* expression was higher in all triple-negative mesenchymal-like breast cancer cell lines compared with luminal cells (Figure 39A). High levels of *AXL* expression were also found in two triple-negative basal-like cells (Figure 39A).

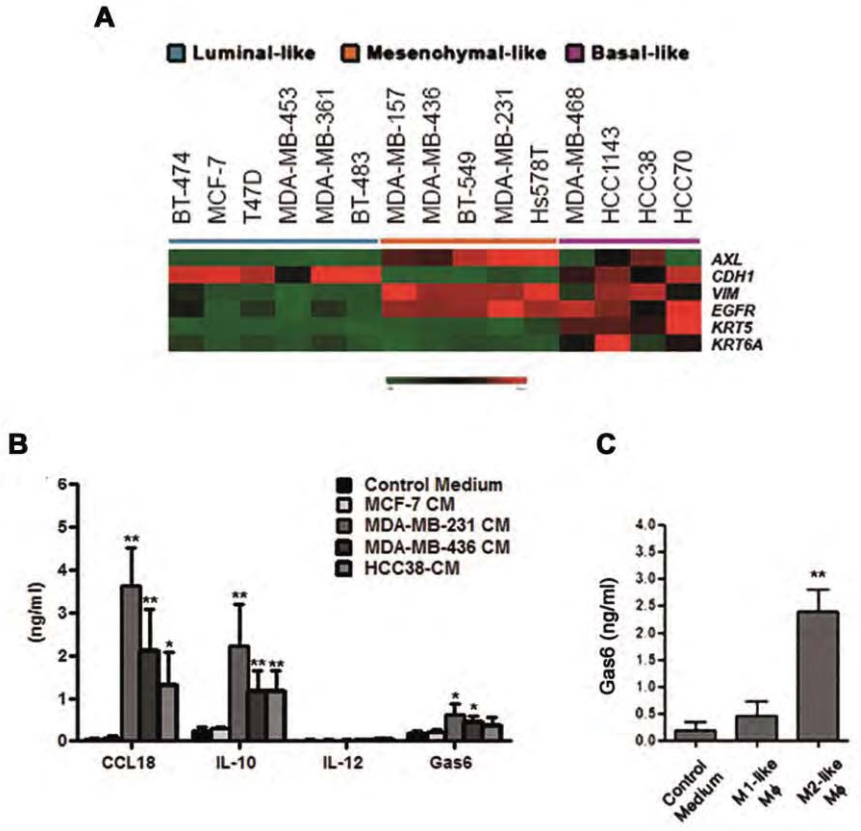

Figure 39. *AXL*-overexpressing breast cancer cells promote the release of pro-tumour cytokines/chemokines. A) Expression analysis of *AXL,* EMT (*CDH1* and *VIM*) and basal (*EGFR, KRT5,* and *KRT6A*) markers in 15 breast cancer cell lines by qRT-PCR. Gene expression levels are visualized in a heatmap. B) Cytokine levels in the media of macrophages cultured in the absence or presence of MCF-7- or TNBC-derived CM measured by ELISA. C) ELISA analysis of Gas6 in the medium of *in vitro* polarized human macrophages (Mφ). *P*-values were obtained using a two-tailed Student's *t* test (mean ± SD, $n = 4$ experiments; $*P < 0.05$; $**P \leq 0.01$).

Then, we investigated the biological mechanisms underlying the cross-talk between *AXL*-expressing breast cancer cells and TAM. To identify the soluble factors potentially mediating the interaction between macrophages and breast cancer cells we measured the release of several major cytokines/chemokines by macrophages exposed to the CM derived from the *AXL*-expressing breast cancer cell lines HCC38, MDA-MB-231, and MDA-MB-436, and from *AXL*-negative MCF-7 cells. We found that the medium of macrophages treated with *AXL*-expressing cells-CM, especially from mesenchymal-like cells, was enriched for tumour-promoting mediators, including CCL18 and IL-10, compared with that from macrophages treated with MCF-7-CM (Figure 39B). Conversely, the presence of

AXL-expressing cells did not affect the release of IL-12, which is commonly associated with the M1 phenotype (Figure 39B). Mesenchymal-like cells also induced an increased production of the AXL ligand Gas6 ($P \leq 0.05$) and a positive trend was also observed for basal-like cells, although not reaching statistical significance (Figure 39B). Consistently, we found that Gas6 was significantly released from *in vitro*-polarized M2-like macrophages, but not from M1-like cells ($P = 1.40E-02$; Figure 39C).

To further investigate the ability of *AXL*-expressing TNBC cells to promote macrophage polarization toward a pro-tumour phenotype we analysed the expression of the M2 specific markers CD206 and CD163 by flow cytometry (Figure 40A).

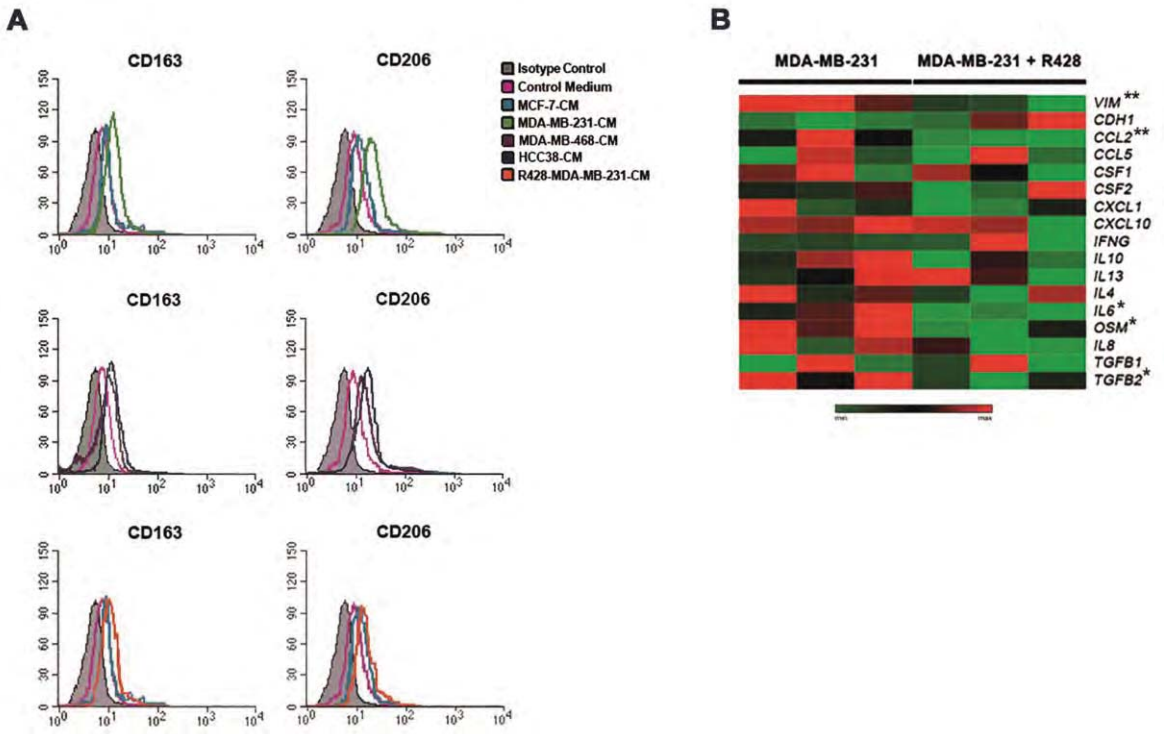

Figure 40. *AXL*-overexpressing breast cancer cells promote the polarization of M2 macrophages. A) Flow cytometric analysis of the M2 markers CD163 and CD206 in human monocytes cultured in the absence (pink) or presence of MCF-7-CM (light blue), MDA-MB-231-CM (green; upper panel), basal-like HCC38-CM (dark blue; middle panel), *AXL*-negative basal-like MDA-MB-468-CM (purple; middle panel), or R428-treated MDA-MB-231-CM (orange; lower panel) for 6 days. Grey histograms represent staining with isotype controls. The histograms are representatives of five independent experiments. B) Heatmap showing the effect of R428 on the expression of EMT markers and relevant cytokines/chemokines in MDA-MB-231 cells. Significant genes are indicated with an asterisks (two-tailed Student's t test; $*P < 0.05$; $**P \leq 0.01$).

AXL-expressing mesenchymal-like TNBC cells, but not MCF-7, were able to polarize macrophages toward an M2 phenotype (Figure 40A, upper panel). Also *AXL*-expressing basal-like cells induced these phenotypic changes in macrophages, although to a lesser extent than mesenchymal-like cells, while the polarizing effect of *AXL*-negative basal-like cells was marginal (Figure 40A, middle panel), suggesting that AXL may sustain the cancer-inflammation cross-talk beyond its primary role in EMT. Noteworthy, the ability of MDA-MB-231 cells to change the expression of these surface markers was impaired by the selective inhibition of AXL with R428 (Figure 40A, lower panel). Consistently, we found that R428-treated MDA-MB-231 cells showed reduced expression of vimentin (P = 0.008), *CCL2* (P = 0.008), *IL6* (P = 0.024), Oncostatin M (*OSM*; P = 0.019), and *TGFB2* (P = 0.029) (Figure 40B), indicating that AXL may contribute to the recruitment and polarization of macrophages by increasing the release of specific cytokines and chemokines.

4.4.6 AXL influences cancer cell aggressiveness and response to chemotherapy in triple-negative breast cancer

We next evaluated the relevance of the reciprocal cross-talk between M2 TAM and cancer cells for tumour progression and chemotherapy response. We demonstrated that the CM from M2-polarized macrophages enhanced the MDA-MB-231 cell migration (P = 2.00E-02; Figures 41A and B) and increased the resistance of MDA-MB-231 and HCC38 TNBC cells to paclitaxel (P = 2.80E-02; P = 3.90E-02, respectively) and doxorubicin (P = 4.30E-02; P = 2.90E-02, respectively) (Figure 41C). Importantly, AXL inhibition with R428 reduced the migratory capacity (P = 3.60E-02, Figures 40A and B) and restored the sensitivity of MDA-MB-231 and HCC38 cells to paclitaxel (P = 1.20E-02; P = 1.90E-02, respectively) and doxorubicin (P = 2.70E-02; P = 2.00E-02, respectively; Figure 41C). In addition to AXL inhibition, the treatment with R428 affected the activation of other oncogenic pathways, including AKT, ERK1/2, and SRC signalling, suggesting possible

cross-talks and escape mechanisms to AXL inhibition in TNBC (Figure 41D). Collectively, these data suggest that the interaction between M2 TAM and TNBC cells through AXL plays an important role in supporting tumour progression and chemoresistance.

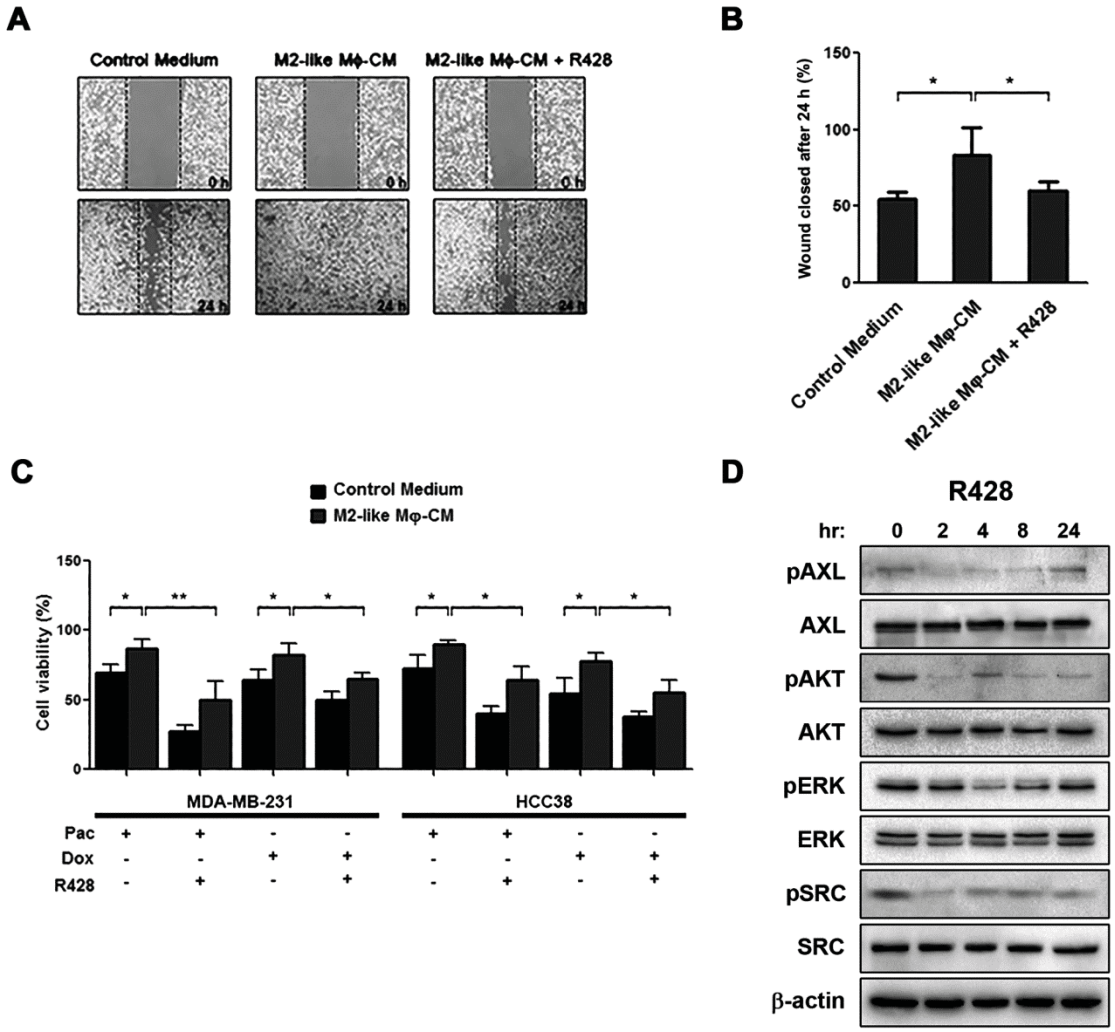

Figure 41. M2-polarized macrophages sustain tumour aggressiveness and influence drug sensitivity of *AXL*-overexpressing breast cancer cells. A) Wound healing assay with untreated or R428-treated MDA-MB-231 cells in the absence (control medium) or presence of conditioned medium (CM) derived from M2 macrophages. B) Statistical analysis of wound closure. Gap size at 0 hours was set to 100% and percentage of closed wound was calculated after 24 hours. C) M2-polarized macrophages increase the resistance of HCC38 and MDA-MB-231 cells to paclitaxel (Pac), and doxorubicin (Dox) treatments compared with cells treated with control medium, while the selective inhibition of AXL with R428 restores drug sensitivity in TNBC cells. D) Western blot with the indicated antibodies of lysates from MDA-MB-231 cells treated with 1 μM R428 at different time points. β-actin was used as a loading control. *P*-values were obtained using a two-tailed Student's *t* test (mean ± SD, $n = 3$ experiments; *$P < 0.05$; **$P \leq 0.01$).

5. Discussion

5.1 Immune gene signatures define different molecular subtypes of triple-negative breast cancer

The hallmarks of cancer comprise specific biological abilities that enable tumour development, progression, and metastatic dissemination (Hanahan and Weinberg, 2011). An increasing body of evidence suggests that genomic instability and immune responses facilitate the acquisition of functional capabilities that allow cancer cells to survive, proliferate, and disseminate (Hanahan and Weinberg, 2011). TNBC is generally characterized by a higher level of genomic aberrations and CIN compared with other breast cancer subtypes (Cancer Genome Atlas Network, 2012; Turner and Reis-Filho, 2013). Noteworthy, a substantial percentage of TNBC are also characterized by a high expression of immune-related genes and by an intense immune cell infiltrate, suggesting a potential connection between the levels of CIN and immune responses in TNBC (Metzger-Filho et al., 2012).

Several gene expression signatures reflecting genomic instability or adaptive and innate immunity have been generated and demonstrated to predict prognosis and response to chemotherapy in breast cancer, including TNBC (Alistar et al., 2014; Amara et al., 2017; Carter et al., 2006; Habermann et al., 2009; Karn et al., 2011; Miller et al., 2016; Mulligan et al., 2014; Nagalla et al., 2013; Rody et al., 2009; Telli et al., 2016; Vollan et al., 2015). Historically, the connection between CIN and immune infiltrates has been explained by the fact that high levels of CIN and mutational load can generate mutant peptides, some of which are immunogenic and can be recognized by T lymphocytes (Disis and Stanton, 2015; Loi, 2013). However, only one-third of mutations have been shown to be expressed in TNBC, suggesting that other factors contribute to the enhanced immune infiltration found in TNBC (Disis and Stanton, 2015; Shah et al., 2012). Accordingly, we found that several immune signatures, especially those reflecting the presence of immune

cells with anti-tumour functions such as NK and CTL, are overexpressed in TNBC with low levels of CIN. This inverse correlation may support the hypothesis that genomic instability influences immune responses not by increasing the immunogenicity of cancer cells, but by allowing immune escape (Loi, 2013). In agreement with our findings, high levels of aneuploidy have been recently found to negatively correlate with the presence of cytotoxic immune responses in several tumour types, including ER-negative/PR-negative breast cancer, and to be associated with reduced response to checkpoint inhibitors (Davoli et al., 2017). Conversely, a high mutational burden and neoantigen load were associated with increased immune signature scores and with durable clinical benefit from immunotherapy in patients with melanoma and non–small cell lung cancer (Davoli et al., 2017; McGranahan et al., 2016; Rizvi et al., 2015; Snyder et al., 2014; Van Allen et al., 2015). Overall, these results indicated that a high mutational load is able to enhance the anti-tumour activity of neoantigen-specific T lymphocytes. However, the presence of high levels of aneuploidy can induce immune suppression that outbalance the immune-promoting effect of mutations, positing CIN as the major genetic driver of immune response in human tumours (Zanetti, 2017). Thus, cancer patients with high levels of CIN, independently from mutational status, may be eligible for alternative immunotherapies that reverse the immunosuppressive status of the tumour microenvironment.

Even though we confirmed that the vast majority of TNBC showed a high level of CIN, distinct biological and molecular features differentially characterize genomically unstable and stable tumours. Accordingly, our results suggest that TNBC with low levels of CIN principally enclose M/MSL and claudin-low tumours, which are characterized by the presence of EMT and CSC-like features and by an intense immune cell infiltrate. This TNBC subset also reflects the characteristics of the IC4 group, displaying a reduced level of genomic instability and massive lymphocytic infiltration (Curtis et al., 2012; Dawson et al., 2013). Conversely, the CIN-high TNBC group, including mostly basal-like breast tumours, which mainly mirror the IC10 group, and a proportion of M/MSL cancers is more

heterogeneous in terms of both biological features and levels of immune infiltrates. Thus, although chemotherapy may be beneficial for a subset of these patients with extreme CIN levels independently of immune infiltrates, novel therapeutic strategies to promote immune response in TNBC refractory to standard chemotherapy warrant further investigation.

The complexity and heterogeneity of the immune microenvironment is also reflected by the finding that different TNBC molecular subgroups are associated with specific immune signatures. Indeed, although the IM subtype was enriched for almost all the immune components, we found that the expression signatures related to NK cells and M2 macrophages were overexpressed in M/MSL cancers, suggesting a potential biological relevance of innate immunity in TNBC with mesenchymal-like properties. Consistent with our findings, recent data provide evidence that TIL strongly contribute to the peculiar gene expression pattern of the IM subtype (Lehmann et al., 2016). Furthermore, the M subgroup showed the lowest correlation with the IM profile among the other TNBC molecular subtypes, suggesting that M tumours are generally characterized by a permissive and immunosuppressive microenvironment (Lehmann et al., 2016). Although IM cancers as well as the MSL subgroup, which principally reflects the high abundance of mesenchymal stromal tissues, have been proposed as simple descriptors of the tumour microenvironment rather than independent subtypes, the relevance of both immune and stromal cells in tumour development and progression, and in determining patient's outcome and response to treatments should not be neglected (Lehmann et al., 2016).

5.2 Immune stratification reveals a subset of PD-1/LAG-3 double-positive triple-negative breast cancers

Recent evidence suggests that the presence of TIL is an important predictor of outcome and response to chemotherapy in TNBC (Adams et al., 2015; Adams et al., 2014; Denkert et al., 2015; Loi et al., 2014; Loi et al., 2013). In our dataset, we confirmed that increasing stromal TIL is an independent prognostic marker for prolonged RFS and OS in TNBC

treated with adjuvant anthracycline-based chemotherapy. Studies evaluating the association of LPBC with survival have reported conflicting results (Adams et al., 2015; Adams et al., 2014; Denkert et al., 2015; Loi et al., 2014; Loi et al., 2013). Indeed, LPBC did not reach a statistically significant association with prognosis, likely due to the reduced number of events, and the small proportion of TNBC displaying this phenotype. Thus, further efforts are needed to improve the quantitative pathological assessment of TIL on HE-stained slides.

In agreement with recent data, we demonstrated that a stromal TIL value ≥ 20% could identify a group of low-risk patients with both lymph node negative and positive early-stage TNBC (Loi et al., 2016). Furthermore, our findings suggest that patients with low TIL may benefit from the generation of an anti-tumour immune response, while boosting the lymphocyte activity (*e.g.,* checkpoint inhibitors) might prove useful in patients with high TIL and high disease burden.

Although the presence of TIL reflects the activation of a local anti-tumour immune response, distinct immune cell subpopulations may have a specific biological significance. In agreement with previous findings, we demonstrated that both CD8+ and FOXP3+ cells were associated with good outcome in TNBC patients and that the clinical significance of FOXP3+ cells was highly dependent on the concurrent presence of CTL (Ali et al., 2014; Jiang et al., 2015; Liu et al., 2014; Mahmoud et al., 2011; West et al., 2013). Interestingly, when stratified based on the presence of CD8+ lymphocytes, a high infiltration of FOXP3+ cells trended towards reduced survival in TNBC cases with low content of CD8+ cells. These results suggest that CD8+ lymphocytes could be the main effectors of anti-tumour immune responses and that the consistent correlation between FOXP3+ and CTL may in part explain the conflicting results reported in previous studies (Dushyanthen et al., 2015b). Overall, our findings indicate that the assessment of single immune components may not be as informative as the global evaluation of stromal TIL. However, the understanding of the biological role of different lymphocyte subpopulations warrants

further investigations and could be useful to select TNBC patients who may benefit from the addition of specific immunomodulatory therapies to conventional chemotherapeutic regimens.

Although TIL are emerging as important prognostic and predictive factors in TNBC, it is worth noting that many TNBC have few TIL, and even in the presence of massive lymphocytic infiltration, immunosuppressive mechanisms should be considered (Loi, 2014). In this scenario, both radiotherapy and chemotherapeutic agents (*e.g.*, anthracyclines) have been shown in preclinical models to be able to shape the tumour microenvironment and to boost an effective immune response against tumour cells (Tsoutsou et al., 2015; Tung and Winer, 2015). These therapies should be evaluated rationally in combination with immunomodulatory drugs to synergize with pre-existing lymphocytes with tumouricidal activity or to elicit a *de novo* local immune response in tumours lacking TIL.

Even though the immune system can recognize and eliminate malignant cells, tumours have evolved multiple mechanisms to evade effective immunosurveillance, including the activation of the immune checkpoints PD-1 and LAG-3 (Fridman et al., 2012; Nguyen and Ohashi, 2015). We demonstrated that PD-1+ and LAG-3+ TIL were present in approximately 30% and 18% of TNBC, respectively, and that their presence in the tumour microenvironment tended to be associated with good prognosis in TNBC. The upregulation of these receptors, especially PD-1, has been classically described as a prominent immune resistance mechanism and analyses performed on tissue microarrays have revealed an inverse correlation with the outcome of breast cancer patients (Muenst et al., 2013; Nguyen and Ohashi, 2015). Indeed, double-positive PD-1/LAG-3 TIL have been recently demonstrated to show a more exhausted phenotype compared with single positive or negative TIL in preclinical model, likely leading to an increased cancer immune evasion (Woo et al., 2012). However, the role of co-inhibitory molecules in the modulation of the tumour immune microenvironment and the mechanisms underlying T cell exhaustion and

anergy are still poorly understood (Nguyen and Ohashi, 2015; Savas et al., 2016). Furthermore, it is worth noting that the activity of immune cells depends on the interaction with cancer cells and recent findings support the idea that the functional relevance of checkpoint proteins is highly sensitive to the context (*e.g.,* amount of antigen, topographical relationships with tumour cells, and PD-L1-expressing cells) (Nguyen and Ohashi, 2015; Okazaki et al., 2013). Consequently, the evaluation of the clinical and biological significance of immune markers, especially those reflecting the activation status of lymphocytes, should be performed on whole tissue sections, reducing sampling bias due to tumour heterogeneity, and providing a more comprehensive understanding of the complex tumour-immune dynamics. Moreover, we found that the expression of both PD-1 and LAG-3 highly correlated with the presence of TIL, especially cytotoxic CD8+ cells. Even though a stratified analysis according to levels of lymphocytic infiltration was not performed due to the low number of cases in each subgroup, our results suggest that the presence of PD-1+ and LAG-3+ TIL in the tumour microenvironment may reflect the occurrence of an active, although partially exhausted, intratumoural immune response, rather than representing a global marker of immunosuppression. Accordingly, emerging evidence revealed that local immunomodulatory factors (*e.g.,* IFN-γ released by TIL) or the activation of oncogenic signalling pathways (*e.g.,* PI3K pathway) can promote the expression of PD-L1, which has been shown to be enriched in triple-negative/basal-like breast cancer and associated with good outcome and response to chemotherapy in patients with TNBC (Ali et al., 2015; Denkert et al., 2015; Gatalica et al., 2014; Mittendorf et al., 2014; Schalper et al., 2014; Wimberly et al., 2015). Interestingly, by analysing two independent cohorts, we found that PD-1+ and LAG-3+ TIL were concurrently expressed in approximately 15% of TNBC. Thus, reversing the phenotype of exhausted T lymphocytes by targeting multiple inhibitory receptors may boost an effective anti-tumour immune response, and represent a novel valuable strategy to treat a subgroup of TNBC. Recently, the blockade of the PD-1/PD-L1 pathway has shown promising clinical activity

in patients with metastatic TNBC, although the molecular preselection of the candidate patients for novel clinical trials would be valuable (Adams et al., 2016; Dirix et al., 2016; Emens et al., 2015; Gibson, 2015; Savas et al., 2016). Preclinical data demonstrated that anti-LAG-3 is mildly effective as a monotherapy, but potently synergize with anti-PD-1, suggesting that the combined immune checkpoint inhibition could enhance T cells activity and improve anti-tumour immunity (Woo et al., 2012). Furthermore, the dual blockade of PD-1 and LAG-3 may exhibit less immune toxicity than that observed with the blockade of other immune receptors (*e.g.,* CTLA-4).

In conclusion, this study highlights the importance of different lymphocyte subpopulations for the selection of primary TNBC patients who may benefit from immunomodulatory drugs. Our data support the clinical evaluation of anti-PD-1/PD-L1 and anti-LAG-3 in combination with chemotherapy in a specific subset of TNBC patients that show concurrent expression of both checkpoints.

5.3 CD103+/PD-1+ T-cells identify a subset of triple-negative breast cancer candidates for targeted checkpoint inhibitors therapy

The presence of tumour-infiltrating immune cells is a hallmark of human cancer and affects the pathological and clinical behaviour of TNBC (Adams et al., 2015; Fridman et al., 2012; Savas et al., 2016). Beside the prognostic and predictive value of TIL in TNBC, the landscape of the immune microenvironment in human tumours is complex and heterogeneous (Adams et al., 2015; Adams et al., 2014; Bottai et al., 2016a; Denkert et al., 2015; Fridman et al., 2012; Loi et al., 2014; Loi et al., 2013; Savas et al., 2016; Stanton et al., 2016). Different subsets of TIL have been found with variable frequencies, localization, and functional status in breast cancer (Fridman et al., 2012; Stanton et al., 2016). According to previous studies, we demonstrated that CD8+ cytotoxic TIL are strongly associated with the outcome of TNBC patients (Ali et al., 2014; Bottai et al., 2016a; Matsumoto et al., 2016; Miyashita et al., 2015). CD8+ cells were more numerous in

tumour stroma, but their presence in both stromal and intraepithelial compartments predicts clinical outcome in TNBC. Even though intraepithelial TIL are quite infrequent and often difficult to evaluate, the prevalent stromal localization of CD8+ cytotoxic lymphocytes may partly explain the superior prognostic value of stromal TIL compared with that of intraepithelial lymphocytes (Adams et al., 2014; Kroemer et al., 2015).

The evaluation of TIL localization, composition, and functionality may increase our understanding of the immune contexture in human cancers and help to identify TNBC patients eligible for immunotherapies. In particular, the mechanisms that promote the localization of CD8+ T cells within the tumour, which may ultimately influence their anti-tumour activity, remain elusive. In this regard, the integrin CD103 plays a pivotal role in the retention of intratumoural T lymphocytes and in the promotion of T cell cytotoxic activity (Djenidi et al., 2015; Le Floc'h et al., 2011; Wang et al., 2016; Webb et al., 2014). Accordingly, we found a consistent correlation between the presence of CD8+ and CD103+ TIL in TNBC. Unlike CD8+ cells, CD103+ lymphocytes were predominantly localized to intraepithelial areas and were associated with prognosis only when they are in direct contact with cancer cells. Importantly, we demonstrated that the concurrent massive infiltration of intraepithelial CD8+ and CD103+ lymphocytes is a strong predictor of good outcome. Overall, our results suggest that CD103 specifically identifies a subset of tumour-reactive CD8+ TIL in TNBC, paving the way for the development of innovative immunotherapeutic approaches.

The functions of CD103 have been suggested to be mediated by the binding of the integrin to E-cadherin on tumour cells (Boutet et al., 2016; Le Floc'h et al., 2011). However, in agreement with previous findings in high-grade serous ovarian cancer, we did not observe a clear association between E-cadherin and the presence of CD103+ cells in TNBC. It is worth noting that a subgroup of TNBC shows features of EMT, which is characterized by the up-regulation of mesenchymal-associated genes (*e.g.,* N-cadherin, fibronectin, and vimentin) and by the loss of E-cadherin (Lamouille et al., 2014; Turner

and Reis-Filho, 2013). Furthermore, TGF-β, which is a key regulator of EMT, has been shown to dampen the expression of E-cadherin and to act as a potent inducer of CD103 expression on CD8+ T cells (Boutet et al., 2016; Lamouille et al., 2014). Thus, our findings suggest that the intraepithelial retention and effector functions of CD103+ cytotoxic TIL may be mediated by mechanisms other than the binding to E-cadherin in TNBC.

EMT and the concurrent loss of E-cadherin have been associated with tumour progression and metastatic spread in TNBC (Kashiwagi et al., 2010; Lamouille et al., 2014). Furthermore, the interaction between cancer cells with mesenchymal features and tumour-associated immune cells is emerging as a hallmark of human cancers, including TNBC (Hanahan and Weinberg, 2011). These distinctive characteristics of the tumour microenvironment may promote intrinsic cancer cells aggressiveness and enable tumours to evade immune destruction. In particular, immune checkpoint receptors such as PD-1 have attracted considerable interest as potential targets for immunotherapy of human tumours, including breast cancer (Savas et al., 2016). We demonstrated that CD103 and PD-1 are frequently co-expressed on intraepithelial TIL in TNBC and that double-positive CD103/PD-1 cells are associated with better outcome compared with patients with double-negative tumours. Even though PD-1 has been historically considered a marker of immune exhaustion, the correlation between the expression of PD-1 on CD103+ TIL and good prognosis rather indicates that it reflects the presence of an active intratumoural immune response. According to recent findings in melanoma, endometrial, ovarian, and non-small cell lung cancers our results suggest that CD103+ cytotoxic T cells expressing PD-1 are partially quiescent in the tumour microenvironment, but might recover their anti-tumour activity following immunogenic chemotherapy (*e.g.,* anthracyclines) and immune modulation (Djenidi et al., 2015; Gros et al., 2014; Webb et al., 2015; Workel et al., 2016). Thus, the presence of PD-1+/CD103+ cytotoxic TIL in tumours warrants further

investigation as a candidate marker for the selection of TNBC patients eligible for immunotherapy.

Collectively, our results suggest that the expression of CD103 on CD8+ TIL in direct contact with cancer cells may identify a subpopulation of lymphocytes with potent anti-tumour activity. However, the effector functions of this TIL subsets as well as the mechanisms mediating T cell retention within tumour epithelium and anti-tumour activity need to be fully elucidated. The expression of PD-1 on CD103+/CD8+ TIL could have potential therapeutic implications, helping to identify TNBC patients eligible for immunomodulatory treatments that boost the anti-tumour activity of potentially quiescent intratumoural T lymphocytes.

5.4 AXL-associated tumour inflammation as a poor prognostic signature in chemotherapy-treated triple-negative breast cancer patients

The tumour microenvironment is of paramount importance in breast cancer progression and accumulating evidence indicates an emerging role of the cross-talk signalling between mesenchymal cancer cells and TAM. In fact, EMT and TAM provide invasive and metastatic capabilities to tumour cells and modulate the tumour microenvironment, leading to suppression of anti-tumour immune response and limiting the effects of cytotoxic chemotherapy (De Craene and Berx, 2013; Drasin et al., 2011; Jung et al., 2015; Lamouille et al., 2014; Reiman et al., 2010; Su et al., 2014b). TNBC, which is often characterized by the presence of both EMT and TAM, is a good model to explore potential molecular markers maintaining the biological intersections between these two signallings (Jung et al., 2015; Reiman et al., 2010; Su et al., 2014a; Su et al., 2014b). In this study, we demonstrated that the receptor AXL was the most significant EMT-related kinase associated with the presence of macrophages in the tumour stroma of TNBC. This receptor is emerging as an important effector of the EMT programme and its activation is responsible for triggering important oncogenic pathways such as PI3K/AKT/mTOR, NF-

κB, EGFR, and MAPK cascades, involved in cell proliferation, survival, and invasion (Asiedu et al., 2014; Elkabets et al., 2015; Gay et al., 2017; Gjerdrum et al., 2010; Graham et al., 2014; Meyer et al., 2013; Paccez et al., 2014). Furthermore, AXL activation has been also involved in the resistance to chemotherapeutic drugs and targeted agents such as cisplatin, taxanes, and EGFR/HER2/MAPK/PI3K inhibitors in multiple cancers (Brand et al., 2014; Byers et al., 2013; Elkabets et al., 2015; Gay et al., 2017; Postel-Vinay and Ashworth, 2012; Tirosh et al., 2016; Wilson et al., 2014). In line with different studies in human tumours, including acute myeloid leukemia, breast cancer, colon cancer, gastric cancer, head and neck squamous cell carcinoma, non-small cell lung cancer, ovarian cancer, and pancreatic cancer, we found that the increased expression of AXL significantly correlated with poor outcome in TNBC patients treated with anthracycline-taxane-based adjuvant chemotherapy (Asiedu et al., 2014; Brand et al., 2015; Dunne et al., 2014; Elkabets et al., 2015; Gjerdrum et al., 2010; Graham et al., 2014; Linger et al., 2010; Lozneanu et al., 2016; Meyer et al., 2013; Paccez et al., 2014). Interestingly, AXL overexpression was associated with distant tumour recurrence, particularly to visceral organs, indicating a specific route of tumour dissemination for a subset of these tumours. *AXL* kinase has been previously shown to be one of the most differentially expressed genes in the mesenchymal stem-like subtype compared with other subgroups of TNBC (Lehmann et al., 2011). Our data demonstrated that the expression of *AXL* was a specific feature of TNBC cells, especially those with mesenchymal features, sustaining the role of AXL in the activation of EMT and in mediating cancer cell aggressiveness (Asiedu et al., 2014; Del Pozo Martin et al., 2015; Gjerdrum et al., 2010; Graham et al., 2014; Paccez et al., 2014). Furthermore, we showed that AXL was involved in the modulation of several immune pathways, including leukocyte migration and chemotaxis, macrophage activation, and agranulocyte adhesion, further supporting the biological relevance of the interaction between *AXL*-expressing cancer cells and cancer-related immune responses in TNBC

(DeNardo et al., 2011; Jung et al., 2015; Lu et al., 2014; Reiman et al., 2010; Su et al., 2014a; Su et al., 2014b; Williams et al., 2016).

Previous studies reported that CD68+ TAM are a potential prognostic marker in breast cancer (Graham et al., 2014; Jinushi et al., 2011; Mahmoud et al., 2012; Tiainen et al., 2015). However, we found that CD68+ TAM in tumour stroma mildly correlated with tumour relapse and were not significantly associated with TNBC patients' outcome. Therefore, given potential differences in the evaluation of protein expression among studies, the clinical significance and utility of CD68 expression in TNBC remains uncertain. These data also highlight the concept that CD68 probably does not accurately reflect the presence and the function of distinct macrophage subpopulations within the tumour stroma, at least in breast cancer (Mukhtar et al., 2011; Ruffell et al., 2012b; Ruffell and Coussens, 2015). Consequently, our results advocate the importance to further evaluate the biological role and functions of different macrophage subpopulations in breast cancer. Indeed, macrophages exhibit remarkable functional and phenotypic plasticity, with activated M2-like cells displaying tumour-promoting activities (Graham et al., 2014; Lu et al., 2014). Accordingly, most human tumours exhibit TAM with an M2-like phenotype, which promote EMT and contribute to tumour progression and drug resistance (DeNardo et al., 2011; Galluzzi et al., 2012; Jinushi et al., 2011; Lu et al., 2014; Mantovani and Allavena, 2015; Pollard, 2004; Qian and Pollard, 2010; Ruffell and Coussens, 2015; Su et al., 2014a; Su et al., 2014b; Williams et al., 2016). Accordingly, we found that the massive presence of M2 macrophages correlated with an aggressive behaviour of TNBC. Moreover, *AXL* was significantly co-expressed with genes associated with M2 macrophages and positively correlated with the infiltration of CD163+ M2 cells, suggesting an important relationship between *AXL*-expressing cells and TAM with pro-tumour activity in a specific subgroup of TNBC.

The cross-talk between mesenchymal cancer cells and tumour microenvironment is recognized as a key factor in tumour progression in several tumours (Del Pozo Martin et

al., 2015; Lu et al., 2014; Reiman et al., 2010; Su et al., 2014a; Su et al., 2014b). However, we demonstrated that CD163+ M2 TAM did not retain their prognostic significance in multivariate analysis, suggesting that CD163+ macrophages likely have a role in sustaining the aggressiveness of cancer cells, but their presence alone may not be sufficient to affect the outcome of TNBC patients.

Although the mechanisms underlying the link between cancer cells and TAM are complex and difficult to dissect *in vitro*, we observed the reciprocal nature of this interaction sustained by AXL. Our data showed that *AXL*-positive TNBC cells with mesenchymal traits activate human macrophages to an M2-like phenotype, modulating a specific pattern of pro-tumour cytokines and chemokines. Indeed, mesenchymal-like cells were able to increase the release of CCL18 and IL-10, which are known macrophage-derived mediators of metastatic dissemination and resistance to chemotherapy in breast cancer (Chen et al., 2011; Ruffell et al., 2014). Furthermore, we demonstrated that the selective inhibition of AXL with R428 impaired the ability of mesenchymal cells to induce the polarization of macrophages, by reducing the release of CCL2, IL-6, OSM, and TGF-β, which are well-known inducers of the M2 phenotype (Tripathi et al., 2014; Williams et al., 2016). Additionally, AXL may be also involved in the recruitment of macrophages at the tumour site, increasing the production of CCL2 that functions as a monocyte chemoattractant protein (Kitamura et al., 2015). Noteworthy, we found that *AXL*-expressing mesenchymal-like cells were also capable of inducing the release of the AXL ligand Gas6, which is selectively secreted by M2-type macrophages. Thus, our results suggest that the AXL/Gas6 signalling may play a role in modulating the interaction between mesenchymal TNBC cells and M2 TAM and support previous findings indicating that tumour cells induced infiltrating TAM to increase the production of Gas6, promoting cell growth and metastasis in different cancer models (Loges et al., 2010). Although also the vitamin K-dependent plasma glycoprotein Protein S was described as a ligand for the TAM receptor family, which includes, AXL, MER, and TYRO3, the ability of this ligand

to bind and activate AXL has never been shown (Linger et al., 2008; van der Meer et al., 2014). Furthermore, alternative ligand-independent mechanisms, including interaction with EGFR, which is frequently express in TNBC, have been demonstrated (Asiedu et al., 2014; Carey et al., 2010; Elkabets et al., 2015; Meyer et al., 2013). Therefore, although the biological modalities of AXL action should be further investigated, our results suggest that TNBC cells with mesenchymal features may "educate" infiltrating TAM to support tumour progression and that targeting AXL may be a novel strategy to reduce both EMT and the pro-tumour activity of TAM in TNBC. Consistently, TAM receptors, particularly AXL and MER, have been found to be expressed in DC, NK cells, and macrophages and to induce immunosuppression by multiple mechanisms, principally by inhibiting pro-inflammatory cytokine signallings and toll-like receptors pathways, and favouring the polarization of M2 macrophages. Thus, although macrophages mostly rely on MER to exert their functions, recent evidence suggests that the inhibition of these receptors can not only impair the intrinsic oncogenic properties of cancer cells, but also affect the tumour microenvironment through the repolarization of the immune response and exert a global anti-cancer action (Aguilera and Giaccia, 2017; Akalu et al., 2017; Antony and Huang, 2017; Graham et al., 2014; Lew et al., 2017; Nemunaitis et al., 2016; Rothlin et al., 2007; van der Meer et al., 2014; Wnuk-Lipinska et al., 2017; Yokoyama et al., 2017; Zizzo et al., 2012).

Finally, we demonstrated that the presence of M2-polarized cells enhanced the migratory potential and chemoresistance of TNBC cells, whereas the selective pharmacological inhibition of AXL was able to drastically reduce cell aggressiveness and to restore response to chemotherapeutic drugs including taxanes and anthracyclines. These results are in agreement with recent findings showing that infiltrating macrophages reduced the primary breast tumour drug response and that R428 enhanced the efficacy of anti-mitotic drugs in mesenchymal-like lung and breast cancer cells (Ruffell et al., 2014; Wilson et al., 2014). Noteworthy, although R428 was shown to be > 100-fold selective for AXL over EGFR, HER2, PDGFRβ, and other kinases, the treatment of TNBC cells with

this inhibitor also affected the activation of other oncogenic pathways, providing evidence of cross-talk signalling between different pathways and the activation of compensatory feedback networks (Holland et al., 2010). Moreover, we showed that *AXL* was also expressed in basal-like breast cancer cells. Even though the effect of *AXL*-expressing basal-like cells on macrophage polarization was mild compared with that of mesenchymal-like cells, TAM were equally able to induce chemoresistance in both TNBC models. These findings suggest that, beyond the role of mesenchymal-like cells in supporting the cross-talk with TAM, AXL inhibition could be a potential therapeutic strategy for a broader range of patients with *AXL*-expressing TNBC.

Even though we provide evidence of the involvement of AXL kinase in macrophage polarization, the specific requirement of AXL for the interaction with TAM and the potentially distinct biological role of different subtypes of TNBC cells warrant further studies. In particular, the direct and indirect role of AXL as potential immunomodulator of macrophage phenotype and functions should be explored through the generation of CRISPR/Cas9-mediated *AXL*-knockout TNBC cells and co-culture experiments. Moreover, the effect of AXL blockade through selective or multi-kinase inhibitors on the modulation of the complex interactions occurring within the tumour microenvironment between TNBC cells and macrophages should be investigated in *in vivo* models of TNBC. Given the retrospective nature of this study and to determine the potential heterogeneity of treatment effects associated with AXL functions, our findings would need to be further validated in a prospective clinical trial. Despite these limitations, our results suggest that AXL is a prognostic indicator of outcome in TNBC treated with chemotherapy. Furthermore, AXL supports the pro-tumour activity of M2-type macrophages, inducing tumour progression and resistance to chemotherapy.

Overall, our data provide support for the use of AXL targeted therapy to reduce tumour aggressiveness, overcome chemotherapy resistance, and impair the cross-talk between cancer cells and TAM in patients with TNBC overexpressing AXL.

6. List of Abbreviations

BL1, basal-like 1; BL2, basal-like 2; CK, cytokeratins; CI, confidence interval; CIN, chromosomal instability; CNA, copy number alterations; CSC, cancer stem cells; DC, dendritic cells; EGFR, epidermal growth factor receptor; EMT, epithelial to mesenchymal transition; ER, estrogen receptor; FFPE, formalin-fixed, paraffin-embedded; HER2, human epidermal growth factor receptor 2; HR, hazard ratio; ieCD8, intraepithelial CD8; ieCD103, intraepithelial CD103; IFN, interferon; IHC, immunohistochemistry; IL, interleukin; IM, immunomodulatory; IQR, Interquartile range; LAG-3, lymphocyte activation gene 3 protein; LAR, luminal androgen receptor; LN, lymph node; LPBC, lymphocyte-predominant breast cancer; LR, likelihood ratio; LVI, lymphovascular invasion; M, mesenchymal; MAPK, mitogen-activated protein kinases; MSL, mesenchymal stem cell-like; NF-κB, nuclear factor-κB; NK, natural killer; OS, overall survival; PD-1, programmed cell death protein 1; PD-L1, programmed cell death 1 ligand 1; PI3K, phosphatidylinositol 3-kinase; PR, progesterone receptor; RFS, relapse-free survival; ROC, receiver operating characteristic; sCD8, stromal CD8; sCD103, stromal CD103; TAM, tumour-associated macrophages; TGF-β, transforming growth factor-β; TIL, tumour-infiltrating lymphocytes; TNBC, triple-negative breast cancers; TNF, tumour necrosis factor.

7. References

Adams, S., Diamond, J., Hamilton, E., Pohlmann, P., Tolaney, S., Molinero, L., Zou, W., Liu, B., Waterkamp, D., Funke, R. and Powderly, J. 2016. Safety and clinical activity of atezolizumab (anti-PDL1) in combination with nab-paclitaxel in patients with metastatic triple-negative breast cancer [abstract]. *In:* Proceedings of the 38th Annual CTRC-AACR San Antonio Breast Cancer Symposium: 2015 Dec 8-12, San Antonio, TX. Philadelphia (PA); AACR; *Cancer Res*, 76(Suppl 4), Abstract nr P2-11-06.

Adams, S., Goldstein, L. J., Sparano, J. A., Demaria, S. and Badve, S. S. 2015. Tumor infiltrating lymphocytes (TILs) improve prognosis in patients with triple negative breast cancer (TNBC). *Oncoimmunology*, 4(9), e985930.

Adams, S., Gray, R. J., Demaria, S., Goldstein, L., Perez, E. A., Shulman, L. N., Martino, S., Wang, M., Jones, V. E., Saphner, T. J., Wolff, A. C., Wood, W. C., Davidson, N. E., Sledge, G. W., Sparano, J. A. and Badve, S. S. 2014. Prognostic value of tumor-infiltrating lymphocytes in triple-negative breast cancers from two phase III randomized adjuvant breast cancer trials: ECOG 2197 and ECOG 1199. *J Clin Oncol*, 32(27), 2959-2966.

Aguilera, T. A. and Giaccia, A. J. 2017. Molecular Pathways: Oncologic Pathways and Their Role in T-cell Exclusion and Immune Evasion-A New Role for the AXL Receptor Tyrosine Kinase. *Clin Cancer Res*, 23(12), 2928-2933.

Akalu, Y. T., Rothlin, C. V. and Ghosh, S. 2017. TAM receptor tyrosine kinases as emerging targets of innate immune checkpoint blockade for cancer therapy. *Immunol Rev*, 276(1), 165-177.

Ali, H. R., Glont, S. E., Blows, F. M., Provenzano, E., Dawson, S. J., Liu, B., Hiller, L., Dunn, J., Poole, C. J., Bowden, S., Earl, H. M., Pharoah, P. D. and Caldas, C. 2015. PD-L1 protein expression in breast cancer is rare, enriched in basal-like tumours and associated with infiltrating lymphocytes. *Ann Oncol*, 26(7), 1488-1493.

Ali, H. R., Provenzano, E., Dawson, S. J., Blows, F. M., Liu, B., Shah, M., Earl, H. M., Poole, C. J., Hiller, L., Dunn, J. A., Bowden, S. J., Twelves, C., Bartlett, J. M., Mahmoud, S. M., Rakha, E., Ellis, I. O., Liu, S., Gao, D., Nielsen, T. O., Pharoah, P. D. and Caldas, C. 2014. Association between CD8+ T-cell infiltration and breast cancer survival in 12,439 patients. *Ann Oncol*, 25(8), 1536-1543.

Alistar, A., Chou, J. W., Nagalla, S., Black, M. A., D'agostino, R., Jr. and Miller, L. D. 2014. Dual roles for immune metagenes in breast cancer prognosis and therapy prediction. *Genome Med*, 6(10), 80.

Allavena, P., Sica, A., Garlanda, C. and Mantovani, A. 2008. The Yin-Yang of tumor-associated macrophages in neoplastic progression and immune surveillance. *Immunol Rev*, 222, 155-161.

Altman, D. G., Mcshane, L. M., Sauerbrei, W. and Taube, S. E. 2012. Reporting Recommendations for Tumor Marker Prognostic Studies (REMARK): explanation and elaboration. *PLoS Med*, 9(5), e1001216.

Amara, D., Wolf, D. M., Van 'T Veer, L., Esserman, L., Campbell, M. and Yau, C. 2017. Co-expression modules identified from published immune signatures reveal five distinct immune subtypes in breast cancer. *Breast Cancer Res Treat*, 161(1), 41-50.

Andersen, M. H., Schrama, D., Thor Straten, P. and Becker, J. C. 2006. Cytotoxic T cells. *J Invest Dermatol*, 126(1), 32-41.

Antony, J. and Huang, R. Y. 2017. AXL-Driven EMT State as a Targetable Conduit in Cancer. *Cancer Res*, 77(14), 3725-3732.

Asiedu, M. K., Beauchamp-Perez, F. D., Ingle, J. N., Behrens, M. D., Radisky, D. C. and Knutson, K. L. 2014. AXL induces epithelial-to-mesenchymal transition and regulates the function of breast cancer stem cells. *Oncogene*, 33(10), 1316-1324.

Aure, M. R., Leivonen, S. K., Fleischer, T., Zhu, Q., Overgaard, J., Alsner, J., Tramm, T., Louhimo, R., Alnaes, G. I., Perala, M., Busato, F., Touleimat, N., Tost, J., Borresen-Dale, A. L., Hautaniemi, S., Troyanskaya, O. G., Lingjaerde, O. C., Sahlberg, K. K. and

Kristensen, V. N. 2013. Individual and combined effects of DNA methylation and copy number alterations on miRNA expression in breast tumors. *Genome Biol*, 14(11), R126.

Balermpas, P., Rodel, F., Liberz, R., Oppermann, J., Wagenblast, J., Ghanaati, S., Harter, P. N., Mittelbronn, M., Weiss, C., Rodel, C. and Fokas, E. 2014. Head and neck cancer relapse after chemoradiotherapy correlates with CD163+ macrophages in primary tumour and CD11b+ myeloid cells in recurrences. *Br J Cancer*, 111(8), 1509-1518.

Bianchini, G., Iwamoto, T., Qi, Y., Coutant, C., Shiang, C. Y., Wang, B., Santarpia, L., Valero, V., Hortobagyi, G. N., Symmans, W. F., Gianni, L. and Pusztai, L. 2010. Prognostic and therapeutic implications of distinct kinase expression patterns in different subtypes of breast cancer. *Cancer Res*, 70(21), 8852-8862.

Bill, R. and Christofori, G. 2015. The relevance of EMT in breast cancer metastasis: Correlation or causality? *FEBS Lett*, 589(14), 1577-1587.

Birkbak, N. J., Eklund, A. C., Li, Q., Mcclelland, S. E., Endesfelder, D., Tan, P., Tan, I. B., Richardson, A. L., Szallasi, Z. and Swanton, C. 2011. Paradoxical relationship between chromosomal instability and survival outcome in cancer. *Cancer Res*, 71(10), 3447-3452.

Biswas, S. K. and Mantovani, A. 2010. Macrophage plasticity and interaction with lymphocyte subsets: cancer as a paradigm. *Nat Immunol*, 11(10), 889-896.

Bonde, A. K., Tischler, V., Kumar, S., Soltermann, A. and Schwendener, R. A. 2012. Intratumoral macrophages contribute to epithelial-mesenchymal transition in solid tumors. *BMC Cancer*, 12, 35.

Bordeaux, J., Welsh, A., Agarwal, S., Killiam, E., Baquero, M., Hanna, J., Anagnostou, V. and Rimm, D. 2010. Antibody validation. *Biotechniques*, 48(3), 197-209.

Bottai, G., Raschioni, C., Losurdo, A., Di Tommaso, L., Tinterri, C., Torrisi, R., Reis-Filho, J. S., Roncalli, M., Sotiriou, C., Santoro, A., Mantovani, A., Loi, S. and Santarpia, L. 2016a. An immune stratification reveals a subset of PD-1/LAG-3 double-positive triple-negative breast cancers. *Breast Cancer Res*, 18(1), 121.

Bottai, G., Raschioni, C., Székely, B., Di Tommaso, L., Szász, A. M., Losurdo, A., Győrffy, B., Ács, B., Torrisi, R., Karachaliou, N., Tőkés, T., Caruso, M., Kulka, J., Roncalli, M., Santoro, A., Mantovani, A., Rosell, R., Reis-Filho, J. S. and Santarpia, L. 2016b. AXL-associated tumor inflammation as a poor prognostic signature in chemotherapy-treated triple-negative breast cancer patients. *NPJ Breast Cancer*, 2, 16033.

Boutet, M., Gauthier, L., Leclerc, M., Gros, G., De Montpreville, V., Theret, N., Donnadieu, E. and Mami-Chouaib, F. 2016. TGFbeta Signaling Intersects with CD103 Integrin Signaling to Promote T-Lymphocyte Accumulation and Antitumor Activity in the Lung Tumor Microenvironment. *Cancer Res*, 76(7), 1757-1769.

Brand, T. M., Iida, M., Stein, A. P., Corrigan, K. L., Braverman, C. M., Coan, J. P., Pearson, H. E., Bahrar, H., Fowler, T. L., Bednarz, B. P., Saha, S., Yang, D., Gill, P. S., Lingen, M. W., Saloura, V., Villaflor, V. M., Salgia, R., Kimple, R. J. and Wheeler, D. L. 2015. AXL Is a Logical Molecular Target in Head and Neck Squamous Cell Carcinoma. *Clin Cancer Res*, 21(11), 2601-2612.

Brand, T. M., Iida, M., Stein, A. P., Corrigan, K. L., Braverman, C. M., Luthar, N., Toulany, M., Gill, P. S., Salgia, R., Kimple, R. J. and Wheeler, D. L. 2014. AXL mediates resistance to cetuximab therapy. *Cancer Res*, 74(18), 5152-5164.

Burkholder, B., Huang, R. Y., Burgess, R., Luo, S., Jones, V. S., Zhang, W., Lv, Z. Q., Gao, C. Y., Wang, B. L., Zhang, Y. M. and Huang, R. P. 2014. Tumor-induced perturbations of cytokines and immune cell networks. *Biochim Biophys Acta*, 1845(2), 182-201.

Burrell, R. A., Mcgranahan, N., Bartek, J. and Swanton, C. 2013. The causes and consequences of genetic heterogeneity in cancer evolution. *Nature*, 501(7467), 338-345.

Byers, L. A., Diao, L., Wang, J., Saintigny, P., Girard, L., Peyton, M., Shen, L., Fan, Y., Giri, U., Tumula, P. K., Nilsson, M. B., Gudikote, J., Tran, H., Cardnell, R. J., Bearss, D. J., Warner, S. L., Foulks, J. M., Kanner, S. B., Gandhi, V., Krett, N., Rosen, S. T.,

Kim, E. S., Herbst, R. S., Blumenschein, G. R., Lee, J. J., Lippman, S. M., Ang, K. K., Mills, G. B., Hong, W. K., Weinstein, J. N., Wistuba, Ii, Coombes, K. R., Minna, J. D. and Heymach, J. V. 2013. An epithelial-mesenchymal transition gene signature predicts resistance to EGFR and PI3K inhibitors and identifies Axl as a therapeutic target for overcoming EGFR inhibitor resistance. *Clin Cancer Res*, 19(1), 279-290.

Campbell, M. J., Tonlaar, N. Y., Garwood, E. R., Huo, D., Moore, D. H., Khramtsov, A. I., Au, A., Baehner, F., Chen, Y., Malaka, D. O., Lin, A., Adeyanju, O. O., Li, S., Gong, C., Mcgrath, M., Olopade, O. I. and Esserman, L. J. 2011. Proliferating macrophages associated with high grade, hormone receptor negative breast cancer and poor clinical outcome. *Breast Cancer Res Treat*, 128(3), 703-711.

Cancer Genome Atlas Network 2012. Comprehensive molecular portraits of human breast tumours. *Nature*, 490(7418), 61-70.

Carey, L., Winer, E., Viale, G., Cameron, D. and Gianni, L. 2010. Triple-negative breast cancer: disease entity or title of convenience? *Nat Rev Clin Oncol*, 7(12), 683-692.

Carey, L. A., Dees, E. C., Sawyer, L., Gatti, L., Moore, D. T., Collichio, F., Ollila, D. W., Sartor, C. I., Graham, M. L. and Perou, C. M. 2007. The triple negative paradox: primary tumor chemosensitivity of breast cancer subtypes. *Clin Cancer Res*, 13(8), 2329-2334.

Carter, S. L., Eklund, A. C., Kohane, I. S., Harris, L. N. and Szallasi, Z. 2006. A signature of chromosomal instability inferred from gene expression profiles predicts clinical outcome in multiple human cancers. *Nat Genet*, 38(9), 1043-1048.

Chen, J., Yao, Y., Gong, C., Yu, F., Su, S., Liu, B., Deng, H., Wang, F., Lin, L., Yao, H., Su, F., Anderson, K. S., Liu, Q., Ewen, M. E., Yao, X. and Song, E. 2011. CCL18 from tumor-associated macrophages promotes breast cancer metastasis via PITPNM3. *Cancer Cell*, 19(4), 541-555.

Chen, X., Li, J., Gray, W. H., Lehmann, B. D., Bauer, J. A., Shyr, Y. and Pietenpol, J. A. 2012. TNBCtype: A Subtyping Tool for Triple-Negative Breast Cancer. *Cancer Inform*, 11, 147-156.

Colotta, F., Allavena, P., Sica, A., Garlanda, C. and Mantovani, A. 2009. Cancer-related inflammation, the seventh hallmark of cancer: links to genetic instability. *Carcinogenesis*, 30(7), 1073-1081.

Comaills, V., Kabeche, L., Morris, R., Buisson, R., Yu, M., Madden, M. W., Licausi, J. A., Boukhali, M., Tajima, K., Pan, S., Aceto, N., Sil, S., Zheng, Y., Sundaresan, T., Yae, T., Jordan, N. V., Miyamoto, D. T., Ting, D. T., Ramaswamy, S., Haas, W., Zou, L., Haber, D. A. and Maheswaran, S. 2016. Genomic Instability Is Induced by Persistent Proliferation of Cells Undergoing Epithelial-to-Mesenchymal Transition. *Cell Rep*, 17(10), 2632-2647.

Coussens, L. M., Zitvogel, L. and Palucka, A. K. 2013. Neutralizing tumor-promoting chronic inflammation: a magic bullet? *Science*, 339(6117), 286-291.

Creighton, C. J., Chang, J. C. and Rosen, J. M. 2010. Epithelial-mesenchymal transition (EMT) in tumor-initiating cells and its clinical implications in breast cancer. *J Mammary Gland Biol Neoplasia*, 15(2), 253-260.

Curtis, C., Shah, S. P., Chin, S. F., Turashvili, G., Rueda, O. M., Dunning, M. J., Speed, D., Lynch, A. G., Samarajiwa, S., Yuan, Y., Graf, S., Ha, G., Haffari, G., Bashashati, A., Russell, R., Mckinney, S., Langerod, A., Green, A., Provenzano, E., Wishart, G., Pinder, S., Watson, P., Markowetz, F., Murphy, L., Ellis, I., Purushotham, A., Borresen-Dale, A. L., Brenton, J. D., Tavare, S., Caldas, C. and Aparicio, S. 2012. The genomic and transcriptomic architecture of 2,000 breast tumours reveals novel subgroups. *Nature*, 486(7403), 346-352.

Davoli, T., Uno, H., Wooten, E. C. and Elledge, S. J. 2017. Tumor aneuploidy correlates with markers of immune evasion and with reduced response to immunotherapy. *Science*, 355(6322).

Dawson, S. J., Provenzano, E. and Caldas, C. 2009. Triple negative breast cancers: clinical and prognostic implications. *Eur J Cancer*, 45(Suppl 1), 27-40.

Dawson, S. J., Rueda, O. M., Aparicio, S. and Caldas, C. 2013. A new genome-driven integrated classification of breast cancer and its implications. *EMBO J*, 32(5), 617-628.

De Craene, B. and Berx, G. 2013. Regulatory networks defining EMT during cancer initiation and progression. *Nat Rev Cancer*, 13(2), 97-110.

Del Pozo Martin, Y., Park, D., Ramachandran, A., Ombrato, L., Calvo, F., Chakravarty, P., Spencer-Dene, B., Derzsi, S., Hill, C. S., Sahai, E. and Malanchi, I. 2015. Mesenchymal Cancer Cell-Stroma Crosstalk Promotes Niche Activation, Epithelial Reversion, and Metastatic Colonization. *Cell Rep*, 13(11), 2456-2469.

Denardo, D. G., Andreu, P. and Coussens, L. M. 2010. Interactions between lymphocytes and myeloid cells regulate pro- versus anti-tumor immunity. *Cancer Metastasis Rev*, 29(2), 309-316.

Denardo, D. G., Brennan, D. J., Rexhepaj, E., Ruffell, B., Shiao, S. L., Madden, S. F., Gallagher, W. M., Wadhwani, N., Keil, S. D., Junaid, S. A., Rugo, H. S., Hwang, E. S., Jirstrom, K., West, B. L. and Coussens, L. M. 2011. Leukocyte complexity predicts breast cancer survival and functionally regulates response to chemotherapy. *Cancer Discov*, 1(1), 54-67.

Denardo, D. G. and Coussens, L. M. 2007. Inflammation and breast cancer. Balancing immune response: crosstalk between adaptive and innate immune cells during breast cancer progression. *Breast Cancer Res*, 9(4), 212.

Denkert, C., Von Minckwitz, G., Brase, J. C., Sinn, B. V., Gade, S., Kronenwett, R., Pfitzner, B. M., Salat, C., Loi, S., Schmitt, W. D., Schem, C., Fisch, K., Darb-Esfahani, S., Mehta, K., Sotiriou, C., Wienert, S., Klare, P., Andre, F., Klauschen, F., Blohmer, J. U., Krappmann, K., Schmidt, M., Tesch, H., Kummel, S., Sinn, P., Jackisch, C., Dietel, M., Reimer, T., Untch, M. and Loibl, S. 2015. Tumor-infiltrating lymphocytes and response to neoadjuvant chemotherapy with or without carboplatin in human epidermal

growth factor receptor 2-positive and triple-negative primary breast cancers. *J Clin Oncol*, 33(9), 983-991.

Dieci, M. V., Mathieu, M. C., Guarneri, V., Conte, P., Delaloge, S., Andre, F. and Goubar, A. 2015. Prognostic and predictive value of tumor-infiltrating lymphocytes in two phase III randomized adjuvant breast cancer trials. *Ann Oncol*, 26(8), 1698-1704.

Dirix, L., Takacs, I., Nikolinakos, P., Jerusalem, G., Arkenau, H.-T., Hamilton, E., Von Heydebreck, A., Grote, H.-J., Chin, K. and Lippman, M. 2016. Avelumab (MSB0010718C), an anti-PD-L1 antibody, in patients with locally advanced or metastatic breast cancer: A phase Ib JAVELIN solid tumor trial [abstract]. *In:* Proceedings of the 38th Annual CTRC-AACR San Antonio Breast Cancer Symposium: 2015 Dec 8-12, San Antonio, TX. AACR; *Cancer Res*, 76(Suppl 4), Abstract nr S1-04.

Disis, M. L. and Stanton, S. E. 2015. Triple-negative breast cancer: immune modulation as the new treatment paradigm. *American Society of Clinical Oncology educational book.* e25-30.

Djenidi, F., Adam, J., Goubar, A., Durgeau, A., Meurice, G., De Montpreville, V., Validire, P., Besse, B. and Mami-Chouaib, F. 2015. CD8+CD103+ tumor-infiltrating lymphocytes are tumor-specific tissue-resident memory T cells and a prognostic factor for survival in lung cancer patients. *J Immunol*, 194(7), 3475-3486.

Drasin, D. J., Robin, T. P. and Ford, H. L. 2011. Breast cancer epithelial-to-mesenchymal transition: examining the functional consequences of plasticity. *Breast Cancer Res*, 13(6), 226.

Dunne, P. D., Mcart, D. G., Blayney, J. K., Kalimutho, M., Greer, S., Wang, T., Srivastava, S., Ong, C. W., Arthur, K., Loughrey, M., Redmond, K., Longley, D. B., Salto-Tellez, M., Johnston, P. G. and Van Schaeybroeck, S. 2014. AXL is a key regulator of inherent and chemotherapy-induced invasion and predicts a poor clinical outcome in early-stage colon cancer. *Clin Cancer Res*, 20(1), 164-175.

Dushyanthen, S., Beavis, P. A., Savas, P., Teo, Z. L., Zhou, C., Mansour, M., Darcy, P. K. and Loi, S. 2015a. Relevance of tumor-infiltrating lymphocytes in breast cancer. *BMC Med*, 13, 202.

Dushyanthen, S., Savas, P., Willard-Gallo, K., Denkert, C., Salgado, R. and Loi, S. 2015b. Tumour-Infiltrating Lymphocytes (TILs) in Breast Cancer: a Predictive or a Prognostic Marker? *Curr Breast Cancer Rep*, 7(1), 59-70.

Elinav, E., Nowarski, R., Thaiss, C. A., Hu, B., Jin, C. and Flavell, R. A. 2013. Inflammation-induced cancer: crosstalk between tumours, immune cells and microorganisms. *Nat Rev Cancer*, 13(11), 759-771.

Elkabets, M., Pazarentzos, E., Juric, D., Sheng, Q., Pelossof, R. A., Brook, S., Benzaken, A. O., Rodon, J., Morse, N., Yan, J. J., Liu, M., Das, R., Chen, Y., Tam, A., Wang, H., Liang, J., Gurski, J. M., Kerr, D. A., Rosell, R., Teixido, C., Huang, A., Ghossein, R. A., Rosen, N., Bivona, T. G., Scaltriti, M. and Baselga, J. 2015. AXL mediates resistance to PI3Kalpha inhibition by activating the EGFR/PKC/mTOR axis in head and neck and esophageal squamous cell carcinomas. *Cancer Cell*, 27(4), 533-546.

Emens, L. A., Braiteh, F. S., Cassier, P., Delord, J.-P., Eder, J. P., Fasso, M., Xiao, Y., Wang, Y., Molinero, L., Chen, D. S. and Krop, I. 2015. Inhibition of PD-L1 by MPDL3280A leads to clinical activity in patients with metastatic triple-negative breast cancer (TNBC). *In:* Proceedings of the 106th Annual Meeting of the American Association for Cancer Research: 2015 Apr 18-22, Philadelphia, PA. Philadelphia, PA; AACR; *Cancer Res*, 75(Suppl 15), Abstract nr 2859.

Farmer, P., Bonnefoi, H., Anderle, P., Cameron, D., Wirapati, P., Becette, V., Andre, S., Piccart, M., Campone, M., Brain, E., Macgrogan, G., Petit, T., Jassem, J., Bibeau, F., Blot, E., Bogaerts, J., Aguet, M., Bergh, J., Iggo, R. and Delorenzi, M. 2009. A stroma-related gene signature predicts resistance to neoadjuvant chemotherapy in breast cancer. *Nat Med*, 15(1), 68-74.

Ferlay, J., Soerjomataram, I., Dikshit, R., Eser, S., Mathers, C., Rebelo, M., Parkin, D. M., Forman, D. and Bray, F. 2015. Cancer incidence and mortality worldwide: sources, methods and major patterns in GLOBOCAN 2012. *Int J Cancer*, 136(5), E359-386.

Finak, G., Bertos, N., Pepin, F., Sadekova, S., Souleimanova, M., Zhao, H., Chen, H., Omeroglu, G., Meterissian, S., Omeroglu, A., Hallett, M. and Park, M. 2008. Stromal gene expression predicts clinical outcome in breast cancer. *Nat Med*, 14(5), 518-527.

Foroutan, M., Cursons, J., Hediyeh-Zadeh, S., Thompson, E. W. and Davis, M. J. 2017. A Transcriptional Program for Detecting TGFbeta-Induced EMT in Cancer. *Mol Cancer Res*, 15(5), 619-631.

Fridman, W. H., Pages, F., Sautes-Fridman, C. and Galon, J. 2012. The immune contexture in human tumours: impact on clinical outcome. *Nat Rev Cancer*, 12(4), 298-306.

Galluzzi, L., Senovilla, L., Zitvogel, L. and Kroemer, G. 2012. The secret ally: immunostimulation by anticancer drugs. *Nat Rev Drug Discov*, 11(3), 215-233.

Gatalica, Z., Snyder, C., Maney, T., Ghazalpour, A., Holterman, D. A., Xiao, N., Overberg, P., Rose, I., Basu, G. D., Vranic, S., Lynch, H. T., Von Hoff, D. D. and Hamid, O. 2014. Programmed cell death 1 (PD-1) and its ligand (PD-L1) in common cancers and their correlation with molecular cancer type. *Cancer Epidemiol Biomarkers Prev*, 23(12), 2965-2970.

Gay, C. M., Balaji, K. and Byers, L. A. 2017. Giving AXL the axe: targeting AXL in human malignancy. *Br J Cancer*, 116(4), 415-423.

Ghebeh, H., Mohammed, S., Al-Omair, A., Qattan, A., Lehe, C., Al-Qudaihi, G., Elkum, N., Alshabanah, M., Bin Amer, S., Tulbah, A., Ajarim, D., Al-Tweigeri, T. and Dermime, S. 2006. The B7-H1 (PD-L1) T lymphocyte-inhibitory molecule is expressed in breast cancer patients with infiltrating ductal carcinoma: correlation with important high-risk prognostic factors. *Neoplasia*, 8(3), 190-198.

Gibson, J. 2015. Anti-PD-L1 for metastatic triple-negative breast cancer. *Lancet Oncol*, 16(6), e264.

Gjerdrum, C., Tiron, C., Hoiby, T., Stefansson, I., Haugen, H., Sandal, T., Collett, K., Li, S., Mccormack, E., Gjertsen, B. T., Micklem, D. R., Akslen, L. A., Glackin, C. and Lorens, J. B. 2010. Axl is an essential epithelial-to-mesenchymal transition-induced regulator of breast cancer metastasis and patient survival. *Proc Natl Acad Sci U S A*, 107(3), 1124-1129.

Goldhirsch, A., Winer, E. P., Coates, A. S., Gelber, R. D., Piccart-Gebhart, M., Thurlimann, B. and Senn, H. J. 2013. Personalizing the treatment of women with early breast cancer: highlights of the St Gallen International Expert Consensus on the Primary Therapy of Early Breast Cancer 2013. *Ann Oncol*, 24(9), 2206-2223.

Graham, D. K., Deryckere, D., Davies, K. D. and Earp, H. S. 2014. The TAM family: phosphatidylserine sensing receptor tyrosine kinases gone awry in cancer. *Nat Rev Cancer*, 14(12), 769-785.

Gros, A., Robbins, P. F., Yao, X., Li, Y. F., Turcotte, S., Tran, E., Wunderlich, J. R., Mixon, A., Farid, S., Dudley, M. E., Hanada, K., Almeida, J. R., Darko, S., Douek, D. C., Yang, J. C. and Rosenberg, S. A. 2014. PD-1 identifies the patient-specific CD8(+) tumor-reactive repertoire infiltrating human tumors. *J Clin Invest*, 124(5), 2246-2259.

Habermann, J. K., Doering, J., Hautaniemi, S., Roblick, U. J., Bundgen, N. K., Nicorici, D., Kronenwett, U., Rathnagiriswaran, S., Mettu, R. K., Ma, Y., Kruger, S., Bruch, H. P., Auer, G., Guo, N. L. and Ried, T. 2009. The gene expression signature of genomic instability in breast cancer is an independent predictor of clinical outcome. *Int J Cancer*, 124(7), 1552-1564.

Hanahan, D. and Weinberg, R. A. 2011. Hallmarks of cancer: the next generation. *Cell*, 144(5), 646-674.

Holland, S. J., Pan, A., Franci, C., Hu, Y., Chang, B., Li, W., Duan, M., Torneros, A., Yu, J., Heckrodt, T. J., Zhang, J., Ding, P., Apatira, A., Chua, J., Brandt, R., Pine, P., Goff, D., Singh, R., Payan, D. G. and Hitoshi, Y. 2010. R428, a selective small molecule

inhibitor of Axl kinase, blocks tumor spread and prolongs survival in models of metastatic breast cancer. *Cancer Res*, 70(4), 1544-1554.

Huang Da, W., Sherman, B. T. and Lempicki, R. A. 2009. Systematic and integrative analysis of large gene lists using DAVID bioinformatics resources. *Nat Protoc*, 4(1), 44-57.

Ignatiadis, M., Singhal, S. K., Desmedt, C., Haibe-Kains, B., Criscitiello, C., Andre, F., Loi, S., Piccart, M., Michiels, S. and Sotiriou, C. 2012. Gene modules and response to neoadjuvant chemotherapy in breast cancer subtypes: a pooled analysis. *J Clin Oncol*, 30(16), 1996-2004.

Ignatiadis, M. and Sotiriou, C. 2013. Luminal breast cancer: from biology to treatment. *Nat Rev Clin Oncol*, 10(9), 494-506.

Jamal-Hanjani, M., A'hern, R., Birkbak, N. J., Gorman, P., Gronroos, E., Ngang, S., Nicola, P., Rahman, L., Thanopoulou, E., Kelly, G., Ellis, P., Barrett-Lee, P., Johnston, S. R., Bliss, J., Roylance, R. and Swanton, C. 2015. Extreme chromosomal instability forecasts improved outcome in ER-negative breast cancer: a prospective validation cohort study from the TACT trial. *Ann Oncol*, 26(7), 1340-1346.

Jiang, D., Gao, Z., Cai, Z., Wang, M. and He, J. 2015. Clinicopathological and prognostic significance of FOXP3+ tumor infiltrating lymphocytes in patients with breast cancer: a meta-analysis. *BMC Cancer*, 15, 727.

Jinushi, M., Chiba, S., Yoshiyama, H., Masutomi, K., Kinoshita, I., Dosaka-Akita, H., Yagita, H., Takaoka, A. and Tahara, H. 2011. Tumor-associated macrophages regulate tumorigenicity and anticancer drug responses of cancer stem/initiating cells. *Proc Natl Acad Sci U S A*, 108(30), 12425-12430.

Jung, H. Y., Fattet, L. and Yang, J. 2015. Molecular pathways: linking tumor microenvironment to epithelial-mesenchymal transition in metastasis. *Clin Cancer Res*, 21(5), 962-968.

Karn, T., Pusztai, L., Holtrich, U., Iwamoto, T., Shiang, C. Y., Schmidt, M., Muller, V., Solbach, C., Gaetje, R., Hanker, L., Ahr, A., Liedtke, C., Ruckhaberle, E., Kaufmann, M. and Rody, A. 2011. Homogeneous datasets of triple negative breast cancers enable the identification of novel prognostic and predictive signatures. *PLoS One*, 6(12), e28403.

Kashiwagi, S., Yashiro, M., Takashima, T., Nomura, S., Noda, S., Kawajiri, H., Ishikawa, T., Wakasa, K. and Hirakawa, K. 2010. Significance of E-cadherin expression in triple-negative breast cancer. *Br J Cancer*, 103(2), 249-255.

Kim, H. J. and Cantor, H. 2014. CD4 T-cell subsets and tumor immunity: the helpful and the not-so-helpful. *Cancer Immunol Res*, 2(2), 91-98.

Kitamura, T., Qian, B. Z., Soong, D., Cassetta, L., Noy, R., Sugano, G., Kato, Y., Li, J. and Pollard, J. W. 2015. CCL2-induced chemokine cascade promotes breast cancer metastasis by enhancing retention of metastasis-associated macrophages. *J Exp Med*, 212(7), 1043-1059.

Kroemer, G., Senovilla, L., Galluzzi, L., Andre, F. and Zitvogel, L. 2015. Natural and therapy-induced immunosurveillance in breast cancer. *Nat Med*, 21(10), 1128-1138.

Lamouille, S., Xu, J. and Derynck, R. 2014. Molecular mechanisms of epithelial-mesenchymal transition. *Nat Rev Mol Cell Biol*, 15(3), 178-196.

Le Du, F., Eckhardt, B. L., Lim, B., Litton, J. K., Moulder, S., Meric-Bernstam, F., Gonzalez-Angulo, A. M. and Ueno, N. T. 2015. Is the future of personalized therapy in triple-negative breast cancer based on molecular subtype? *Oncotarget*, 6(15), 12890-12908.

Le Floc'h, A., Jalil, A., Franciszkiewicz, K., Validire, P., Vergnon, I. and Mami-Chouaib, F. 2011. Minimal engagement of CD103 on cytotoxic T lymphocytes with an E-cadherin-Fc molecule triggers lytic granule polarization via a phospholipase Cgamma-dependent pathway. *Cancer Res*, 71(2), 328-338.

Lee, C. H., Espinosa, I., Vrijaldenhoven, S., Subramanian, S., Montgomery, K. D., Zhu, S., Marinelli, R. J., Peterse, J. L., Poulin, N., Nielsen, T. O., West, R. B., Gilks, C. B. and Van De Rijn, M. 2008. Prognostic significance of macrophage infiltration in leiomyosarcomas. *Clin Cancer Res*, 14(5), 1423-1430.

Lehmann, B. D., Bauer, J. A., Chen, X., Sanders, M. E., Chakravarthy, A. B., Shyr, Y. and Pietenpol, J. A. 2011. Identification of human triple-negative breast cancer subtypes and preclinical models for selection of targeted therapies. *J Clin Invest*, 121(7), 2750-2767.

Lehmann, B. D., Jovanovic, B., Chen, X., Estrada, M. V., Johnson, K. N., Shyr, Y., Moses, H. L., Sanders, M. E. and Pietenpol, J. A. 2016. Refinement of Triple-Negative Breast Cancer Molecular Subtypes: Implications for Neoadjuvant Chemotherapy Selection. *PLoS One*, 11(6), e0157368.

Lehmann, B. D. and Pietenpol, J. A. 2014. Identification and use of biomarkers in treatment strategies for triple-negative breast cancer subtypes. *J Pathol*, 232(2), 142-150.

Lew, E. D., Tindall, E. A., Oh, J., Walsh, C., Barrera, M., Ely, H., Diliberto, A., Yokoyama, Y., Li, G. and Albert, A. 2017. RXDX-106, a novel, selective and potent small molecule TAM (TYRO3, AXL, MER) inhibitor, demonstrates efficacy in TAM-driven tumors. *In:* Proceedings of the 108th American Association for Cancer Research Annual Meeting: 2017 Apr 1-5, Washington, DC. Philadelphia (PA); AACR; *Cancer Res*, 77(Suppl 13), Abstract nr 4191.

Li, Q., Birkbak, N. J., Gyorffy, B., Szallasi, Z. and Eklund, A. C. 2011. Jetset: selecting the optimal microarray probe set to represent a gene. *BMC Bioinformatics*, 12, 474.

Linger, R. M., Keating, A. K., Earp, H. S. and Graham, D. K. 2008. TAM receptor tyrosine kinases: biologic functions, signaling, and potential therapeutic targeting in human cancer. *Adv Cancer Res*, 100, 35-83.

Linger, R. M., Keating, A. K., Earp, H. S. and Graham, D. K. 2010. Taking aim at Mer and Axl receptor tyrosine kinases as novel therapeutic targets in solid tumors. *Expert Opin Ther Targets*, 14(10), 1073-1090.

Liu, R., Wang, X., Chen, G. Y., Dalerba, P., Gurney, A., Hoey, T., Sherlock, G., Lewicki, J., Shedden, K. and Clarke, M. F. 2007. The prognostic role of a gene signature from tumorigenic breast-cancer cells. *N Engl J Med*, 356(3), 217-226.

Liu, S., Foulkes, W. D., Leung, S., Gao, D., Lau, S., Kos, Z. and Nielsen, T. O. 2014. Prognostic significance of FOXP3+ tumor-infiltrating lymphocytes in breast cancer depends on estrogen receptor and human epidermal growth factor receptor-2 expression status and concurrent cytotoxic T-cell infiltration. *Breast Cancer Res*, 16(5), 432.

Liu, S., Lachapelle, J., Leung, S., Gao, D., Foulkes, W. D. and Nielsen, T. O. 2012. CD8+ lymphocyte infiltration is an independent favorable prognostic indicator in basal-like breast cancer. *Breast Cancer Res*, 14(2), R48.

Llosa, N. J., Cruise, M., Tam, A., Wicks, E. C., Hechenbleikner, E. M., Taube, J. M., Blosser, R. L., Fan, H., Wang, H., Luber, B. S., Zhang, M., Papadopoulos, N., Kinzler, K. W., Vogelstein, B., Sears, C. L., Anders, R. A., Pardoll, D. M. and Housseau, F. 2015. The vigorous immune microenvironment of microsatellite instable colon cancer is balanced by multiple counter-inhibitory checkpoints. *Cancer Discov*, 5(1), 43-51.

Loges, S., Schmidt, T., Tjwa, M., Van Geyte, K., Lievens, D., Lutgens, E., Vanhoutte, D., Borgel, D., Plaisance, S., Hoylaerts, M., Luttun, A., Dewerchin, M., Jonckx, B. and Carmeliet, P. 2010. Malignant cells fuel tumor growth by educating infiltrating leukocytes to produce the mitogen Gas6. *Blood*, 115(11), 2264-2273.

Loi, S. 2013. Tumor-infiltrating lymphocytes, breast cancer subtypes and therapeutic efficacy. *Oncoimmunology*, 2(7), e24720.

Loi, S. 2014. Host antitumor immunity plays a role in the survival of patients with newly diagnosed triple-negative breast cancer. *J Clin Oncol*, 32(27), 2935-2937.

Loi, S., Drubay, D., Adams, S., Francis, P., Joensuu, H., Dieci, M., Badve, S., Demaria, S., Gray, R., Piccart, M., Kellokumpa-Lehtinen, P.-L., Andre, F., Dufaure-Gare, I., Denkert, C., Salgado, R. and Michiels, S. 2016. Pooled individual patient data analysis of stromal tumor infiltrating lymphocytes in primary triple negative breast cancer treated with anthracycline-based chemotherapy. *In:* Proceedings of the 38th Annual CTRC-AACR San Antonio Breast Cancer Symposium: 2015 Dec 8-12, San Antonio, TX. Philadelphia (PA); AACR; *Cancer Res*, 76(Suppl 4), Abstract nr S1-03.

Loi, S., Michiels, S., Salgado, R., Sirtaine, N., Jose, V., Fumagalli, D., Kellokumpu-Lehtinen, P. L., Bono, P., Kataja, V., Desmedt, C., Piccart, M. J., Loibl, S., Denkert, C., Smyth, M. J., Joensuu, H. and Sotiriou, C. 2014. Tumor infiltrating lymphocytes are prognostic in triple negative breast cancer and predictive for trastuzumab benefit in early breast cancer: results from the FinHER trial. *Ann Oncol*, 25(8), 1544-1550.

Loi, S., Sirtaine, N., Piette, F., Salgado, R., Viale, G., Van Eenoo, F., Rouas, G., Francis, P., Crown, J. P., Hitre, E., De Azambuja, E., Quinaux, E., Di Leo, A., Michiels, S., Piccart, M. J. and Sotiriou, C. 2013. Prognostic and predictive value of tumor-infiltrating lymphocytes in a phase III randomized adjuvant breast cancer trial in node-positive breast cancer comparing the addition of docetaxel to doxorubicin with doxorubicin-based chemotherapy: BIG 02-98. *J Clin Oncol*, 31(7), 860-867.

Lozneanu, L., Pinciroli, P., Ciobanu, D. A., Carcangiu, M. L., Canevari, S., Tomassetti, A. and Caruntu, I. D. 2016. Computational and Immunohistochemical Analyses Highlight AXL as a Potential Prognostic Marker for Ovarian Cancer Patients. *Anticancer Res*, 36(8), 4155-4163.

Lu, H., Clauser, K. R., Tam, W. L., Frose, J., Ye, X., Eaton, E. N., Reinhardt, F., Donnenberg, V. S., Bhargava, R., Carr, S. A. and Weinberg, R. A. 2014. A breast cancer stem cell niche supported by juxtacrine signalling from monocytes and macrophages. *Nat Cell Biol*, 16(11), 1105-1117.

Mahmoud, S. M., Lee, A. H., Paish, E. C., Macmillan, R. D., Ellis, I. O. and Green, A. R. 2012. Tumour-infiltrating macrophages and clinical outcome in breast cancer. *J Clin Pathol*, 65(2), 159-163.

Mahmoud, S. M., Paish, E. C., Powe, D. G., Macmillan, R. D., Grainge, M. J., Lee, A. H., Ellis, I. O. and Green, A. R. 2011. Tumor-infiltrating CD8+ lymphocytes predict clinical outcome in breast cancer. *J Clin Oncol*, 29(15), 1949-1955.

Mak, M. P., Tong, P., Diao, L., Cardnell, R. J., Gibbons, D. L., William, W. N., Skoulidis, F., Parra, E. R., Rodriguez-Canales, J., Wistuba, Ii, Heymach, J. V., Weinstein, J. N., Coombes, K. R., Wang, J. and Byers, L. A. 2016. A Patient-Derived, Pan-Cancer EMT Signature Identifies Global Molecular Alterations and Immune Target Enrichment Following Epithelial-to-Mesenchymal Transition. *Clin Cancer Res*, 22(3), 609-620.

Mallini, P., Lennard, T., Kirby, J. and Meeson, A. 2014. Epithelial-to-mesenchymal transition: what is the impact on breast cancer stem cells and drug resistance. *Cancer Treat Rev*, 40(3), 341-348.

Mantovani, A. and Allavena, P. 2015. The interaction of anticancer therapies with tumor-associated macrophages. *J Exp Med*, 212(4), 435-445.

Mantovani, A., Sozzani, S., Locati, M., Allavena, P. and Sica, A. 2002. Macrophage polarization: tumor-associated macrophages as a paradigm for polarized M2 mononuclear phagocytes. *Trends Immunol*, 23(11), 549-555.

Marotta, L. L., Almendro, V., Marusyk, A., Shipitsin, M., Schemme, J., Walker, S. R., Bloushtain-Qimron, N., Kim, J. J., Choudhury, S. A., Maruyama, R., Wu, Z., Gonen, M., Mulvey, L. A., Bessarabova, M. O., Huh, S. J., Silver, S. J., Kim, S. Y., Park, S. Y., Lee, H. E., Anderson, K. S., Richardson, A. L., Nikolskaya, T., Nikolsky, Y., Liu, X. S., Root, D. E., Hahn, W. C., Frank, D. A. and Polyak, K. 2011. The JAK2/STAT3 signaling pathway is required for growth of CD44(+)CD24(-) stem cell-like breast cancer cells in human tumors. *J Clin Invest*, 121(7), 2723-2735.

Martinez-Lostao, L., Anel, A. and Pardo, J. 2015. How Do Cytotoxic Lymphocytes Kill Cancer Cells? *Clin Cancer Res*, 21(22), 5047-5056.

Masuda, H., Baggerly, K. A., Wang, Y., Zhang, Y., Gonzalez-Angulo, A. M., Meric-Bernstam, F., Valero, V., Lehmann, B. D., Pietenpol, J. A., Hortobagyi, G. N., Symmans, W. F. and Ueno, N. T. 2013. Differential response to neoadjuvant chemotherapy among 7 triple-negative breast cancer molecular subtypes. *Clin Cancer Res*, 19(19), 5533-5540.

Matsumoto, H., Thike, A. A., Li, H., Yeong, J., Koo, S. L., Dent, R. A., Tan, P. H. and Iqbal, J. 2016. Increased CD4 and CD8-positive T cell infiltrate signifies good prognosis in a subset of triple-negative breast cancer. *Breast Cancer Res Treat*, 156(2), 237-247.

Mcgranahan, N., Furness, A. J., Rosenthal, R., Ramskov, S., Lyngaa, R., Saini, S. K., Jamal-Hanjani, M., Wilson, G. A., Birkbak, N. J., Hiley, C. T., Watkins, T. B., Shafi, S., Murugaesu, N., Mitter, R., Akarca, A. U., Linares, J., Marafioti, T., Henry, J. Y., Van Allen, E. M., Miao, D., Schilling, B., Schadendorf, D., Garraway, L. A., Makarov, V., Rizvi, N. A., Snyder, A., Hellmann, M. D., Merghoub, T., Wolchok, J. D., Shukla, S. A., Wu, C. J., Peggs, K. S., Chan, T. A., Hadrup, S. R., Quezada, S. A. and Swanton, C. 2016. Clonal neoantigens elicit T cell immunoreactivity and sensitivity to immune checkpoint blockade. *Science*, 351(6280), 1463-1469.

Medrek, C., Ponten, F., Jirstrom, K. and Leandersson, K. 2012. The presence of tumor associated macrophages in tumor stroma as a prognostic marker for breast cancer patients. *BMC Cancer*, 12, 306.

Metzger-Filho, O., Tutt, A., De Azambuja, E., Saini, K. S., Viale, G., Loi, S., Bradbury, I., Bliss, J. M., Azim, H. A., Jr., Ellis, P., Di Leo, A., Baselga, J., Sotiriou, C. and Piccart-Gebhart, M. 2012. Dissecting the heterogeneity of triple-negative breast cancer. *J Clin Oncol*, 30(15), 1879-1887.

Meyer, A. S., Miller, M. A., Gertler, F. B. and Lauffenburger, D. A. 2013. The receptor AXL diversifies EGFR signaling and limits the response to EGFR-targeted inhibitors in triple-negative breast cancer cells. *Sci Signal*, 6(287), ra66.

Miller, L. D., Chou, J. A., Black, M. A., Print, C., Chifman, J., Alistar, A., Putti, T., Zhou, X., Bedognetti, D., Hendrickx, W., Pullikuth, A., Rennhack, J., Andrechek, E. R., Demaria, S., Wang, E. and Marincola, F. M. 2016. Immunogenic Subtypes of Breast Cancer Delineated by Gene Classifiers of Immune Responsiveness. *Cancer Immunol Res*, 4(7), 600-610.

Mittendorf, E. A., Philips, A. V., Meric-Bernstam, F., Qiao, N., Wu, Y., Harrington, S., Su, X., Wang, Y., Gonzalez-Angulo, A. M., Akcakanat, A., Chawla, A., Curran, M., Hwu, P., Sharma, P., Litton, J. K., Molldrem, J. J. and Alatrash, G. 2014. PD-L1 expression in triple-negative breast cancer. *Cancer Immunol Res*, 2(4), 361-370.

Miyashita, M., Sasano, H., Tamaki, K., Hirakawa, H., Takahashi, Y., Nakagawa, S., Watanabe, G., Tada, H., Suzuki, A., Ohuchi, N. and Ishida, T. 2015. Prognostic significance of tumor-infiltrating CD8+ and FOXP3+ lymphocytes in residual tumors and alterations in these parameters after neoadjuvant chemotherapy in triple-negative breast cancer: a retrospective multicenter study. *Breast Cancer Res*, 17, 124.

Muenst, S., Soysal, S. D., Gao, F., Obermann, E. C., Oertli, D. and Gillanders, W. E. 2013. The presence of programmed death 1 (PD-1)-positive tumor-infiltrating lymphocytes is associated with poor prognosis in human breast cancer. *Breast Cancer Res Treat*, 139(3), 667-676.

Mukhtar, R. A., Nseyo, O., Campbell, M. J. and Esserman, L. J. 2011. Tumor-associated macrophages in breast cancer as potential biomarkers for new treatments and diagnostics. *Expert Rev Mol Diagn*, 11(1), 91-100.

Mulligan, J. M., Hill, L. A., Deharo, S., Irwin, G., Boyle, D., Keating, K. E., Raji, O. Y., Mcdyer, F. A., O'brien, E., Bylesjo, M., Quinn, J. E., Lindor, N. M., Mullan, P. B., James, C. R., Walker, S. M., Kerr, P., James, J., Davison, T. S., Proutski, V., Salto-

Tellez, M., Johnston, P. G., Couch, F. J., Paul Harkin, D. and Kennedy, R. D. 2014. Identification and validation of an anthracycline/cyclophosphamide-based chemotherapy response assay in breast cancer. *J Natl Cancer Inst*, 106(1), djt335.

Nagalla, S., Chou, J. W., Willingham, M. C., Ruiz, J., Vaughn, J. P., Dubey, P., Lash, T. L., Hamilton-Dutoit, S. J., Bergh, J., Sotiriou, C., Black, M. A. and Miller, L. D. 2013. Interactions between immunity, proliferation and molecular subtype in breast cancer prognosis. *Genome Biol*, 14(4), R34.

Negrini, S., Gorgoulis, V. G. and Halazonetis, T. D. 2010. Genomic instability--an evolving hallmark of cancer. *Nat Rev Mol Cell Biol*, 11(3), 220-228.

Nemunaitis, J., Borghaei, H., Akerley, W., Gadgeel, S., Spira, A., Rybkin, I., Faltaos, D., Chen, I., Christensen, J., Potvin, D., Velastegui, K., Levisetti, M. and Husain, H. 2016. Phase 2 Study of Glesatinib or Sitravatinib with Nivolumab in Non-Small Cell Lung Cancer (NSCLC) after Checkpoint Inhibitor Therapy. *In:* Proceedings of the 17th IASLC World Conference on Lung Cancer: 2016 Dec 4-7, Vienna, Austria. Elsevier; *J Thorac Oncol*, 12(Suppl), Abstract nr P2.06-014.

Nguyen, L. T. and Ohashi, P. S. 2015. Clinical blockade of PD1 and LAG3--potential mechanisms of action. *Nat Rev Immunol*, 15(1), 45-56.

Nielsen, F. C., Van Overeem Hansen, T. and Sorensen, C. S. 2016. Hereditary breast and ovarian cancer: new genes in confined pathways. *Nat Rev Cancer*, 16(9), 599-612.

Okazaki, T., Chikuma, S., Iwai, Y., Fagarasan, S. and Honjo, T. 2013. A rheostat for immune responses: the unique properties of PD-1 and their advantages for clinical application. *Nat Immunol*, 14(12), 1212-1218.

Ostuni, R., Kratochvill, F., Murray, P. J. and Natoli, G. 2015. Macrophages and cancer: from mechanisms to therapeutic implications. *Trends Immunol*, 36(4), 229-239.

Paccez, J. D., Vogelsang, M., Parker, M. I. and Zerbini, L. F. 2014. The receptor tyrosine kinase Axl in cancer: biological functions and therapeutic implications. *Int J Cancer*, 134(5), 1024-1033.

Park, S. Y., Lee, H. E., Li, H., Shipitsin, M., Gelman, R. and Polyak, K. 2010. Heterogeneity for stem cell-related markers according to tumor subtype and histologic stage in breast cancer. *Clin Cancer Res*, 16(3), 876-887.

Perou, C. M., Sorlie, T., Eisen, M. B., Van De Rijn, M., Jeffrey, S. S., Rees, C. A., Pollack, J. R., Ross, D. T., Johnsen, H., Akslen, L. A., Fluge, O., Pergamenschikov, A., Williams, C., Zhu, S. X., Lonning, P. E., Borresen-Dale, A. L., Brown, P. O. and Botstein, D. 2000. Molecular portraits of human breast tumours. *Nature*, 406(6797), 747-752.

Piras, F., Colombari, R., Minerba, L., Murtas, D., Floris, C., Maxia, C., Corbu, A., Perra, M. T. and Sirigu, P. 2005. The predictive value of CD8, CD4, CD68, and human leukocyte antigen-D-related cells in the prognosis of cutaneous malignant melanoma with vertical growth phase. *Cancer*, 104(6), 1246-1254.

Pitroda, S., Bao, R., Andrade, J., Weichselbaum, R. R. and Connell, P. P. 2017. Low Recombination Proficiency Score (RPS) predicts heightened sensitivity to DNA-damaging chemotherapy in breast cancer. *Clin Cancer Res*, 10.1158/1078-0432.CCR-16-2845.

Pollard, J. W. 2004. Tumour-educated macrophages promote tumour progression and metastasis. *Nat Rev Cancer*, 4(1), 71-78.

Polyak, K. and Weinberg, R. A. 2009. Transitions between epithelial and mesenchymal states: acquisition of malignant and stem cell traits. *Nat Rev Cancer*, 9(4), 265-273.

Postel-Vinay, S. and Ashworth, A. 2012. AXL and acquired resistance to EGFR inhibitors. *Nat Genet*, 44(8), 835-836.

Prat, A., Carey, L. A., Adamo, B., Vidal, M., Tabernero, J., Cortes, J., Parker, J. S., Perou, C. M. and Baselga, J. 2014. Molecular features and survival outcomes of the intrinsic subtypes within HER2-positive breast cancer. *J Natl Cancer Inst*, 106(8).

Prat, A., Parker, J. S., Karginova, O., Fan, C., Livasy, C., Herschkowitz, J. I., He, X. and Perou, C. M. 2010. Phenotypic and molecular characterization of the claudin-low intrinsic subtype of breast cancer. *Breast Cancer Res*, 12(5), R68.

Prat, A. and Perou, C. M. 2011. Deconstructing the molecular portraits of breast cancer. *Mol Oncol*, 5(1), 5-23.

Qian, B. Z. and Pollard, J. W. 2010. Macrophage diversity enhances tumor progression and metastasis. *Cell*, 141(1), 39-51.

Rakha, E. A., Reis-Filho, J. S. and Ellis, I. O. 2008. Basal-like breast cancer: a critical review. *J Clin Oncol*, 26(15), 2568-2581.

Reiman, J. M., Knutson, K. L. and Radisky, D. C. 2010. Immune promotion of epithelial-mesenchymal transition and generation of breast cancer stem cells. *Cancer Res*, 70(8), 3005-3008.

Rivenbark, A. G., O'connor, S. M. and Coleman, W. B. 2013. Molecular and cellular heterogeneity in breast cancer: challenges for personalized medicine. *Am J Pathol*, 183(4), 1113-1124.

Rizvi, N. A., Hellmann, M. D., Snyder, A., Kvistborg, P., Makarov, V., Havel, J. J., Lee, W., Yuan, J., Wong, P., Ho, T. S., Miller, M. L., Rekhtman, N., Moreira, A. L., Ibrahim, F., Bruggeman, C., Gasmi, B., Zappasodi, R., Maeda, Y., Sander, C., Garon, E. B., Merghoub, T., Wolchok, J. D., Schumacher, T. N. and Chan, T. A. 2015. Cancer immunology. Mutational landscape determines sensitivity to PD-1 blockade in non-small cell lung cancer. *Science*, 348(6230), 124-128.

Rody, A., Holtrich, U., Pusztai, L., Liedtke, C., Gaetje, R., Ruckhaeberle, E., Solbach, C., Hanker, L., Ahr, A., Metzler, D., Engels, K., Karn, T. and Kaufmann, M. 2009. T-cell metagene predicts a favorable prognosis in estrogen receptor-negative and HER2-positive breast cancers. *Breast Cancer Res*, 11(2), R15.

Rothlin, C. V., Ghosh, S., Zuniga, E. I., Oldstone, M. B. and Lemke, G. 2007. TAM receptors are pleiotropic inhibitors of the innate immune response. *Cell*, 131(6), 1124-1136.

Rouzier, R., Perou, C. M., Symmans, W. F., Ibrahim, N., Cristofanilli, M., Anderson, K., Hess, K. R., Stec, J., Ayers, M., Wagner, P., Morandi, P., Fan, C., Rabiul, I., Ross, J. S., Hortobagyi, G. N. and Pusztai, L. 2005. Breast cancer molecular subtypes respond differently to preoperative chemotherapy. *Clin Cancer Res*, 11(16), 5678-5685.

Roylance, R., Endesfelder, D., Gorman, P., Burrell, R. A., Sander, J., Tomlinson, I., Hanby, A. M., Speirs, V., Richardson, A. L., Birkbak, N. J., Eklund, A. C., Downward, J., Kschischo, M., Szallasi, Z. and Swanton, C. 2011. Relationship of extreme chromosomal instability with long-term survival in a retrospective analysis of primary breast cancer. *Cancer Epidemiol Biomarkers Prev*, 20(10), 2183-2194.

Ruffell, B., Affara, N. I. and Coussens, L. M. 2012a. Differential macrophage programming in the tumor microenvironment. *Trends Immunol*, 33(3), 119-126.

Ruffell, B., Au, A., Rugo, H. S., Esserman, L. J., Hwang, E. S. and Coussens, L. M. 2012b. Leukocyte composition of human breast cancer. *Proc Natl Acad Sci U S A*, 109(8), 2796-2801.

Ruffell, B., Chang-Strachan, D., Chan, V., Rosenbusch, A., Ho, C. M., Pryer, N., Daniel, D., Hwang, E. S., Rugo, H. S. and Coussens, L. M. 2014. Macrophage IL-10 blocks CD8+ T cell-dependent responses to chemotherapy by suppressing IL-12 expression in intratumoral dendritic cells. *Cancer Cell*, 26(5), 623-637.

Ruffell, B. and Coussens, L. M. 2015. Macrophages and therapeutic resistance in cancer. *Cancer Cell*, 27(4), 462-472.

Salgado, R., Denkert, C., Demaria, S., Sirtaine, N., Klauschen, F., Pruneri, G., Wienert, S., Van Den Eynden, G., Baehner, F. L., Penault-Llorca, F., Perez, E. A., Thompson, E. A., Symmans, W. F., Richardson, A. L., Brock, J., Criscitiello, C., Bailey, H., Ignatiadis, M., Floris, G., Sparano, J., Kos, Z., Nielsen, T., Rimm, D. L., Allison, K. H., Reis-Filho,

J. S., Loibl, S., Sotiriou, C., Viale, G., Badve, S., Adams, S., Willard-Gallo, K. and Loi, S. 2015. The evaluation of tumor-infiltrating lymphocytes (TILs) in breast cancer: recommendations by an International TILs Working Group 2014. *Ann Oncol*, 26(2), 259-271.

Sangaletti, S., Di Carlo, E., Gariboldi, S., Miotti, S., Cappetti, B., Parenza, M., Rumio, C., Brekken, R. A., Chiodoni, C. and Colombo, M. P. 2008. Macrophage-derived SPARC bridges tumor cell-extracellular matrix interactions toward metastasis. *Cancer Res*, 68(21), 9050-9059.

Santarpia, L., Bottai, G., Kelly, C. M., Gyorffy, B., Szekely, B. and Pusztai, L. 2016. Deciphering and Targeting Oncogenic Mutations and Pathways in Breast Cancer. *Oncologist*, 21(9), 1063-1078.

Santarpia, L., Iwamoto, T., Di Leo, A., Hayashi, N., Bottai, G., Stampfer, M., Andre, F., Turner, N. C., Symmans, W. F., Hortobagyi, G. N., Pusztai, L. and Bianchini, G. 2013. DNA repair gene patterns as prognostic and predictive factors in molecular breast cancer subtypes. *Oncologist*, 18(10), 1063-1073.

Savas, P., Salgado, R., Denkert, C., Sotiriou, C., Darcy, P. K., Smyth, M. J. and Loi, S. 2016. Clinical relevance of host immunity in breast cancer: from TILs to the clinic. *Nat Rev Clin Oncol*, 13(4), 228-241.

Schalper, K. A., Velcheti, V., Carvajal, D., Wimberly, H., Brown, J., Pusztai, L. and Rimm, D. L. 2014. In situ tumor PD-L1 mRNA expression is associated with increased TILs and better outcome in breast carcinomas. *Clin Cancer Res*, 20(10), 2773-2782.

Senkus, E., Kyriakides, S., Ohno, S., Penault-Llorca, F., Poortmans, P., Rutgers, E., Zackrisson, S. and Cardoso, F. 2015. Primary breast cancer: ESMO Clinical Practice Guidelines for diagnosis, treatment and follow-up. *Ann Oncol*, 26 (Suppl 5), v8-30.

Shah, S. P., Roth, A., Goya, R., Oloumi, A., Ha, G., Zhao, Y., Turashvili, G., Ding, J., Tse, K., Haffari, G., Bashashati, A., Prentice, L. M., Khattra, J., Burleigh, A., Yap, D., Bernard, V., Mcpherson, A., Shumansky, K., Crisan, A., Giuliany, R., Heravi-

Moussavi, A., Rosner, J., Lai, D., Birol, I., Varhol, R., Tam, A., Dhalla, N., Zeng, T., Ma, K., Chan, S. K., Griffith, M., Moradian, A., Cheng, S. W., Morin, G. B., Watson, P., Gelmon, K., Chia, S., Chin, S. F., Curtis, C., Rueda, O. M., Pharoah, P. D., Damaraju, S., Mackey, J., Hoon, K., Harkins, T., Tadigotla, V., Sigaroudinia, M., Gascard, P., Tlsty, T., Costello, J. F., Meyer, I. M., Eaves, C. J., Wasserman, W. W., Jones, S., Huntsman, D., Hirst, M., Caldas, C., Marra, M. A. and Aparicio, S. 2012. The clonal and mutational evolution spectrum of primary triple-negative breast cancers. *Nature*, 486(7403), 395-399.

Shipitsin, M., Campbell, L. L., Argani, P., Weremowicz, S., Bloushtain-Qimron, N., Yao, J., Nikolskaya, T., Serebryiskaya, T., Beroukhim, R., Hu, M., Halushka, M. K., Sukumar, S., Parker, L. M., Anderson, K. S., Harris, L. N., Garber, J. E., Richardson, A. L., Schnitt, S. J., Nikolsky, Y., Gelman, R. S. and Polyak, K. 2007. Molecular definition of breast tumor heterogeneity. *Cancer Cell*, 11(3), 259-273.

Snyder, A., Makarov, V., Merghoub, T., Yuan, J., Zaretsky, J. M., Desrichard, A., Walsh, L. A., Postow, M. A., Wong, P., Ho, T. S., Hollmann, T. J., Bruggeman, C., Kannan, K., Li, Y., Elipenahli, C., Liu, C., Harbison, C. T., Wang, L., Ribas, A., Wolchok, J. D. and Chan, T. A. 2014. Genetic basis for clinical response to CTLA-4 blockade in melanoma. *N Engl J Med*, 371(23), 2189-2199.

Solinas, G., Schiarea, S., Liguori, M., Fabbri, M., Pesce, S., Zammataro, L., Pasqualini, F., Nebuloni, M., Chiabrando, C., Mantovani, A. and Allavena, P. 2010. Tumor-conditioned macrophages secrete migration-stimulating factor: a new marker for M2-polarization, influencing tumor cell motility. *J Immunol*, 185(1), 642-652.

Sotiriou, C. and Pusztai, L. 2009. Gene-expression signatures in breast cancer. *N Engl J Med*, 360(8), 790-800.

Stanton, S. E., Adams, S. and Disis, M. L. 2016. Variation in the Incidence and Magnitude of Tumor-Infiltrating Lymphocytes in Breast Cancer Subtypes: A Systematic Review. *JAMA Oncol*, 2(10), 1354-1360.

Steidl, C., Lee, T., Shah, S. P., Farinha, P., Han, G., Nayar, T., Delaney, A., Jones, S. J., Iqbal, J., Weisenburger, D. D., Bast, M. A., Rosenwald, A., Muller-Hermelink, H. K., Rimsza, L. M., Campo, E., Delabie, J., Braziel, R. M., Cook, J. R., Tubbs, R. R., Jaffe, E. S., Lenz, G., Connors, J. M., Staudt, L. M., Chan, W. C. and Gascoyne, R. D. 2010. Tumor-associated macrophages and survival in classic Hodgkin's lymphoma. *N Engl J Med*, 362(10), 875-885.

Su, S., Liu, Q., Chen, J., Chen, F., He, C., Huang, D., Wu, W., Lin, L., Huang, W., Zhang, J., Cui, X., Zheng, F., Li, H., Yao, H., Su, F. and Song, E. 2014a. A positive feedback loop between mesenchymal-like cancer cells and macrophages is essential to breast cancer metastasis. *Cancer Cell*, 25(5), 605-620.

Su, S., Wu, W., He, C., Liu, Q. and Song, E. 2014b. Breaking the vicious cycle between breast cancer cells and tumor-associated macrophages. *Oncoimmunology*, 3(8), e953418.

Susan G. Komen. 2015. *Molecular Subtypes of Breast Cancer* [Online]. Available at http://ww5.komen.org/BreastCancer/SubtypesofBreastCancer.html [Accessed 6 October 2016].

Swanton, C., Nicke, B., Schuett, M., Eklund, A. C., Ng, C., Li, Q., Hardcastle, T., Lee, A., Roy, R., East, P., Kschischo, M., Endesfelder, D., Wylie, P., Kim, S. N., Chen, J. G., Howell, M., Ried, T., Habermann, J. K., Auer, G., Brenton, J. D., Szallasi, Z. and Downward, J. 2009. Chromosomal instability determines taxane response. *Proc Natl Acad Sci U S A*, 106(21), 8671-8676.

Tan, T. Z., Miow, Q. H., Miki, Y., Noda, T., Mori, S., Huang, R. Y. and Thiery, J. P. 2014. Epithelial-mesenchymal transition spectrum quantification and its efficacy in deciphering survival and drug responses of cancer patients. *EMBO Mol Med*, 6(10), 1279-1293.

Taube, J. H., Herschkowitz, J. I., Komurov, K., Zhou, A. Y., Gupta, S., Yang, J., Hartwell, K., Onder, T. T., Gupta, P. B., Evans, K. W., Hollier, B. G., Ram, P. T., Lander, E. S.,

Rosen, J. M., Weinberg, R. A. and Mani, S. A. 2010. Core epithelial-to-mesenchymal transition interactome gene-expression signature is associated with claudin-low and metaplastic breast cancer subtypes. *Proc Natl Acad Sci U S A*, 107(35), 15449-15454.

Taube, J. M., Young, G. D., Mcmiller, T. L., Chen, S., Salas, J. T., Pritchard, T. S., Xu, H., Meeker, A. K., Fan, J., Cheadle, C., Berger, A. E., Pardoll, D. M. and Topalian, S. L. 2015. Differential Expression of Immune-Regulatory Genes Associated with PD-L1 Display in Melanoma: Implications for PD-1 Pathway Blockade. *Clin Cancer Res*, 21(17), 3969-3976.

Telli, M. L., Timms, K. M., Reid, J., Hennessy, B., Mills, G. B., Jensen, K. C., Szallasi, Z., Barry, W. T., Winer, E. P., Tung, N. M., Isakoff, S. J., Ryan, P. D., Greene-Colozzi, A., Gutin, A., Sangale, Z., Iliev, D., Neff, C., Abkevich, V., Jones, J. T., Lanchbury, J. S., Hartman, A. R., Garber, J. E., Ford, J. M., Silver, D. P. and Richardson, A. L. 2016. Homologous Recombination Deficiency (HRD) Score Predicts Response to Platinum-Containing Neoadjuvant Chemotherapy in Patients with Triple-Negative Breast Cancer. *Clin Cancer Res*, 22(15), 3764-3773.

Tiainen, S., Tumelius, R., Rilla, K., Hamalainen, K., Tammi, M., Tammi, R., Kosma, V. M., Oikari, S. and Auvinen, P. 2015. High numbers of macrophages, especially M2-like (CD163-positive), correlate with hyaluronan accumulation and poor outcome in breast cancer. *Histopathology*, 66(6), 873-883.

Tirosh, I., Izar, B., Prakadan, S. M., Wadsworth, M. H., 2nd, Treacy, D., Trombetta, J. J., Rotem, A., Rodman, C., Lian, C., Murphy, G., Fallahi-Sichani, M., Dutton-Regester, K., Lin, J. R., Cohen, O., Shah, P., Lu, D., Genshaft, A. S., Hughes, T. K., Ziegler, C. G., Kazer, S. W., Gaillard, A., Kolb, K. E., Villani, A. C., Johannessen, C. M., Andreev, A. Y., Van Allen, E. M., Bertagnolli, M., Sorger, P. K., Sullivan, R. J., Flaherty, K. T., Frederick, D. T., Jane-Valbuena, J., Yoon, C. H., Rozenblatt-Rosen, O., Shalek, A. K., Regev, A. and Garraway, L. A. 2016. Dissecting the multicellular ecosystem of metastatic melanoma by single-cell RNA-seq. *Science*, 352(6282), 189-196.

Topalian, S. L., Drake, C. G. and Pardoll, D. M. 2015. Immune checkpoint blockade: a common denominator approach to cancer therapy. *Cancer Cell*, 27(4), 450-461.

Tripathi, C., Tewari, B. N., Kanchan, R. K., Baghel, K. S., Nautiyal, N., Shrivastava, R., Kaur, H., Bhatt, M. L. and Bhadauria, S. 2014. Macrophages are recruited to hypoxic tumor areas and acquire a pro-angiogenic M2-polarized phenotype via hypoxic cancer cell derived cytokines Oncostatin M and Eotaxin. *Oncotarget*, 5(14), 5350-5368.

Tsoutsou, P. G., Bourhis, J. and Coukos, G. 2015. Tumor-infiltrating lymphocytes in triple-negative breast cancer: a biomarker for use beyond prognosis? *J Clin Oncol*, 33(11), 1297-1298.

Tung, N. M. and Winer, E. P. 2015. Tumor-infiltrating lymphocytes and response to platinum in triple-negative breast cancer. *J Clin Oncol*, 33(9), 969-971.

Turner, N., Tutt, A. and Ashworth, A. 2004. Hallmarks of 'BRCAness' in sporadic cancers. *Nat Rev Cancer*, 4(10), 814-819.

Turner, N. C. and Reis-Filho, J. S. 2013. Tackling the diversity of triple-negative breast cancer. *Clin Cancer Res*, 19(23), 6380-6388.

Van Allen, E. M., Miao, D., Schilling, B., Shukla, S. A., Blank, C., Zimmer, L., Sucker, A., Hillen, U., Geukes Foppen, M. H., Goldinger, S. M., Utikal, J., Hassel, J. C., Weide, B., Kaehler, K. C., Loquai, C., Mohr, P., Gutzmer, R., Dummer, R., Gabriel, S., Wu, C. J., Schadendorf, D. and Garraway, L. A. 2015. Genomic correlates of response to CTLA-4 blockade in metastatic melanoma. *Science*, 350(6257), 207-211.

Van Der Meer, J. H., Van Der Poll, T. and Van 'T Veer, C. 2014. TAM receptors, Gas6, and protein S: roles in inflammation and hemostasis. *Blood*, 123(16), 2460-2469.

Vassilakopoulou, M., Parisi, F., Siddiqui, S., England, A. M., Zarella, E. R., Anagnostou, V., Kluger, Y., Hicks, D. G., Rimm, D. L. and Neumeister, V. M. 2015. Preanalytical variables and phosphoepitope expression in FFPE tissue: quantitative epitope assessment after variable cold ischemic time. *Lab Invest*, 95(3), 334-341.

Vollan, H. K., Rueda, O. M., Chin, S. F., Curtis, C., Turashvili, G., Shah, S., Lingjaerde, O. C., Yuan, Y., Ng, C. K., Dunning, M. J., Dicks, E., Provenzano, E., Sammut, S., Mckinney, S., Ellis, I. O., Pinder, S., Purushotham, A., Murphy, L. C., Kristensen, V. N., Brenton, J. D., Pharoah, P. D., Borresen-Dale, A. L., Aparicio, S. and Caldas, C. 2015. A tumor DNA complex aberration index is an independent predictor of survival in breast and ovarian cancer. *Mol Oncol*, 9(1), 115-127.

Wang, Z. Q., Milne, K., Derocher, H., Webb, J. R., Nelson, B. H. and Watson, P. H. 2016. CD103 and Intratumoral Immune Response in Breast Cancer. *Clin Cancer Res*, 22(24), 6290-6297.

Webb, J. R., Milne, K. and Nelson, B. H. 2015. PD-1 and CD103 Are Widely Coexpressed on Prognostically Favorable Intraepithelial CD8 T Cells in Human Ovarian Cancer. *Cancer Immunol Res*, 3(8), 926-935.

Webb, J. R., Milne, K., Watson, P., Deleeuw, R. J. and Nelson, B. H. 2014. Tumor-infiltrating lymphocytes expressing the tissue resident memory marker CD103 are associated with increased survival in high-grade serous ovarian cancer. *Clin Cancer Res*, 20(2), 434-444.

West, N. R., Kost, S. E., Martin, S. D., Milne, K., Deleeuw, R. J., Nelson, B. H. and Watson, P. H. 2013. Tumour-infiltrating FOXP3(+) lymphocytes are associated with cytotoxic immune responses and good clinical outcome in oestrogen receptor-negative breast cancer. *Br J Cancer*, 108(1), 155-162.

Williams, C. B., Yeh, E. S. and Soloff, A. C. 2016. Tumor-associated macrophages: unwitting accomplices in breast cancer malignancy. *NPJ Breast Cancer*, 2.

Wilson, C., Ye, X., Pham, T., Lin, E., Chan, S., Mcnamara, E., Neve, R. M., Belmont, L., Koeppen, H., Yauch, R. L., Ashkenazi, A. and Settleman, J. 2014. AXL inhibition sensitizes mesenchymal cancer cells to antimitotic drugs. *Cancer Res*, 74(20), 5878-5890.

Wimberly, H., Brown, J. R., Schalper, K., Haack, H., Silver, M. R., Nixon, C., Bossuyt, V., Pusztai, L., Lannin, D. R. and Rimm, D. L. 2015. PD-L1 Expression Correlates with Tumor-Infiltrating Lymphocytes and Response to Neoadjuvant Chemotherapy in Breast Cancer. *Cancer Immunol Res*, 3(4), 326-332.

Wnuk-Lipinska, K., Davidsen, K., Blø, M., Engelsen, A., Kang, J., Hodneland, L., Lie, M., Bougnaud, S., Aguilera, K., Ahmed, L., Rybicka, A., Nævdal, E. M., Deyna, P., Boniecka, A., Oddbjørn, S., Chouaib, S., Brekken, R., Gausdal, G. and Lorens, J. B. 2017. BGB324, a selective small molecule inhibitor of receptor tyrosine kinase AXL, abrogates tumor intrinsic and microenvironmental immune suppression and enhances immune checkpoint inhibitor efficacy in lung and mammary adenocarcinoma models. *In:* Proceedings of the 108th American Association for Cancer Research Annual Meeting: 2017 Apr 1-5, Washington, DC. Philadelphia (PA); AACR; *Cancer Res*, 77(Suppl 13), Abstract nr 626.

Woo, S. R., Turnis, M. E., Goldberg, M. V., Bankoti, J., Selby, M., Nirschl, C. J., Bettini, M. L., Gravano, D. M., Vogel, P., Liu, C. L., Tangsombatvisit, S., Grosso, J. F., Netto, G., Smeltzer, M. P., Chaux, A., Utz, P. J., Workman, C. J., Pardoll, D. M., Korman, A. J., Drake, C. G. and Vignali, D. A. 2012. Immune inhibitory molecules LAG-3 and PD-1 synergistically regulate T-cell function to promote tumoral immune escape. *Cancer Res*, 72(4), 917-927.

Workel, H. H., Komdeur, F. L., Wouters, M. C., Plat, A., Klip, H. G., Eggink, F. A., Wisman, G. B., Arts, H. J., Oonk, M. H., Mourits, M. J., Yigit, R., Versluis, M., Duiker, E. W., Hollema, H., De Bruyn, M. and Nijman, H. W. 2016. CD103 defines intraepithelial CD8+ PD1+ tumour-infiltrating lymphocytes of prognostic significance in endometrial adenocarcinoma. *Eur J Cancer*, 60, 1-11.

Yokoyama, Y., Lew, E. D., Seelige, R., Walsh, C., Barrera, M., Tindall, E., Oh, J., Ely, H., Diliberto, A., Albert, A., Bui, J. and Li, G. 2017. Immuno-oncological efficacy of RXDX-106, a novel, selective and potent small molecule TAM (TYRO3, AXL, MER)

inhibitor. *In:* Proceedings of the 108th American Association for Cancer Research Annual Meeting: 2017 Apr 1-5, Washington, DC. Philadelphia (PA); AACR; *Cancer Res*, 77(Suppl 13), Abstract nr 4698.

Zanetti, M. 2017. Chromosomal chaos silences immune surveillance. *Science*, 355(6322), 249-250.

Zhang, L., Zhou, F. and Ten Dijke, P. 2013. Signaling interplay between transforming growth factor-beta receptor and PI3K/AKT pathways in cancer. *Trends Biochem Sci*, 38(12), 612-620.

Zizzo, G., Hilliard, B. A., Monestier, M. and Cohen, P. L. 2012. Efficient clearance of early apoptotic cells by human macrophages requires M2c polarization and MerTK induction. *J Immunol*, 189(7), 3508-3520.